



Escola Universitària d'Enginyeria
Tècnica Industrial de Barcelona
Consorci Escola Industrial de Barcelona

UNIVERSITAT POLITÈCNICA DE CATALUNYA

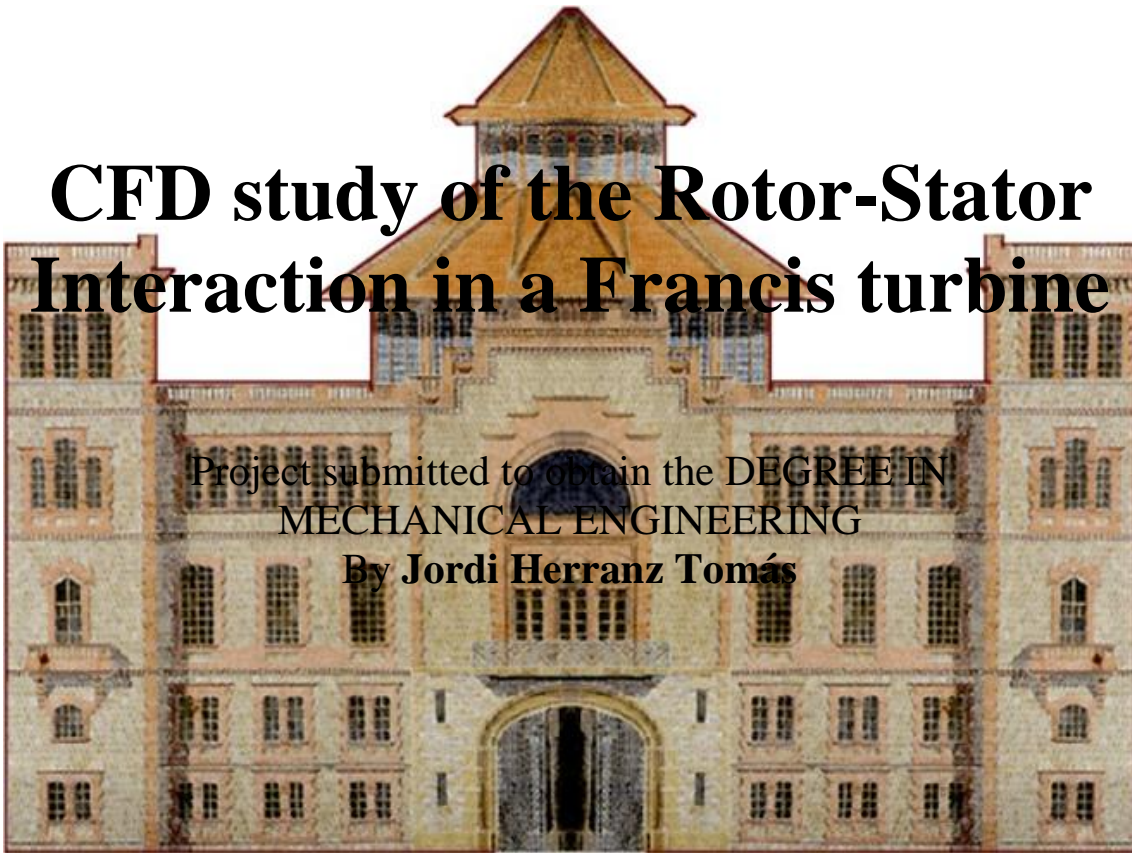
Volume I
Report – Budget – Annexes

B.Eng. Thesis

CFD study of the Rotor-Stator Interaction in a Francis turbine

Project submitted to obtain the DEGREE IN
MECHANICAL ENGINEERING

By **Jordi Herranz Tomás**



Barcelona, 26th April 2016

Director: Alfredo Guardo Zabaleta
Fluids Mechanics Department (MF)
Universitat Politècnica de Catalunya (UPC)

GENERAL TABLE OF CONTENTS

VOLUME I (Report - Budget - Annexes)

REPORT TABLE OF CONTENTS

Visit i plau d'autorització de defensa de TFG	i
Report table of contents.....	ii
Resum.....	iv
Resumen.....	iv
Abstract	iv
Preface.....	vi
List of figures	viii
List of tables.....	x
CHAPTER 1. Introduction.....	1
1.1. Rotor-stator interaction.....	1
1.1.1. Generalities and problematic.....	2
1.1.2. State of the art	5
1.2. Computational fluid dynamics.....	8
1.2.1. Generalities and applications	8
1.3. CFD of RSI in turbomachinery.....	8
1.4. Objective and project scope.....	10
1.5. Limitations.....	10
CHAPTER 2. Flow modeling	11
2.1. Fluid mechanics governing equations.....	12
2.1.1. Mass conservation.....	12
2.1.2. Conservation of the amount of movement	13
2.2. Turbulence models.....	16
2.2.1. Reynolds Averaged Navier Stokes (RANS)	17
CHAPTER 3. Methodology	19
3.1. Problem identification.....	20
3.2. Pre-processing.....	20
3.2.1. CAD Geometries.....	20
3.2.2. Meshing.....	24

3.2.3. Physics	26
3.2.4. Solver settings.....	28
3.3. Solve	31
3.4. Post-processing	32
CHAPTER 4. Results and discussion	33
4.1. Pressure and velocity contours	33
4.2. Velocity vectors	36
4.3. Frequency analysis.....	37
4.3.1. Drag and lift coefficients.....	37
4.3.2. Pressure monitors	39
4.3.3. Surface Monitor	42
4.4. Comparison between theoretical and numerical study	42
CHAPTER 5. Conclusions.....	43
CHAPTER 6. Bibliography	45
6.1. Reference bibliography.....	45
6.2. Consultation bibliography.....	48

BUDGET TABLE OF CONTENTS

Budget table of contents	i
CHAPTER 1. Previous considerations.....	1
CHAPTER 2. Budget	2

ANNEXES TABLE OF CONTENTS

Annexes table of contents	i
CHAPTER 1. Meshing.....	1
1.1. Annex A: Rotor meshing quality	1
1.2. Annex B: Stator meshing quality	3
CHAPTER 2. Results.....	5
2.1. Annex C: Static pressure point monitors	5
2.2. Annex D: Frequencies of the pressure monitors.....	32



Escola Universitària d'Enginyeria
Tècnica Industrial de Barcelona
Consorci Escola Industrial de Barcelona

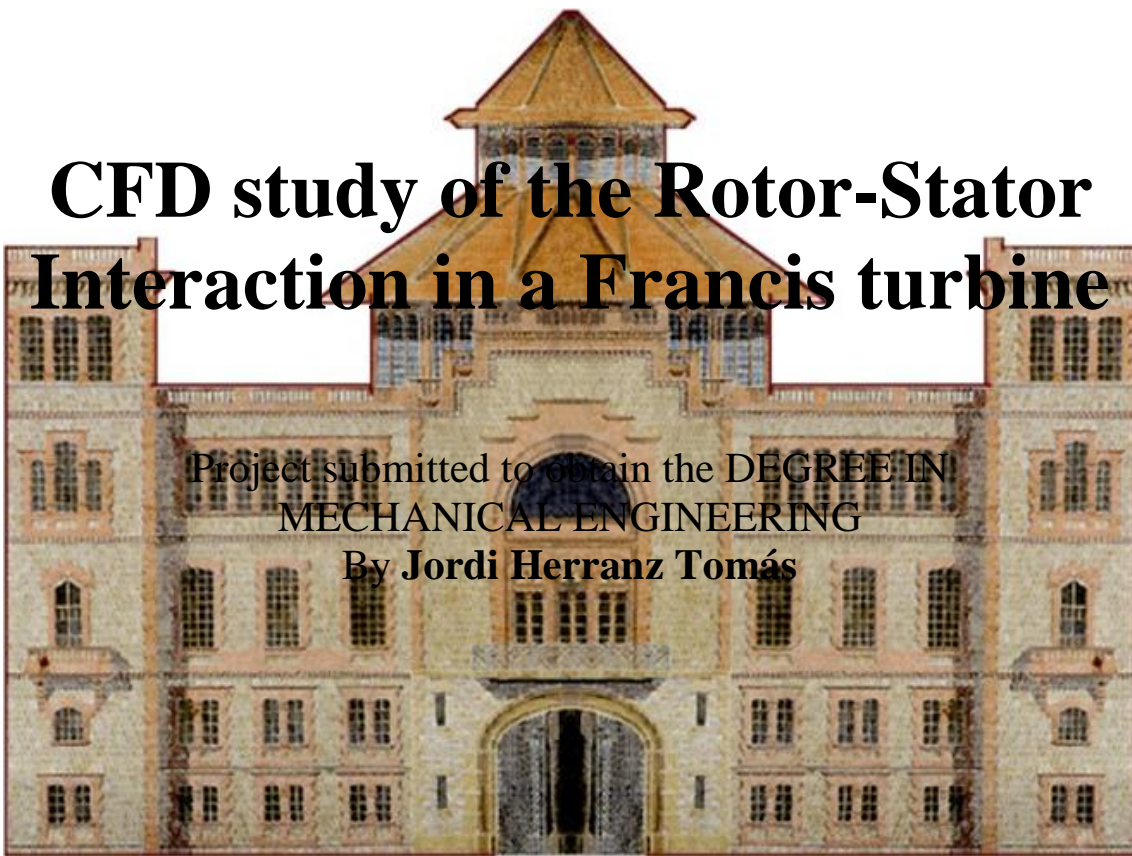
UNIVERSITAT POLITÈCNICA DE CATALUNYA

Report

CFD study of the Rotor-Stator Interaction in a Francis turbine

Project submitted to obtain the **DEGREE IN
MECHANICAL ENGINEERING**

By Jordi Herranz Tomás



Barcelona, 26th April 2016

Director: Alfredo Guardo Zabaleta
Fluids Mechanics Department (MF)
Universitat Politècnica de Catalunya (UPC)



VISIT I PLAU D'AUTORITZACIÓ DE DEFENSA DE TFG

Jo, *ALFREDO GUARDO ZABALETA* Director/a del TFG

dut a terme per l'estudiant/a:

Nom : *JORDI*

Cognoms : *HERRANZ TOMÁS*

DNI : *46774803-W*

Grau en Enginyeria : *MECÀNICA*

A C R E D I T O:

Que l'estudiant/a ha assolit els requisits establerts en la normativa acadèmica dels estudis de Grau de l'Escola Universitària d'Enginyeria Tècnica Industrial de Barcelona i que es troba en condicions de realitzar, en la present convocatòria, la defensa del treball de fi de Grau que a continuació es relaciona:

Títol del TFG: *CFD study of the rotor-stator interaction in a Francis turbine*

.....

.....

.....

I perquè consti, a petició de l'interessat i als efectes d'autorització de defensa de TFG, signo el present vist i plau.

Barcelona a, ... *25* ... de *ABRIL* de *2016*

El/la Director/a del TFG

Signatura:

REPORT TABLE OF CONTENTS

Visit i plau d'autorització de defensa de TFG	i
Report table of contents.....	ii
Resum.....	iv
Resumen	iv
Abstract	iv
Preface.....	v
List of figures	vii
List of tables.....	ix
CHAPTER 1. Introduction.....	1
1.1. Rotor-stator interaction	1
1.1.1. Generalities and problematic.....	2
1.1.2. State of the art	5
1.2. Computational fluid dynamics.....	8
1.2.1. Generalities and applications	8
1.3. CFD of RSI in turbomachinery.....	8
1.4. Objective and project scope.....	10
1.5. Limitations.....	10
CHAPTER 2. Flow modeling.....	11
2.1. Fluid mechanics governing equations.....	12
2.1.1. Mass conservation.....	12
2.1.2. Conservation of the amount of movement	13
2.2. Turbulence models.....	16
2.2.1. Reynolds Averaged Navier Stokes (RANS)	17
CHAPTER 3. Methodology	19
3.1. Problem identification.....	20
3.2. Pre-processing.....	20
3.2.1. CAD Geometries.....	20
3.2.2. Meshing.....	24
3.2.3. Physics	26
3.2.4. Solver settings.	28
3.3. Solve	31
3.4. Post-processing	32

CHAPTER 4. Results and discussion	33
4.1. Pressure and velocity contours	33
4.2. Velocity vectors	36
4.3. Frequency analysis.....	37
4.3.1. Drag and lift coefficients.....	37
4.3.2. Pressure monitors	39
4.3.3. Surface Monitor	42
4.4. Comparison between theoretical and numerical study	42
CHAPTER 5. Conclusions.....	43
CHAPTER 6. Bibliography	45
6.1. Reference bibliography.....	45
6.2. Consultation bibliography.....	48

RESUM

En el següent treball de fi de grau, el qual forma part d'un projecte dirigit pel CDIF (Centre de Diagnòstic Industrial i Fluidodinàmica), es pretén realitzar l'estudi del model geomètric d'un prototip real d'una turbina hidràulica. En el present projecte es pretén modelar numèricament mitjançant la mecànica de fluids computacional, a partir d'ara CFD, la màquina hidràulica en qüestió per tal de discretitzar els fenòmens fluidodinàmics implicats en el seu funcionament.

El cos principal de l'estudi es centrarà essencialment en l'anàlisi dels fenòmens que intervenen en la interacció Rotor-Estator: l'efecte potencial i l'efecte de la estela en menor mesura. Per mitja d'imatges de contorns y vectors es pretendrá observar com es el comportament del flux amb el pas dels alebs del rotor en les zones de major interès.

Per altra banda, es definiran diversos monitors dins del domini computacional per tal de capturar la informació dels repetits cicles presents en el sistema. Així com determinar les seves principals freqüències característiques.

RESUMEN

En el siguiente trabajo de fin de grado, el cual forma parte de un proyecto dirigido por el CDIF (Centro de Diagnóstico Industrial y Fluidodinámica), se pretende realizar el estudio del modelo geométrico de un prototipo real de una turbina hidráulica. En el presente proyecto se pretende modelizar numéricamente mediante la mecánica de fluidos computacional, a partir de ahora CFD, la máquina hidráulica en cuestión y de este modo poder discretizar los fenómenos fluidodinámicos implicados en su funcionamiento.

El cuerpo principal del estudio se va a centrar esencialmente en el análisis de los fenómenos que intervienen en la interacción Rotor-Estator: el efecto potencial y el efecto de la estela en menor medida. Por medio de imágenes de contornos y vectores se pretenderá observar como es el comportamiento del flujo con el paso de los álabes del rotor en las zonas de mayor interés.

Por otro lado, se definirán varios monitores dentro del dominio computacional con el objetivo de capturar la información de los repetidos ciclos presentes en el sistema. Así como determinar sus principales frecuencias características.

ABSTRACT

In the following degree paper, which is part of a project led by CDIF (Centre for Industrial Diagnostics and Fluid Dynamics), is pretended to study a geometrical model of a real prototype of a hydraulic turbine. The main point of this paper is to make a discrete numerical model of the hydraulic machine with Computational Fluid Dynamics, from now CFD, to get the characteristic fluid dynamics phenomena when it is operating.

The study will focus mainly on the analysis of the phenomena involved in the rotor-stator interaction: potential effect and the wake effect in lesser importance. Through vectors and contour images is intended to observe how is the flow behaviour with the rotor blade passing in the areas of greatest interest.

On the other hand, multiple monitors within the computational domain will be defined in order to capture the information from the repeated cycles of the system. As well as determining its principal characteristic frequencies.

PREFACE

PROJECT ORIGIN

The CDIF researches the area of Fluid Mechanics and Turbomachinery.

It investigates the fluid-structure interaction phenomena in simple structures such as blades and more complex as the rotors of the turbomachines.

The basic knowledge is used to investigate the dynamic behavior of turbine-pump of big dimensions as those used in the field of renewable energy.

The research includes the study of fluid dynamics excitations generated by fluid and dynamic response of stationary structures such as the rotating blades and the rotors.

The analysis of the dynamic behavior is fundamental in the slim structures design or when the vibrations and excitations magnitude can generate excessive tensions that can lead to fatigue cracks.

The rotor of a turbopump is a complex structure submerged in water in a case with very small clearances. In these conditions the effects of added mass, damping affect the modal response thereby calculating frequencies, amplitudes and modes presents many uncertainties. On the other hand, with the increase of the power concentration, the excitation forces in the rotor are more intense especially those generated by the interaction rotor-stator. It is also studied the excitement generated by wakes and cavitations.

PREVIOUS REQUIREMENTS

For carrying out a proper study of CFD is highly recommended and advisable to have minimal notions about the fluids behavior and the theory that surrounds them. Thus, aside from being able to design a conscious and justified model, we can go beyond obtain certain results and be able to understand and give a coherent and substantiated explanation of why of such behavior.

Unfortunately, for carrying out a computer simulation, is not enough simply to know the theoretical framework behind this big world as fluid mechanics. Clearly, the role of powerful CFD software is irrefutably essential.

Prior to embarking on such a project described below it is of vital necessity to do an intensive course, either face to face or based on tutorials to improve our fluency with this type of software.

Currently in the market, there is a wide range of CFD software available to everyone for free or with fee required. In my case I have increased my knowledge of ANSYS, Inc. in the pre-processing software as well as post-processing. In this way, as part of the same company, the interaction and the importing files among them is faster and more intuitive. For this reason, I had to spend two months for learning and understanding almost the entire software of both.

MOTIVATION

I have always been curious to go a step further and understand every detail of physical phenomena.

Likewise, despite I acquired the interest in engineering from when I was a child, I realized, in the second year of my studies that the sector which is more interesting to me is CAE (Computer-Aided Engineering) applied to the Fluid mechanics.

Later, when I joined the Formula Student team from EUETIB, I saw that the area that attracted me more was Aerodynamics. The main tool was CFD, essentially used to analyze the areas of high and low pressure and afterwards modify the geometry and thus achieve greater or lower adhesion.

Through this experience I reaffirm definitely that my interest in the world of engineering was CFD. For this reason I decided to make this project based on Computational Fluid Mechanics and later to continue my studies with a Master in this sector.

ACKNOWLEDGEMENTS

First of all my sincere thanks to my tutor Alfredo Guardo Zabaleta for letting me be part of this project. As well as provide practical and efficient solutions in unproductive moments.

Secondly I would like to give my thanks to the whole CDIF team for giving me support, based on theoretical and indirect participation in my project.

I would also like to thank my family for their patience, trust and understanding they have shown in me regarding to this project.

Finally a special and highlighted thanks to my two fellow from University, Jordi Parra Porcar for sharing his experience and time dedicated to teaching me to use entirely the software used. And Jordi Lahoz for lending me his project data many times as necessary without delay some. As well as offer me help when needed.

LIST OF FIGURES

Figure 1.1 Unsteadiness of rotor and stator interaction RSI	2
Figure 1.2 Streak lines in the wake behind a circular cylinder in a stream of oil.....	3
Figure 1.3 Regimes of fluid flow across smooth circular cylinders	4
Figure 1.4 Top view of Von Kármán vortex street cavitation: a) Lock-in condition, b) Lock-off condition.....	5
Figure 1.5 Wake interaction between rotor and stator.	9
Figure 1.6 Airfoil wake and vortex shedding. LES Simulation and Soap-Film Experiments.....	9
Figure 1.7 Locations of the monitoring points in the distributor channel	10
Figure 2.1 X component of the parameters involved in the infinitesimal control volume	12
Figure 2.2 Efforts notation	14
Figure 3.1 Diagram of the methodology to follow.....	19
Figure 3.2 Computational domain.....	20
Figure 3.3 a) 2D sketch of the rotor (top view), b) Full rotor extruded	21
Figure 3.4 Stator computational domain; a) Sketch, b) Solid	21
Figure 3.5 Reduced computational domain.....	22
Figure 3.6 a) Geometry exported to ANSYS Icem 15.0, b) Surface creation in the imported geometry	22
Figure 3.7 Detail of the created fluid volume location.....	23
Figure 3.8 Division of the geometry in parts.....	23
Figure 3.9 a) Strategy employed in distributing the blocks, b) Overview of the stator mesh	24
Figure 3.10 a) O-grid mesh refined, b) mesh density at the guide vane trailing edge.....	25
Figure 3.11 Detail view of the stator periodic zones.....	25
Figure 3.12 a) General view of the rotor mesh, b) Detail view of the tetrahedral elements that conform the rotor mesh.....	26
Figure 3.13 Defined boundary conditions in the computational domain	27
Figure 3.14 Unit vectors of drag and lift of the guide vane.....	29
Figure 3.15 Unit vectors of drag and lift of the wicket gate.....	29
Figure 3.16 Flowchart of the numerical solution in commercial CFD programs.....	32
Figure 4.1 Static pressure variation in real time in one complete rotor revolution	33
Figure 4.2 Single static pressure cycle at real time	34
Figure 4.3 Static pressure contours showing the potential phenomena at different time steps; a) Time=2,7396 s b) Time=2,7402 s c) Time=2,7408 s d) Time=2,7414 s	34
Figure 4.4 Velocity contours of the rotor-stator domain.....	35

Figure 4.5 Detail A view showing the contours of velocity around the wicket gate trailing edge at different time steps; a) Time=2,7396 s b) Time=2,7402 s c) Time=2,7408 s d) Time=2,7414 s 36

Figure 4.6 Detail B view of the vortex shedding due to the wake effect 37

Figure 4.7 Drag coefficient values depending on the vane 38

Figure 4.8 Lift coefficient values depending on the vane 38

Figure 4.9 Frequencies of the a) C_D around the guide vane, b) C_L around the guide vane, c) C_D around the wicket gate and d) C_L around the wicket gate 39

Figure 4.10 Detail of the point monitors location 40

Figure 4.11 Static pressure monitors variation in one complete cycle 40

Figure 4.12 Frequencies of the static pressure in the monitor point 1 41

Figure 4.13 Volumetric flow-rate variation..... 42

LIST OF TABLES

Table 2.1 Mass flow relation at the inlet and the outlet for the conservation of mass	13
Table 2.2 Flow relation at the inlet and outlet for the conservation of momentum.....	13
Table 2.3 Surface forces relation in the inlet and outlet for the x-direction	15
Table 3.1 Features Summary of both meshes	26
Table 3.2 Initial pre-established general parameters	27
Table 3.3 Detail of the used boundary conditions	28
Table 3.4 Established relaxing parameters	28
Table 3.5 Pre-defined limit values.....	28
Table 3.6 Unit vectors components of the C_L and C_D	30
Table 3.7 Geometric coordinates of the punctual monitors.....	30
Table 3.8 Characteristic frequencies of the C_D and C_L coefficients	39
Table 3.9 Frequencies of the static pressure monitor points.....	41

CHAPTER 1. INTRODUCTION

In order to obtain more efficient turbomachine designs it has been reduced the gap between the rotor and the stator increasing thereby the performance of the machine. Despite carrying out more efficient models, the fact of minimize the distance mentioned causes strong interactions between the rotor blades and the stator guide vanes. These interactions affect adversely on the fluid dynamics and on the structure of the system. This phenomenon is called rotor-stator interaction (from now RSI) and plays an essential role on the behavior of the machine. That is why the design of turbomachinery is not a trivial task.

In order to study efficiently and reliably the effects that take place due to the RSI phenomenon, has resorted the use of the technique of numerical methods using computational fluid dynamics (CFD). In fact nowadays, it is inconceivable to study in an analytical way almost any real phenomenon because of the high mathematical complexity that we should deal with. However, we still require experimentation, since it is a good complement to confirm numerical studies.

In this case, the analysis of the RSI phenomenon requires a high cost of experimentation and this is why we must make sure to choose a good turbulence model that suits to our case as well as make an appropriate treatment of the boundary layer to obtain results as reliable as possible.

This work aims to study and analyze the effects on the RSI phenomenon in a real model of a Francis turbine that is composed of a 7 bladed moving rotor and a stator of 16 vanes. It will be made by CFD including the prior CAD modeling in order to meet the complex pattern of fluid characteristics, pressure fluctuations as well as their fundamental frequencies and harmonics in this type of turbomachine.

1.1. Rotor-stator interaction

For the vast majority of the engineering and industrial applications, the features of any turbomachine are evaluated from the Euler equation for steady flow. In a way, this global and functional description only attends to the difference in the flow energy content between the input and the output, giving to the machine the ability to produce this exchange, but without trying to understand or analyze the phenomena that take place inside.

On the other hand, if what is intended is to study the interaction between fixed and movable crowns, which have relative movement between them inside the machine, must rethink the study until the consideration of non-stationary conditions. The fact of observing in a fixed reference the regular blade passing, reveals the unsteady nature of the flow.

1.1.1. Generalities and problematic

The great complexity that the flow has inside the turbomachine is given by the existence of these movable surfaces that move regard to other fixed. Moreover, the existence of various boundary layers associated with each surface, generate wakes, which being carried by the flow among the constituent crowns of the machine, are responsible for new non-stationary phenomena. Therefore, for each fixed point of the space where the blades will be passing by, there will be a signal of velocity and pressure, which will change in a periodically way with the pass of the blades. This is equivalent to stating that inside the machine is established a pressure field that is variable in time, a non-stationary field direct consequence of the passing blade frequency.

The interactions between the rotor blades and the stator wicket gates is one of the most important reason of the hydraulic machines vibrations (Zobeiri et al. 2006) [1]. The phenomenology of rotor-stator interactions may be considered as a combination of inviscid flow, potential, and viscous flow, wake, interactions (Dring et al. 1982) [2]. The RSI can generate, under certain conditions, unfavourable effects like high pressure pulses, noise and structural vibrations that they are unwanted. These effects are important harmful sources not only for the blades but also for the entire machine as in some cases can cause failure fatigue.

The above mentioned fluid dynamic effects linked to the existence of non-stationarity constitute RSI phenomenon. The RSI can be divided into the following mechanisms: potential interaction or wake interaction [2] y (Ardnt et al. 1989) [3], and in smaller measure shock interactions (in turbomachine of incompressible fluid).

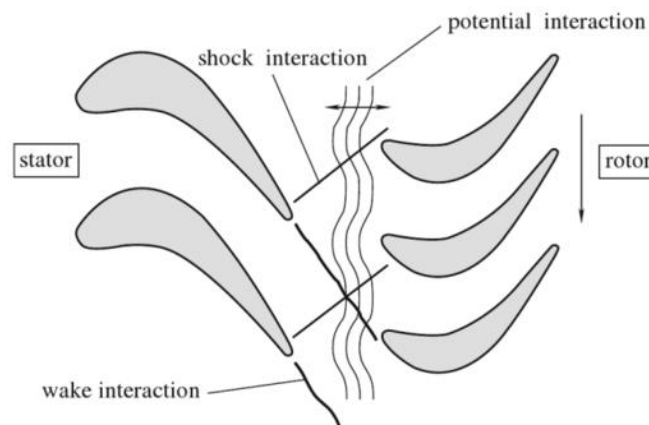


Figure 1.1 Unsteadiness of rotor and stator interaction RSI (Adameczyk 2000)

- Potential Interaction.

The flow in the channel of the distributor is periodically disturbed by the movable blades of the rotor. It is one of the main sources that generate pressure fluctuations. The existing pressure field between the crowns is modifying in time in function of the relative position that is adopted by the movable blades crown regard to the fixed. Each time a blade passes in front of successive stator channels, there are variations in the pressure field modify the upstream flow and the response of the machine. Thus the pressure peak will be reached when the guide vanes are fully open and one of the movable rotor blades is in line with a wicket gate trailing edge.

The essential operating parameter of the potential interaction that controls the intensity of the rotor-stator interactions is the clearance gap between the wicket gates below the rotor blade (Giesing 1968) [4-5], the passage among cascades and the speed rotation (interactions frequency).

- Wake Interaction.

A phenomenon associated with the presence of a stator upstream of the rotor is the generation of wakes which reach the rotor, getting a non-stationary flow because of non-uniform flux conditions at the entrance. The thickness of the boundary layers on the wicket gates trailing edge governs the speed variable distribution in the midst of the wakes. Consequently the rotor responds to that effect by inducing vibrations and decreasing the performance of the machine.

Under certain operating conditions, the flow can suffer separation of the boundary layer along the blade trailing edge due to the appearance of an adverse pressure gradient caused by the divergence geometry flow . This generates some typically three-dimensional turbulent structures called vortices which cause vibrations.

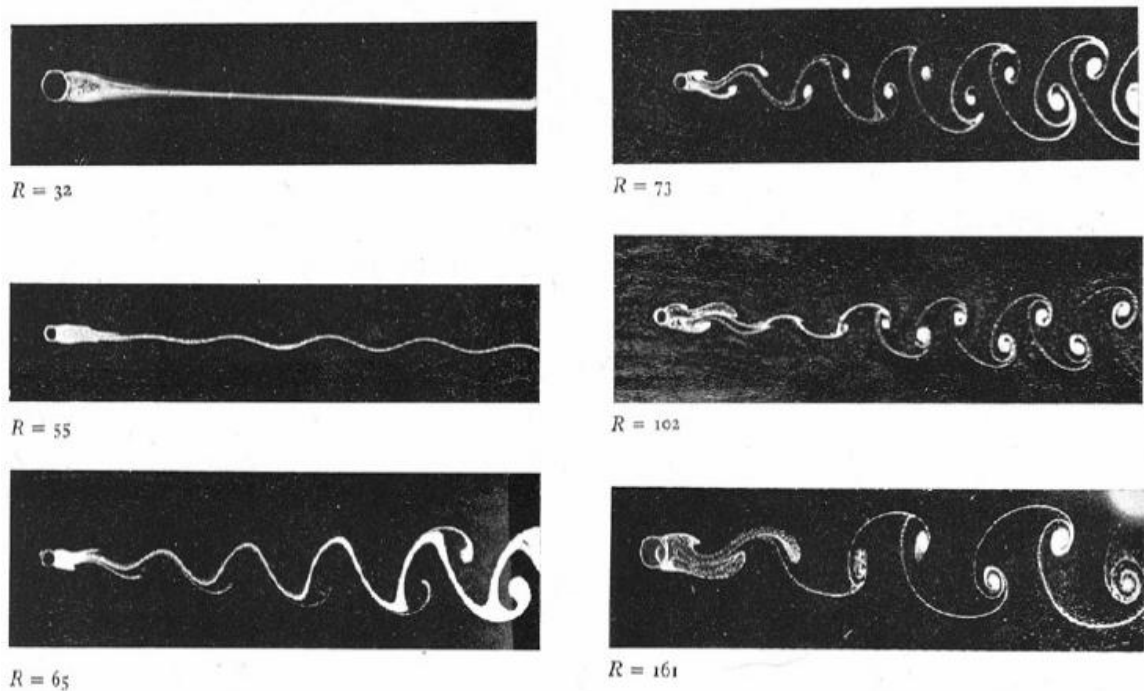


Figure 1.2 Streak lines in the wake behind a circular cylinder in a stream of oil (Homann 1936a)

Viscous effects are characteristic of this phenomenon as vortex shedding is given by shearing forces created due to the existence of a given velocity gradient. The velocity field outside the wake is higher than the internal one and this produces shearing stresses which induces flow spins . This effect depends entirely on the flow turbulence degree and thus of the number of Re. We can view the detail in the Figure 1.3 shown below.

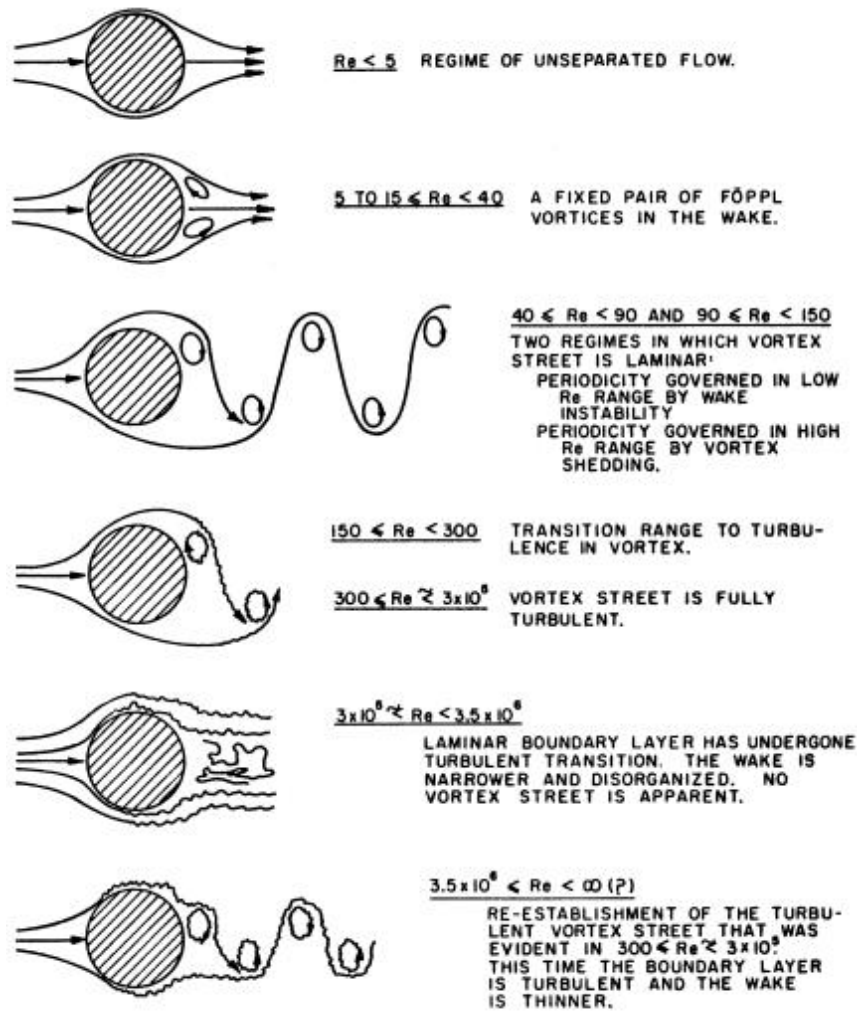


Figure 1.3 Regimes of fluid flow across smooth circular cylinders (Lienhard 1966) [6]

As a result of the vortex shedding phenomenon, the pressure distribution on the blade changes periodically, generating thereby a periodic variation in the blade force component. These force components can be divided into cross-flow direction (perpendicular to the flow) and in-line direction (parallel to the flow). The force perpendicular to the flow is called lift force (F_L) as long as the force parallel to the flow is called drag force (F_D). Because of the non-stationary flow both forces vary in time. Their corresponding dimensionless coefficients C_L and C_D can be written as shown below:

$$C_L = \frac{L(t)}{\frac{1}{2} \rho U^2 d} \quad (1.1)$$

$$C_D = \frac{D(t)}{\frac{1}{2} \rho U^2 d} \quad (1.2)$$

As it is shown in the Figure 1.4, when these shedding is not simultaneously generated throughout the vane (lock-off), the pressure derivation over the vane makes the resultant force be small and thereby has low excitation. However, when the vortex sheds alternatively (lock-in), the pressure derivation produces high oscillating forces. Consequently, this produces a sum of the excitation modules (frequencies), inducing structural vibrations and resonance which could generate mechanical failures on the system.

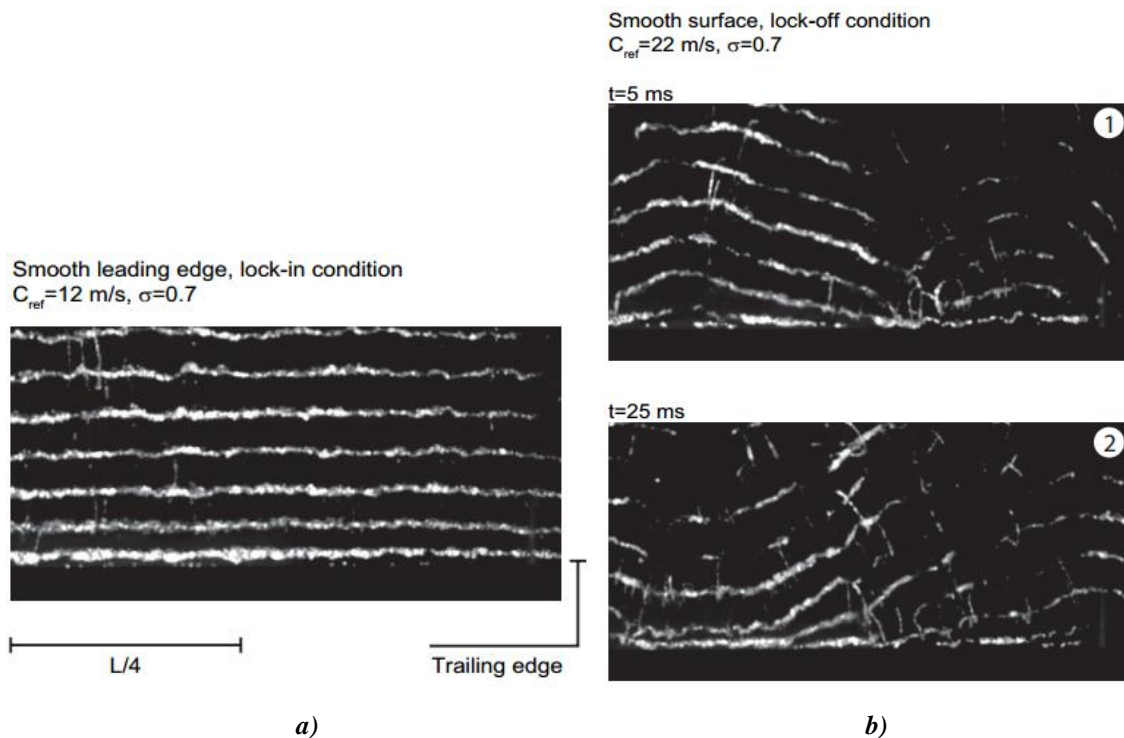


Figure 1.4 Top view of Von Kármán vortex street cavitation: a) Lock-in condition, b) Lock-off condition. (Ausoni P., Farhat M., Avellan F. 2007) [7]

- Shock interaction.

This effect is governed by unsteady flow and occurs only in incomprehensible flow turbomachines. The generated wake by the stator hits the rotor blade row downstream causing small vibrations.

1.1.2. State of the art

The first studies about the RSI, were focused on a cascade of blades that was attacked by a flow stream so that the blade line responded to a periodic perturbation on the input flow.

From the knowledge acquired by Von Karman in the study of the boundary layer (1921) [8], Von Kármán 1938 [9] and Sears 1939 [10], applied the bases to study the disturbances of a bi-dimensional flow on a flat plate. Later Kemp (1952) [11] provided his effort in obtaining an expression to evaluate the pressure on the flat plate in function of a flow with certain disturbances, and the length of the plate. The obtained expression included the function of Theodorsen (Silkowski, 2001) [12] and allowed to calculate the lift and drag forces and observe the response on the plate depending on the disturbances frequency.

In 1968, Horlock [13] extends the study including both horizontal and vertical components of the incident burst. Horlock concluded that from greater than 10° angles of the plate inclination in relation to the flow velocity average, the horizontal components of the disturbance become important.

The analytical and semi-analytical study solutions continued with the development of three-dimensional incompressible theories in the early 70s. The exact problem was solved by Graham (1970) [14] with infinite series for an infinite dimension blade. Filotas (1969) [15] y Mugridge (1971) [16] also suggested approximate solutions from certain disturbances. The next step was an extension towards compressible flow developed by Adamczyk (1974) [17] using numerical solutions for obtaining the non-stationary lift. At this time, Sears (1971) and Osborne (1971) [18] formulated simplified analytical solutions for the same two-dimensional compressible flow problem.

There have been other experimental studies that have highlighted the importance of RSI, such [2] y Dunn (1984). As well as contributions from Kemp y Sears (1955), Parker and Watson (1972) [19], Kerrebrock y Mikolajczak (1970) [20], Gilles y Hodson (1984) o Haldeman and Dunn (2000) [21].

With the birth of CFD techniques from the 70s, numerical methods started to be highlighted as the most widely used tool for studying the RSI. The main disciplines were: Aeromechanics and aeroelasticity, aeroacoustics and aerodynamics and fluid dynamics.

Since then, when numerical solutions of bi-dimensional channels under potential flow hypothesis were achieved, technology has been advancing through Eulerian codes (early 80s) and finally codes Navier-Stokes (90s). As major drivers of these developments are included Denton (1975), Ni (1988) y Dawes (1988) (Hirsch, 2003).

From the RSI numerical simulation point of view, it should be taken into account all the involved effects related to RSI as wake flow and the potential effect if is required a well modeling of the phenomena. A first step is the correct boundary layer modeling through the vane and of its trailing edge behind it. Many serious efforts have been done to obtain both experimental and numerical results to the boundary layer along some volumes (cylinders, profiles, ...) and to the trailing edge flow where the most amount of cases is used a cylinder.

Hwang and Yao (1997) [22] studied the behavior of the wake vortices created by a square cylinder placed in a laminar flow boundary layer. The calculations were made by solving the non stationary equations of Navier-Stokes with the finite volume method. Jordan and Ragab (1998) [23], and Doolan (2010) [24], carried out LES simulations in the circular cylinder wake which determined the velocity field there and non stationary induced forces. In his work Doolan, 2010, obtained numerically that the speed fluctuations were associated with the emergence of vortex pair and its explosion. As its shown in the experimental results of Brun et al., (2008) [25]. Ovchinnikov, et al. (2006) [26], they studied with DNS and LES the vortices of Von Karman in the circular cylinder wake as well as the induction effects in the transition produced in their interaction with the laminar boundary layer of a plate.

An experimental and numerical study in a NACA 0009 truncated profile was carried out by Vu et al., (2007) [27], in which he determined numerically the representative frequencies of the vortex shedding and the velocity profiles in the boundary layer with the help of SST model. At his work there was a comparison of the vortex shedding frequency when the boundary layer made a natural transition to turbulence and when the boundary layer was forced to move to laminar zone.

They found that when the transition to turbulence was forced on the profile, the SST model presented the best vortex shedding frequency results and when the transition was produced naturally, the best results were obtained with the SST model with transition. In his study were not used other turbulence models to determine the SST skills in determining the vortex shedding frequencies.

Munch et al, (2010) [28], simulated the forces due to the fluid interaction and the structure of an oscillating NACA0009 profile and obtained an excellent agreement when they compared them with the obtained data in a hydrodynamic tunnel experiment. They performed a mesh sensitivity study and time step and they determined the pressures and the hydrodynamic torque on the profile because its oscillation. In his work only they used the SST turbulence model in a 2D mesh and did not determine the velocities at the boundary layer and in the wake.

There have been studied several numerical studies of flow in hydraulic machines. Shi et al., (2001) [29], determined numerically the pressure fluctuations in a pump due to the interaction between the rotor and the stator. The results obtained in a RANS simulation, collected the potential and wake effects in the pressure fluctuation. 2D and 3D pump simulations were carried out. However, the results did not show great differences because the potential effects type predominated to the effects of the wake. In his work used only the model k- ϵ . Wang et al., (2001) [30], also determined pressure

fluctuations with the 2D same pump, using a vortex method and they obtained similar results to [29]. In their works Shi and Wang, studied only the behaviour of the pump working at design conditions.

Zhang et al., (2005) [31], determined experimentally the hydrodynamic forces in a pump with the same number of blades in the rotor as in the stator. The work shows that the forces of the fluid in the rotor were smaller than with other combinations, but the pressure fluctuations were higher. They performed a numerical study of the pump in 3D, using a RANS code and the k- ϵ model by using a vortex method 2D. They obtained better results with k- ϵ model. He worked only at design conditions and with a RANS model.

Byskov et al., (2003) [32], carried out an experimental and numerical study about a centrifugal pump rotor without diffuser working on design and partial load conditions. Velocities in the pump rotor, made with LES, presented good results in design and partial load conditions. They also made a stationary study to the same pump using Baldwin-Lomax and Chien k- ϵ RANS models, in order to compare the obtained velocities with experimental velocities values. They obtained that with partial load conditions, the RANS models did not reproduce complicated flow in the two rotor channels, where the flow stagnating occurred. In his work Byskov did not do any study of pressure fluctuation of the pump rotor, nor an unsteady flow study with a RANS model.

Guleren i Pinarbasi, (2004) [33], studied a centrifugal pump with diffuser working at different load conditions. The pressures among the rotor outlet and the stator inlet were determined in the space as well as the pump flow patterns with the k- ϵ model. They obtained that stagnation occurred in the stator, close to the volute cut water and the effect was increased when they were working at partial load conditions. Also, at partial load conditions jet flow and stagnation channels were alternately generated in the stator. In their study they did not determine the frequencies associated with the RSI effects on the diffuser.

González et al. (2006) [34] carried out an experimental and numerical study about a pump. They determined pressure fluctuations and radial forces in the volute of a centrifugal pump without diffuser. The work was performed with two different rotor size and making the pump work in different load conditions. Numerically, only the k- ϵ model were used and they did not determine the velocity fields of the pump.

Feng et al., (2007) [35] studied a pump with diffuser working in different operating conditions, different gap spaces between the rotor and the stator, and different number configurations of rotor blades and stator vanes. They used a 3D mesh with a wall functions treatment. They obtained the velocities at the rotor outlet, the pressure fluctuations and hydrodynamic forces on the stator vanes using the SST k- ω model, but he did not determine the RSI interaction frequencies between the rotor and the stator.

Vasudeva et al., (2009) [36] studied numerically the behavior of a fan when working with different gap separations between the impeller blades and diffuser. Per each spacing configuration, they determined the efficiencies and the pressure fluctuations. In their work they used a k- ϵ model and they did not determine the RSI interaction frequencies.

In other work Feng et al., 2011, made an experimental and numerical study about a radial pump with diffuser in which they got a good correlation of the obtained results with the SST k- ω model, of the relative radial and tangential velocities among the rotor and the diffuser. In the results they collected the potential effect of the rotor blades and the stator wicket gates interaction as well as the wake effects. However, they did not determine the pressure fluctuations. Finally they concluded that with high quality meshes and with an appropriate turbulence model is possible to prevent the complex flow in the pump diffuser.

Cavazzini et al. 2011 [38], carried out a numerical and experimental acoustic and fluid dynamic studies about the large scale instabilities in a centrifugal pump with diffuser. The goal was to identify and characterize the developed instabilities in the flow inside turbomachinery. As well as to determine

the correlation between the fluid dynamics and the noise generated. For simulating the turbulence they used DES model with which obtained a good frequency spectrum characterization due to pressure pulsations in the diffuser, working at partial load and overload conditions.

1.2. Computational fluid dynamics

1.2.1. *Generalities and applications*

Fluid dynamics is the science that studies the movement of a fluid. This has always used two action ways: theory and experiments, and it hasn't been until the ends of the twentieth century that started the development of a third way: by numerical methods: CFD.

The development of these numerical simulations has represented a breakthrough in the engineering world, using the results extracted from CFD for improving all kinds of conceptual designs, improved product details, as well as quick access in the troubleshooting or the need for redesign.

The main advantages of CFD regarding to experimental studies are:

- a) Reduction of deadlines and new design costs.
- b) Possibility of studying systems under dangerous conditions or outside of the work conditions.
- c) Possibility of studying systems in which an experiment is difficult to control.
- d) Results with a large number of data.

Currently, in industrial level are many applications in which the use of CFD is essential for better product development. The technique of numerical methods is presented in almost all fields of engineering. Some examples would be:

- Mechanical Engineering: study of turbomachine, mold filling problems, ...
- Civil Engineering: force analysis of off shore structures, structural analysis of dams, ...
- Aeronautical Engineering: optimization of wing profiles, aerodynamic studies on airplanes, ...
- Naval Engineering: Hydrodynamic studies ships, ...
- Biomedical Engineering: analysis of blood flow or pressure fields in the arteries, ...

1.3. CFD of RSI in turbomachinery

The present paper focuses the study of RSI in a turbomachine, particularly in a Francis pump-turbine in turbine operating conditions. The nature of the flow inside it is turbulent and nonstationary due to the interaction of the wake and therefore it is not easy to use tools of computational fluid dynamics (CFD) to fix the flow structure. Currently, the use of CFD helps to know in detail the structure of the flow in RSI. Due to the flow conditions, a convenient choice of turbulence is really important for obtaining good results in the CFD (Coussirat, 2003).

The current trend in hydraulic machines is to make lighter designs, involving a reduction in the thickness of the blades, that reduce its resistance and therefore are more sensitive to excitation. That is why one of the main current aims in the design of hydraulic machines is to reduce fluid dynamic excitation, reducing vortex shedding and achieve to break down consistency in its shedding to prevent high vibrations.

Moreover, the number of blades on a turbine / pump is an important parameter in the determination of the rotor flow. The ideal situation would be one in which the flow leded well due to a large number of blades, but this would increase frictional losses and decrease efficiency. Reducing the number of blades reduces the friction losses, but this increase the flow vorticity on the rotor channel, causing flux recirculation. Usually the choice of the rotor blades numbers presents a balance between losses and rotation leading to high efficiency values. Rotor configurations with reduced number of blades have their applications when the flow to transport has solid particles in suspension and require large channels.

With the help of numerical codes we can understand more deeply the behavior that have the characteristic effects of the RSI phenomena either vortex shedding (Figure 1.6) or the wake interaction (Figure 1.5) and thus design more efficient prototypes.

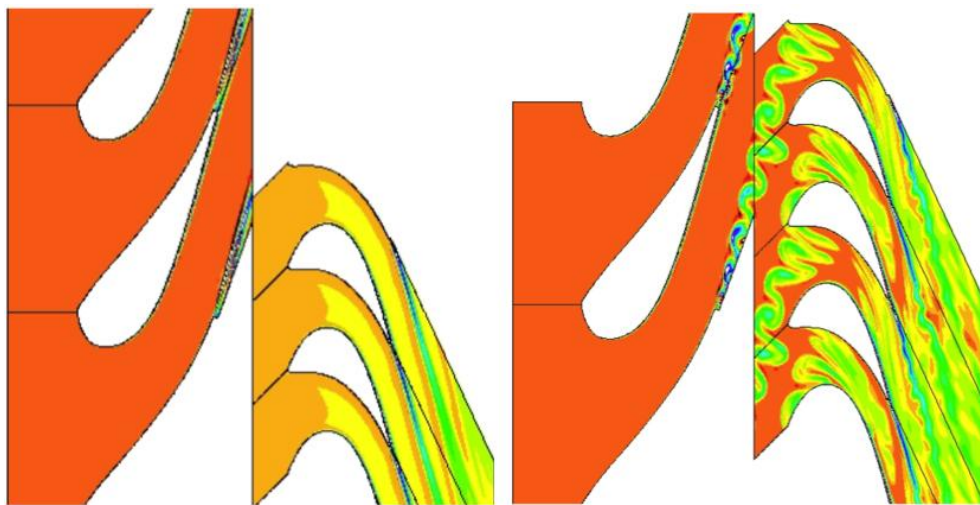


Figure 1.5 Wake interaction between rotor and stator. (John D. Denton, ASME Turbo Expo, 2010) [39]

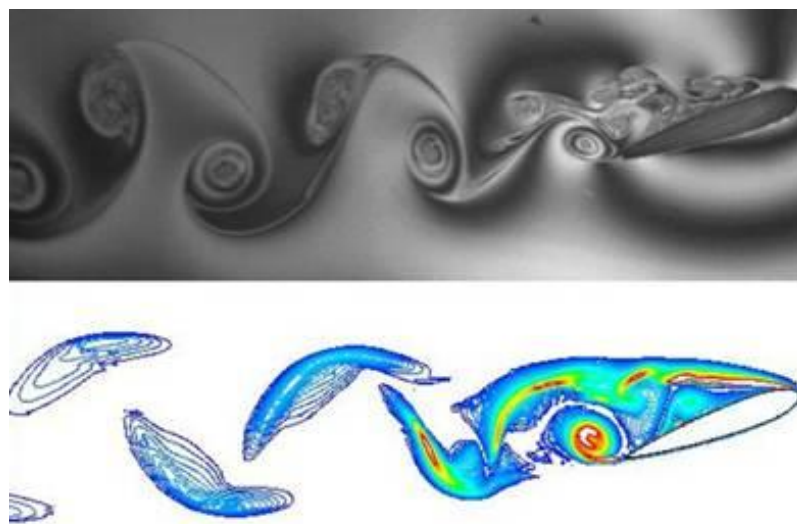


Figure 1.6 Airfoil wake and vortex shedding. LES Simulation and Soap-Film Experiments [Concordia University, Department of Mechanical and Industrial Engineering, Research Group]

In order to capture how varies the pressure field values and velocities that take place in the RSI phenomenon due to the potential effect on a turbomachine it is highly recommended to allocate monitors on one of the stator channels as shown in Figure 1.7.

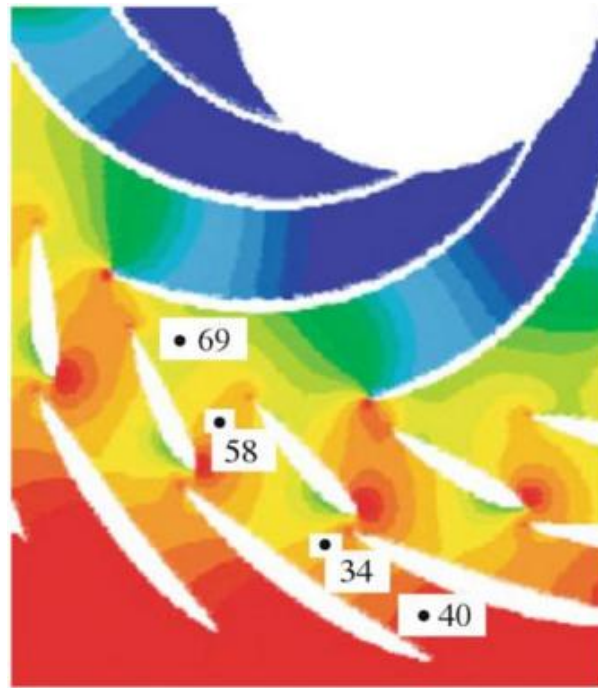


Figure 1.7 Locations of the monitoring points in the distributor channel [1]

1.4. Objective and project scope

The effects generated by the RSI of a turbomachine can cause great destroys on the blades of it or can even damage the installation. The consecutive stress-relaxation cycles caused by the pressure pulses present in each alignment of the rotor and stator blades can potentially cause fatigue failure.

That is why the main purpose of this project is to perform an approximate numerical study in order to capture the characteristic effects involved in the RSI phenomena, as well as determine the fundamental frequencies and its harmonics, present in our study case. Thus, in future projects, it will be possible to propose other alternative geometries which maybe reduce these harmful interactions.

1.5. Limitations

For carrying out this project we must take into account certain limitations that hinder the resolution of the problem to deal with. First of all will be highlighted the complexity of the software usage due to the large number of tools and possibilities that offers to us. As mentioned in the preface, it is why in the beginning of the project it was needed to invest more than three months in the self-learning based in video tutorials, guides and manuals. Another point to remark not less important as the previous is that we cannot lose sight of is the limitation of our PC features as this will directly affect the mesh quality and therefore the reliability and accuracy of the results.

CHAPTER 2. FLOW MODELING

The CFD solves the Navier-Stokes equations, of the energy and the material balance. These differential equations are solved along many control volumes, which are infinitesimal elements in which the geometry is divided. All together conform the entire mesh where these equations will be solved. The magnitude and number of all these control volumes is one of the determining factors in achieving good numerical results. Once the boundary conditions of the problem are defined, are numerically solved the flow energy balances. The process is performed by iterating loop, which can reduce the error until achieving satisfactory results.

The current commercial CFD codes are based on three different ways to space discretizing, finite difference (FD), finite volume (VF) and finite element (FE). The finite differences have a major drawback that only allow structured meshes and therefore cannot be applied to complex geometries which non structured meshes are required, for this reason currently finite volumes and finite element methods are the most used as they let us to work with both structured and non structured meshes.

ANSYS Fluent v15.0, the CFD software we will use works with the method of finite volumes. It is an alternative method to the finite difference and finite element and it was originally introduced by McDonald (1971).

ANSYS Fluent provides comprehensive modeling capabilities for a wide range of incompressible and compressible, laminar and turbulent fluid flow problems. Steady-state or transient analyses can be performed. A broad range of mathematical models for transport phenomena is combined with the ability to model complex geometries.

To permit modeling of fluid flow and related transport phenomena in industrial equipment and processes, various useful features are provided. These include porous media, lumped parameter periodic stream wise flow and heat transfer, swirl, moving reference frame models and dynamic mesh model. The moving reference frame family of models includes the ability to model single or multiple reference frames.

Other very useful group of models in ANSYS Fluent is the set of free surface and multiphase flow models, various models of heat transfer as well as other models that are very useful for reacting flow applications.

Turbulence models are a vital component of the ANSYS Fluent suite of models. have a broad range of applicability, and they include the effects of other physical phenomena. Particular care has been devoted to addressing issues of near-wall accuracy via the use of extended wall functions and zonal models.

In our particular case, which attempts to model the flow through the interior of a Francis turbine, we will consider a model of incompressible turbulent flow through a non-stationary analysis. We will use the method of sliding mesh, which is a particular case of dynamic mesh model in which all of the

boundaries and the cells of a given mesh zone move together in a rigid-body motion. In this situation, the nodes of the mesh move in space but the cells, defined by the nodes do not deform. This model is useful for modeling multiple stages in turbomachinery applications and is typical for studies where is desired to model the RSI between a moving blade and a stationary vane in a turbine.

2.1. Fluid mechanics governing equations

By applying the Reynolds's transport theorem to the mass, the amount of movement, the kinetic momentum and the energy to a infinitesimal control volume, are obtained three differential relationships that govern the fluid dynamics. The equation of the kinetic momentum is completely canceled due to the symmetry of the shearing forces. Moreover the energy equation will not be considered for not being relevant in this study. In this section is presented the governing equations for a laminar flow in a inertial reference frame.

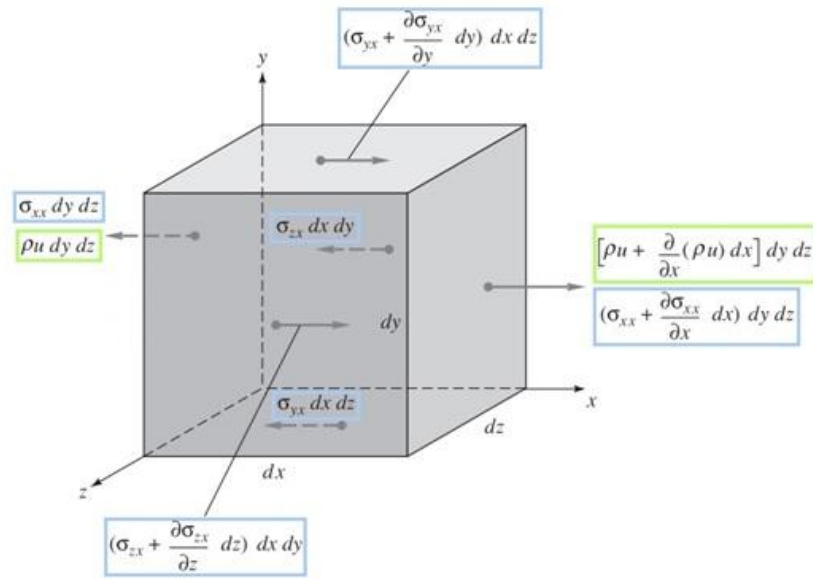


Figure 2.1 X component of the parameters involved in the infinitesimal control volume

2.1.1. Mass conservation

According to the Reynolds's transport theorem, the relation of the mass conservation can be written in the following way:

$$\left(\frac{dm}{dt}\right)_{\text{sis}} = \left(\int_{VC} \frac{\partial \rho}{\partial t} dV\right) + \sum_i (\rho_i C_i A_i)_{\text{sal}} - \sum_i (\rho_i C_i A_i)_{\text{ent}} = S_m \quad (2.1)$$

The source S_m is the mass added to the continuous phase from the dispersed second phase (for example, due to vaporization of liquid droplets) and any user-defined sources.

Being an infinitesimal control volume, the volume integral is reduced to a differential term:

$$\int_{VC} \frac{\partial \rho}{\partial t} dV = \frac{\partial \rho}{\partial t} dx dy dz \quad (2.2)$$

As we see in the Figure 2.1 for the mass conservation, the surface of infinitesimal control volume contains six faces crossed by three inlet mass flows and three outlet mass flows that they are detailed below:

Face	Inlet mass flow	Outlet mass flow
x	$\rho u \, dy \, dz$	$\left[\rho u + \frac{\partial}{\partial x}(\rho u) dx \right] dy dz$
y	$\rho v \, dx \, dz$	$\left[\rho v + \frac{\partial}{\partial y}(\rho v) dy \right] dx dz$
z	$\rho w \, dx \, dy$	$\left[\rho w + \frac{\partial}{\partial z}(\rho w) dz \right] dx dy$

Table 2.1 Mass flow relation at the inlet and the outlet for the conservation of mass

Grouping terms and simplifying we arrive at the differential equation of continuity for infinitesimal control volume:

$$\frac{\partial \rho}{\partial t} + \frac{\partial}{\partial x}(\rho u) + \frac{\partial}{\partial y}(\rho v) + \frac{\partial}{\partial z}(\rho w) = \frac{\partial \rho}{\partial t} + \nabla \cdot (\rho \mathbf{C}) = S_m \quad (2.3)$$

2.1.2. Conservation of the amount of movement

For the same elemental control volume of Figure 2.1., here Reynolds's transport theorem will take the following form:

$$\frac{d}{dt}(\mathbf{mC})_{\text{ sist }} = \sum \mathbf{F} = \left(\int_{V_C} \frac{\partial}{\partial t} \rho \mathbf{C} dV \right) + \sum_i (\dot{m}_i \mathbf{C}_i)_{\text{ sal }} - \sum_i (\dot{m}_i \mathbf{C}_i)_{\text{ ent }} \quad (2.4)$$

We will divide the analysis into two equations:

1. Second member of the equation (2.4):

Being an infinitesimal volume control, the volume integral is reduced to the differential term:

$$\int_{V_C} \frac{\partial}{\partial t} (\rho \mathbf{C}) dV = \frac{\partial}{\partial t} (\rho \mathbf{C}) dx \, dy \, dz \quad (2.5)$$

Analogously to the previous case, as we see in Figure 2.1 for the momentum conservation, the control surface of infinitesimal volume contains six faces crossed by three inlet flows and three outlet flows that are detailed below:

Face	Inlet flow	Outlet flow
x	$\rho u \mathbf{C} \, dy \, dz$	$\left[\rho u \mathbf{C} + \frac{\partial}{\partial x}(\rho u \mathbf{C}) dx \right] dy dz$
y	$\rho v \mathbf{C} \, dx \, dz$	$\left[\rho v \mathbf{C} + \frac{\partial}{\partial y}(\rho v \mathbf{C}) dy \right] dx dz$
z	$\rho w \mathbf{C} \, dx \, dy$	$\left[\rho w \mathbf{C} + \frac{\partial}{\partial z}(\rho w \mathbf{C}) dz \right] dx dy$

Table 2.2 Flow relation at the inlet and outlet for the conservation of momentum

Grouping terms and simplifying:

$$\begin{aligned}
 dx dy dz \left[\frac{\partial}{\partial t}(\rho C) + \frac{\partial}{\partial x}(\rho u C) + \frac{\partial}{\partial y}(\rho v C) + \frac{\partial}{\partial z}(\rho w C) \right] \\
 = dx dy dz \left[C \left(\frac{\partial \rho}{\partial t} + \nabla \cdot (\rho C) \right) + \rho \left(\frac{\partial C}{\partial t} + u \frac{\partial C}{\partial x} + v \frac{\partial C}{\partial y} + w \frac{\partial C}{\partial z} \right) \right]
 \end{aligned} \quad (2.6)$$

The first term in parenthesis of the second member is canceled as by definition is the equation of continuity. Thus the second member of the equation (2.4) is simplified to:

$$\sum \mathbf{F} = \rho \frac{dC}{dt} dx dy dz \quad (2.7)$$

2. First member of the equation (2.4):

The element undergoes two types of forces in each of the three axes:

- a) Surface forces: sum of hydrostatic pressure and viscous forces acting directly on the control surface of the fluid element.
- b) Volumetric forces: centrifugal force, gravity, Coriolis, electromagnetic forces, which act directly on the mass of the element volume.
- c) External forces: arise, for example, from the interaction with dispersed phases. It can also be considered as a source of other forces defined by the user.

$$\sum \mathbf{F} = d\mathbf{F}_{vol} + d\mathbf{F}_{sup} = d\mathbf{f} + (d\mathbf{F}_p + d\mathbf{F}_{viscosa}) + d\mathbf{F}_{ext} \quad (2.8)$$

Concerning to surface forces on one hand we have viscous forces τ . We can represent those grouped in the following matrix of the tensor σ .

$$\sigma_{ij} = \begin{bmatrix} \sigma_{xx} & \sigma_{yx} & \sigma_{zx} \\ \sigma_{yx} & \sigma_{yy} & \sigma_{yz} \\ \sigma_{zx} & \sigma_{zy} & \sigma_{zz} \end{bmatrix} = \begin{bmatrix} -p + \tau_{xx} & \tau_{yx} & \tau_{zx} \\ \tau_{yx} & -p + \tau_{yy} & \tau_{yz} \\ \tau_{zx} & \tau_{zy} & -p + \tau_{zz} \end{bmatrix} \quad (2.9)$$

They require two subscripts to define each component. The usual notation of the two τ_{ij} suffixes are applied to indicate the direction of such efforts. The suffix j indicates the viscous forces acting in that direction on a normal surface to the axis i .

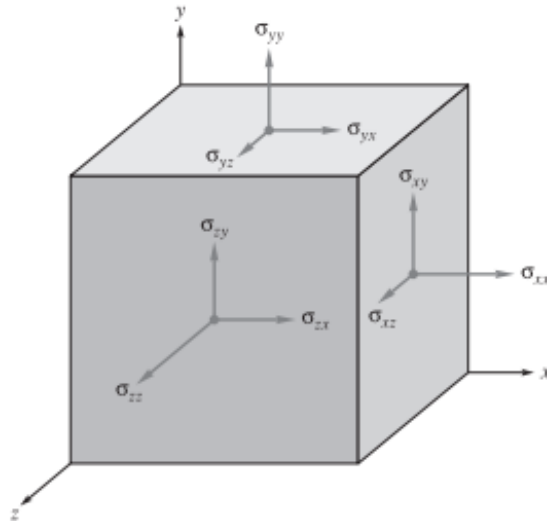


Figure 2.2 Efforts notation

For the x direction, the surface force balance will be:

Face	Inlet flow	Outlet flow
x	$-\sigma_{xx} dy dz$	$\left[\sigma_{xx} + \frac{\partial \sigma_{xx}}{\partial x} dx \right] dydz$
y	$-\sigma_{yx} dx dz$	$\left[\sigma_{yx} + \frac{\partial \sigma_{yx}}{\partial y} dy \right] dx dz$
z	$-\sigma_{zx} dx dy$	$\left[\sigma_{zx} + \frac{\partial \sigma_{zx}}{\partial z} dz \right] dx dy$

Table 2.3 Surface forces relation in the inlet and outlet for the x-direction

Grouping terms and simplifying:

$$dF_{x,sup} = \left[\frac{\partial \sigma_{xx}}{\partial x} + \frac{\partial \sigma_{yx}}{\partial y} + \frac{\partial \sigma_{zx}}{\partial z} \right] dx dy dz = \left[-\frac{\partial p}{\partial x} + \frac{\partial}{\partial x}(\tau_{xx}) + \frac{\partial}{\partial y}(\tau_{yx}) + \frac{\partial}{\partial z}(\tau_{zx}) \right] dx dy dz \quad (2.10)$$

In the same way we can obtain surface forces for directions y y z:

$$dF_{y,sup} = \left[-\frac{\partial p}{\partial y} + \frac{\partial}{\partial x}(\tau_{xy}) + \frac{\partial}{\partial y}(\tau_{yy}) + \frac{\partial}{\partial z}(\tau_{zy}) \right] dx dy dz \quad (2.11)$$

$$dF_{z,sup} = \left[-\frac{\partial p}{\partial z} + \frac{\partial}{\partial x}(\tau_{xz}) + \frac{\partial}{\partial y}(\tau_{yz}) + \frac{\partial}{\partial z}(\tau_{zz}) \right] dx dy dz \quad (2.12)$$

In this way we can obtain an vectorial expression for the net surface force per volume unit:

$$d\mathbf{F}_{sup} = [-\nabla p + d\mathbf{F}_{viscosa}] dx dy dz = [-\nabla p + \nabla \cdot \boldsymbol{\tau}_{ij}] dx dy dz \quad (2.13)$$

where,

$$\boldsymbol{\tau}_{ij} = \begin{bmatrix} \tau_{xx} & \tau_{yx} & \tau_{zx} \\ \tau_{yx} & \tau_{yy} & \tau_{yz} \\ \tau_{zx} & \tau_{zy} & \tau_{zz} \end{bmatrix} \quad (2.14)$$

On the other hand we have the volumetric character forces. We will denote \mathbf{f} the vectorial force per mass unit that acts in the three directions of the element at issue:

$$dF_{x,vol} = \rho f_x dx dy dz \quad (2.15)$$

$$dF_{y,vol} = \rho f_y dx dy dz \quad (2.16)$$

$$dF_{z,vol} = \rho f_z dx dy dz \quad (2.17)$$

In this way we can obtain a vectorial expression for the resultant volumetric force per mass unit:

$$d\mathbf{F}_{vol} = \rho \mathbf{f} dx dy dz \quad (2.18)$$

Referring to external forces, we will denote \mathbf{F}_{ext} vector force per volume unit acting in the three directions of the element at issue:

$$dF_{ext,x} = F_{ext,x} dx dy dz \quad (2.19)$$

$$dF_{ext,y} = F_{ext,y} dx dy dz \quad (2.20)$$

$$dF_{ext,z} = F_{ext,z} dx dy dz \quad (2.21)$$

Analogously to the previous case, we can obtain a vectorial expression for the net external force per volume unit:

$$d\mathbf{F}_{ext} = \mathbf{F}_{ext} dx dy dz \quad (2.22)$$

Substituting the equations (2.13) and (2.18) into equation (2.7) we obtain the momentum equation in differential form:

$$\rho \mathbf{f} - \nabla p + \nabla \cdot \boldsymbol{\tau}_{ij} + \mathbf{F}_{ext} = \rho \frac{d\mathcal{C}}{dt} \quad (2.23)$$

- Newtonian fluid case: Navier-Stokes equations.

For Newtonian fluids, viscous forces are defined by deformation velocity and the coefficient of viscosity as it follows:

$$\begin{aligned} \tau_{xx} &= 2\mu \frac{\partial u}{\partial x} & \tau_{yy} &= 2\mu \frac{\partial v}{\partial y} & \tau_{zz} &= 2\mu \frac{\partial w}{\partial z} \\ \tau_{xy} = \tau_{yx} &= \mu \left(\frac{\partial u}{\partial y} + \frac{\partial v}{\partial x} \right) & \tau_{xz} = \tau_{zx} &= \mu \left(\frac{\partial w}{\partial x} + \frac{\partial u}{\partial z} \right) \\ \tau_{yz} = \tau_{zy} &= \mu \left(\frac{\partial v}{\partial z} + \frac{\partial w}{\partial y} \right) \end{aligned} \quad (2.24)$$

In this way, for viscous and incompressible flows, the equation (2.19) can be rewritten in the following way:

$$\rho f_x - \frac{\partial p}{\partial x} + \mu \left(\frac{\partial^2 u}{\partial x^2} + \frac{\partial^2 u}{\partial y^2} + \frac{\partial^2 u}{\partial z^2} \right) + F_{ext,x} = \rho \frac{du}{dt} \quad (2.25)$$

$$\rho f_y - \frac{\partial p}{\partial y} + \mu \left(\frac{\partial^2 v}{\partial x^2} + \frac{\partial^2 v}{\partial y^2} + \frac{\partial^2 v}{\partial z^2} \right) + F_{ext,y} = \rho \frac{dv}{dt} \quad (2.26)$$

$$\rho f_z - \frac{\partial p}{\partial z} + \mu \left(\frac{\partial^2 w}{\partial x^2} + \frac{\partial^2 w}{\partial y^2} + \frac{\partial^2 w}{\partial z^2} \right) + F_{ext,z} = \rho \frac{dw}{dt} \quad (2.27)$$

2.2. Turbulence models

Prandtl in 1904 showed that the friction effects within the fluid are only present at a very thin layer close to solid surfaces called boundary layer and the rest of the flow field can be analyzed with Euler and Bernoulli equations. If the velocity in a fluid is high enough, as the time proceed the flow in this layer undergoes a disorder by generating eddies without any sense, leading to turbulent regime.

There are two radically different flow states that are easily identified and distinguished as laminar flow and turbulent flow.

The laminar flow is characterized by do not create cross currents of the velocity fields in space and time within they move. These flows are presented when the viscosity of the fluid is large enough to absorb any disturbances in the flow that can occur due to imperfections or boundary irregularities. These flows are produced in low Reynolds number values.

In contrast, the turbulent flows are characterized by large fluctuations, almost at random speed and pressure in space and time. These fluctuations arise from instabilities that grow to non-linear interactions that cause more and more subtle turns that eventually dissipate (in heat) through the action of viscosity. The turbulent flows occur at high Reynolds numbers values.

The most amount of fluids have a chaotic nature, unpredictable. In recent decades has been able to predict the behavior of fluids in motion by numerical methods in an approximate way.

The CFD tools can manipulate laminar flows easily, but it is impossible to solve turbulent flows without having to resort the use of turbulence models. It does not exist a universal turbulence model and the CFD solution of turbulent flow depends directly on the appropriate turbulence model in each application. In spite of this limitation, the current turbulence models produce good results for many engineering problems nowadays.

The approaches to solve the equations that govern a turbulent flow field can be divided into different classes: Reynolds Averaged Navier Stokes (RANS), Scale-Resolving-Simulation (SRS) i Direct Numerical Simulations (DNS).

1. In fluent software there are different turbulence models options that we can choose. These are RANS models and SRS models.
2. RANS turbulence methods to FLUENT:
 - a) Spallart-Almaras (1 eqn)
 - b) K-epsilon (2 eqn)
 - c) K-omega (2eqn)
 - d) Transition k-kl-omega (3 eqn)
 - e) Transition SST (4 eqn)
 - f) Reynolds Stress (7 eqn)
3. SRS turbulence methods to FLUENT:
 - a) Scale-Adaptative-Simulation (SAS)
 - b) Detached Eddy Simulation (DES)
 - c) Large Eddy Simulation (LES)

Of the three methods mentioned above, the one we have implemented is the RANS as it is offering a better relation of computational cost versus reliability. In our case, after several tests, we observed that within the RANS method, the turbulence model that best suits our study is the Spallart-Almaras because it offers a more realistic and reliable results regarding to the turbulence phenomena.

2.2.1. Reynolds Averaged Navier Stokes (RANS)

When cases of non-stationary flows are solved by CFD, the Navier-Stokes equations for turbulent flows in complex geometries and large Reynolds numbers, cannot solve the smallest movements magnitude due to the high computational cost. The averages of Reynolds (Reynolds-averaging) can be used to make the Navier-Stokes equations treated in a way that small turbulence fluctuations are not simulated directly. This method introduces additional terms to the equations to be modeled, in order to close the unknown variables.

The time average of the Navier Stokes equations leads to RANS equations (Reynolds Averaged Navier Stokes equations) that govern the flow average quantities transport, where the full range of turbulence scales are modeled. The model based on the RANS approach greatly, reduces the computational forces and is widely adapted to the practical engineering applications. It is available a wide range of closing models, including the Spalart-Allmaras, the RSM, the k- ϵ , the k- ω and their variants.

The RANS equations are often used to solve time dependent flows, in which instabilities can be externally imposed (for example conditions of non stationary contour or sources), or the same flow

(for example vortex shedding, flow instability with frequencies lower than those are used for the temporary average Navier Stokes equations, implying lower frequencies regarding to the vortex / "energetic" and "dissipative" swirls).

- Spallart-Almaras

The Spalart-Allmaras model (Spalart and Aymaras, 1992) is a one simple equation model the transport of the kinematic eddy viscosity equation. The model was designed specifically for aerospace applications in flows to the walls and has been demonstrated that gives good results in boundary layers subjected to adverse pressure gradients. Also it is gaining in popularity for applications in turbomachines.

In its original form the Spalart-Allmaras model is effectively a low Reynolds number model, requiring properly resolve the viscous boundary layer area. This could be the best choice for simulations relatively unsuitable with medium size meshes which good results of turbulent flow are not critical. On the other hand the transported variable gradients near the wall are much smaller than the transported variable gradients of k - ϵ and k - ω models. That could make the model be more sensible to the numerical errors when only a few layers near the wall are used. Furthermore one equation models are criticized for its inability to accommodate quickly to the changes in the large eddies scales.

CHAPTER 3. METHODOLOGY

All commercial CFD software, are made by four different modules where the different areas of the process will be developed (see Figure 3.1).

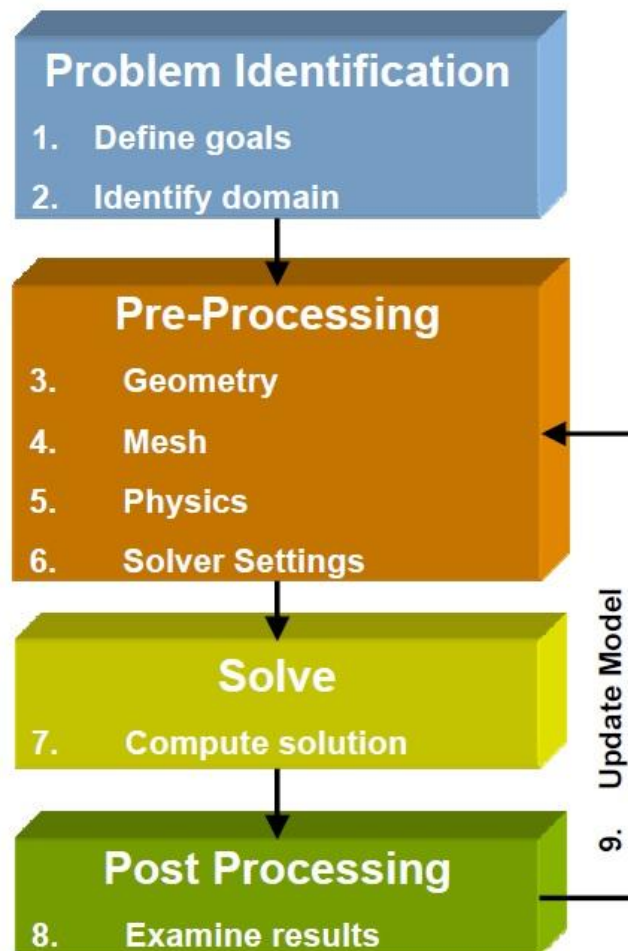


Figure 3.1 Diagram of the methodology to follow

For carrying out numerical simulations in CFD, the software used has been ANSYS Fluent 15.0, for the CAD creation of the CAD geometry SolidWorks 2012 and for the geometry treatment and meshing ANSYS ICEM CFD 15.0.

3.1. Problem identification

Previously the turbine geometry was done in other software and later was exported to .igs format in which was given to us. During the export of a particular IGES format a significant loss of information is produced and that is why we had to modify the geometry until to achieve the desired model and as much like the original.

The interest computational domain (Figure 3.2) consists only with the rotor and the stator. This is because, as has been introduced in Chapter 1, the RSI phenomenon to study happen in the area between both. The rest of the typical Francis turbine effects will not take part in this project for not being relevant.

Thus the flow will enter to the domain through the stator periphery with the arrow direction of the guide vanes towards the rotor center. The vortices and chaotic effects that would take place at the entrance of the draft tube will not be considered for not taking relevant importance in this paper.

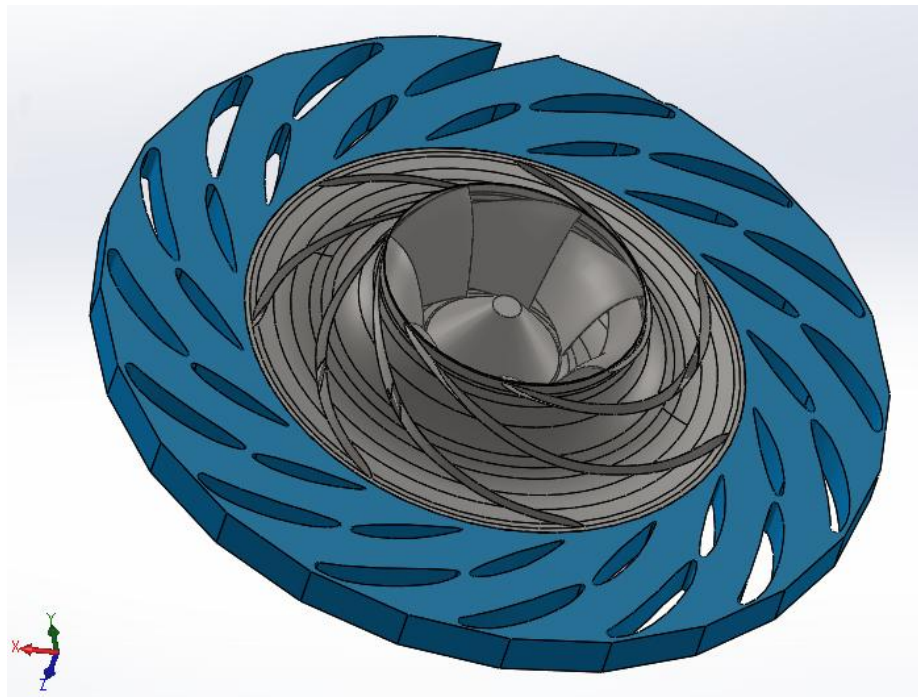


Figure 3.2 Computational domain

3.2. Pre-processing

Having defined the problem, we will start from the pre-processing creating the CAD geometry. Unnecessary items that could complicate the subsequent meshing will not be considered. We should see also if the problem could be simplified from 3D to 2D or to reduce the geometry due to symmetry. Then will be introduced the geometry mesh to study and in the end a solver setup will be defined.

3.2.1. CAD Geometries

Due to the potential effect and the wake effect practically it is not affected by the vertical axis, to simplify the work without losing almost precisely effect we will focus on a 2D plane of a fully qualified domain rotor obtaining in this way an extruded two-dimensional model of the fully qualified domain, as well as it is shown in Figure 3.3. The rotor is made by 7 rotor blades.

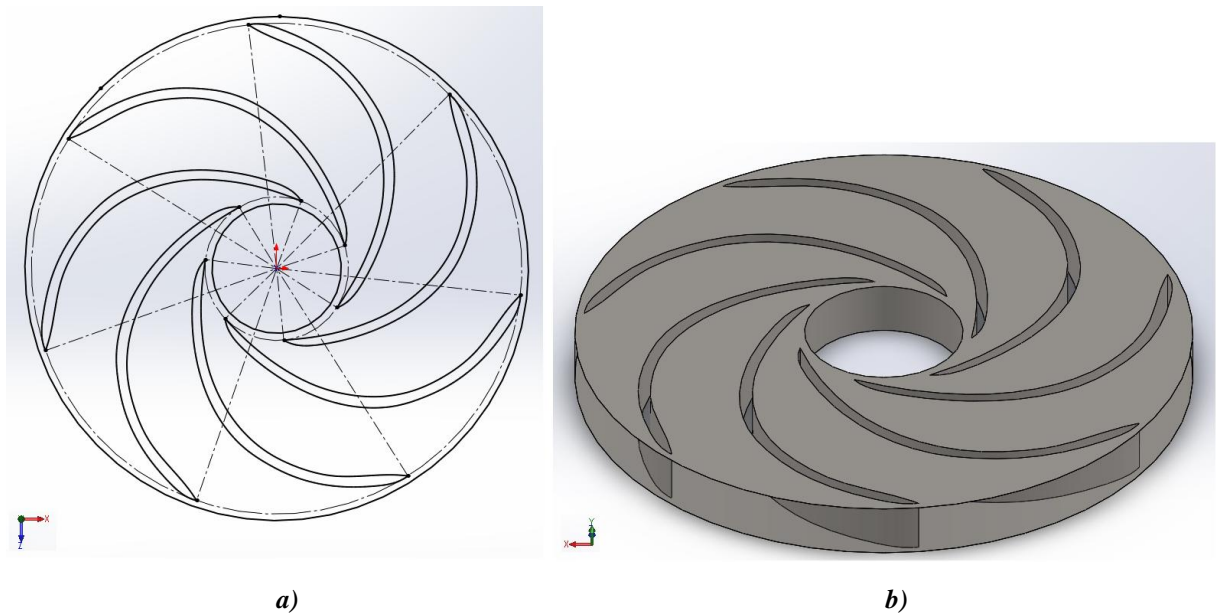


Figure 3.3 a) 2D sketch of the rotor (top view), b) Full rotor extruded

By circular symmetry to simplify the subsequent mesh and as it is shown in Figure 3.4 the geometry stator has been reduced to a portion of 180° . The complete stator is made by 16 guide vanes and 16 wicket gates. The defined computational portion by periodicities will be made by 8 guide vanes and 8 fixed blades.

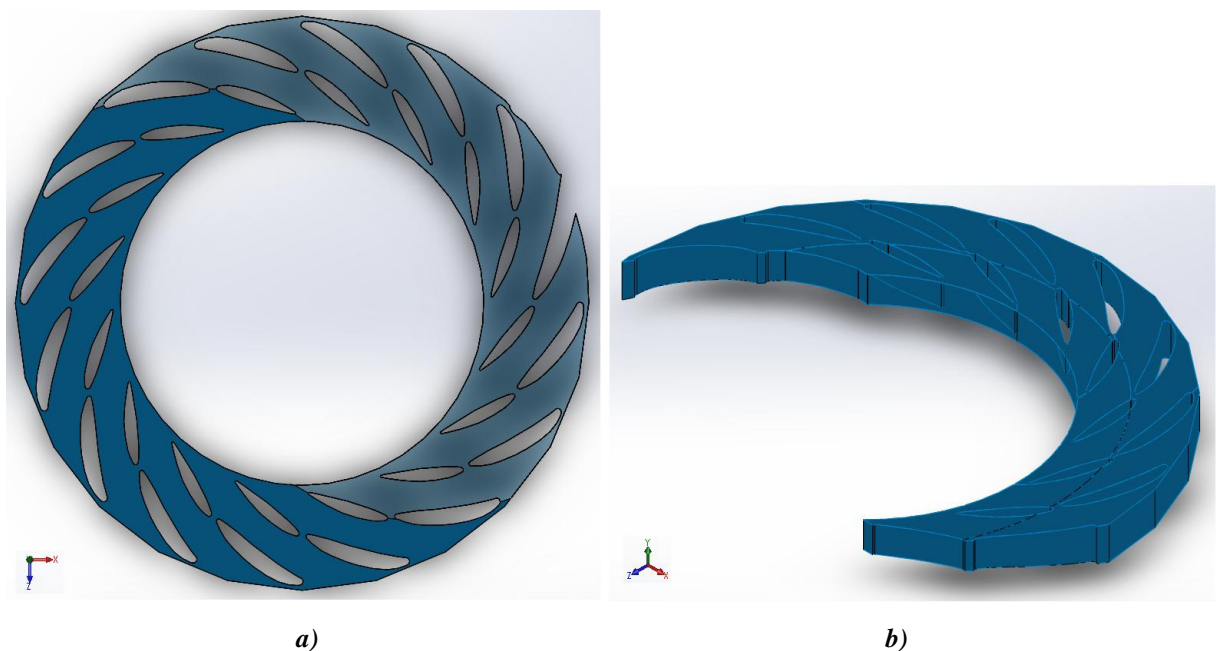


Figure 3.4 Stator computational domain; a) Sketch, b) Solid

Subsequently to the simplification of both sides of the geometry, rotor and stator, they have been assembled to create the reduced computational domain. As it is shown in Figure 3.5., The initial model has been reduced only to the elements that will be important in the future simulation. This geometry will be the definitely one in which the CFD study will be developed.

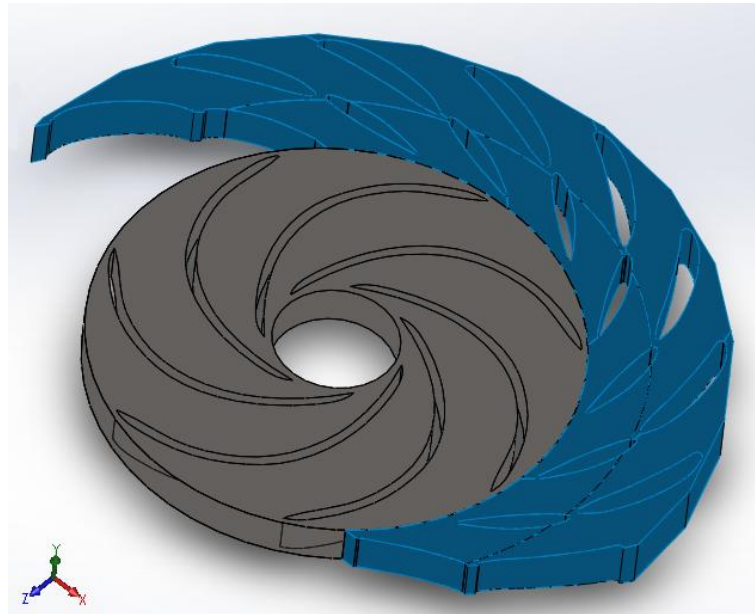


Figure 3.5 *Reduced computational domain*

The rotor and the stator have been treated separately. It is assumed that the following steps have been carried out analogously for the stator. For more information see [40].

Before turning to geometry meshing, both .sldprt files will be exported to .igs in order to be opened in ANSYS ICEM CFD 15.0. The treaty of the geometry consists basically the following four step:

- Create the surfaces:

In the solid export, the transferred geometric elements are curves and points. That is why the first thing that has been done was to delimit the boundary by using surfaces as it is shown in Figure 3.6. In paragraph 3.2.3. the boundary conditions are defined in these surfaces.

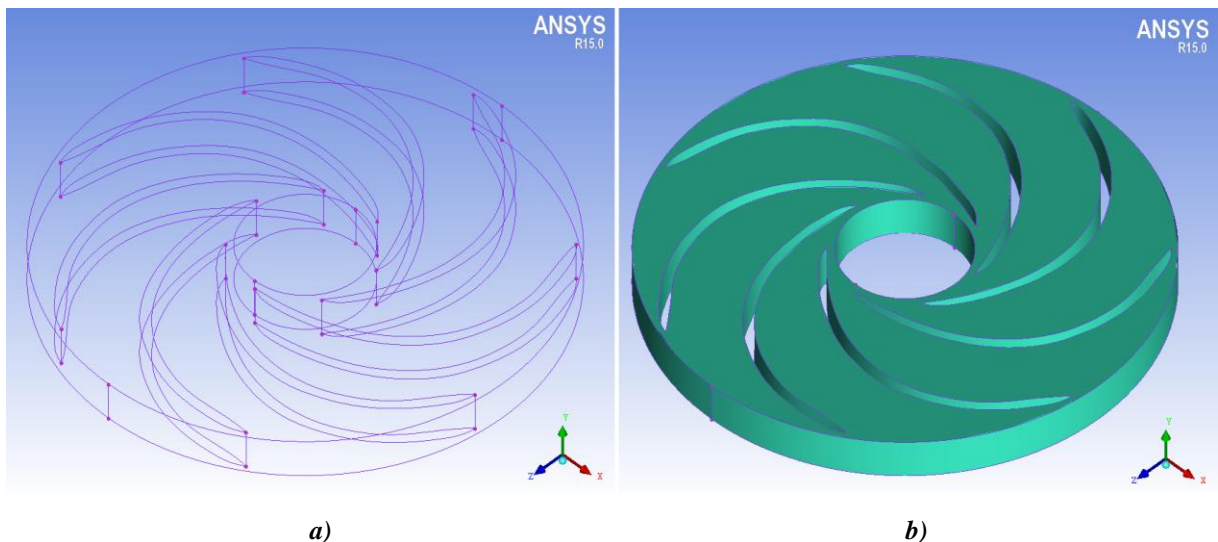


Figure 3.6 *a) Geometry exported to ANSYS Icem 15.0, b) Surface creation in the imported geometry*

- Create flow volume:

In this step the computational volume (Figure 3.7.) that delimits the previously created surfaces has been defined. Subsequently, this volume is discretized in the meshing process to solve the governing equations in each infinitesimal element.

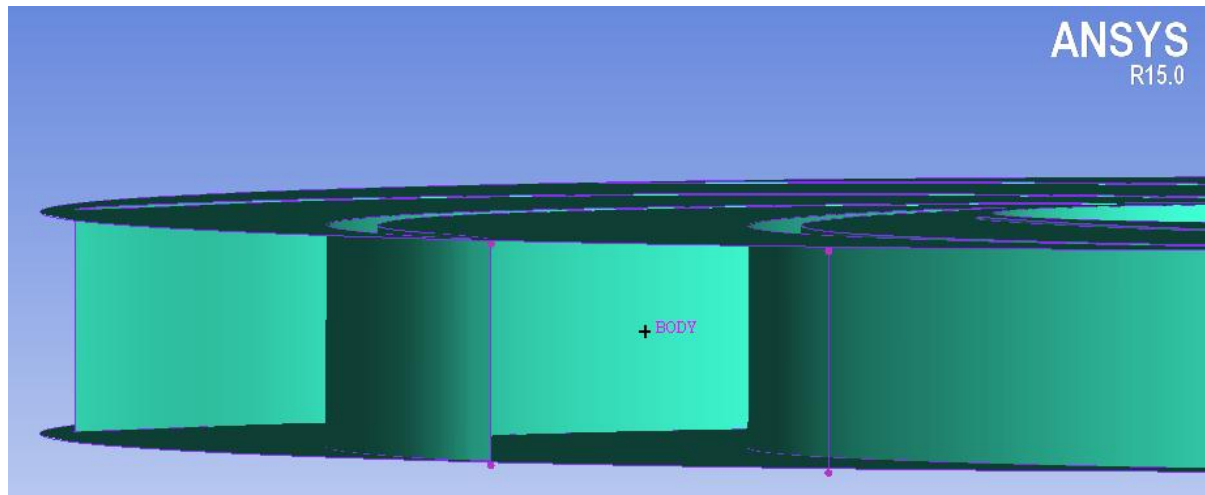


Figure 3.7 Detail of the created fluid volume location

- Define the geometry parts:

Afterward, as it is shown in Figure 3.8., it has been associated a name to each surface or surfaces group, leaving the geometry divided into different parts. In this way, in paragraph 3.2.3., a boundary condition to each part or group of surfaces will be awarded.

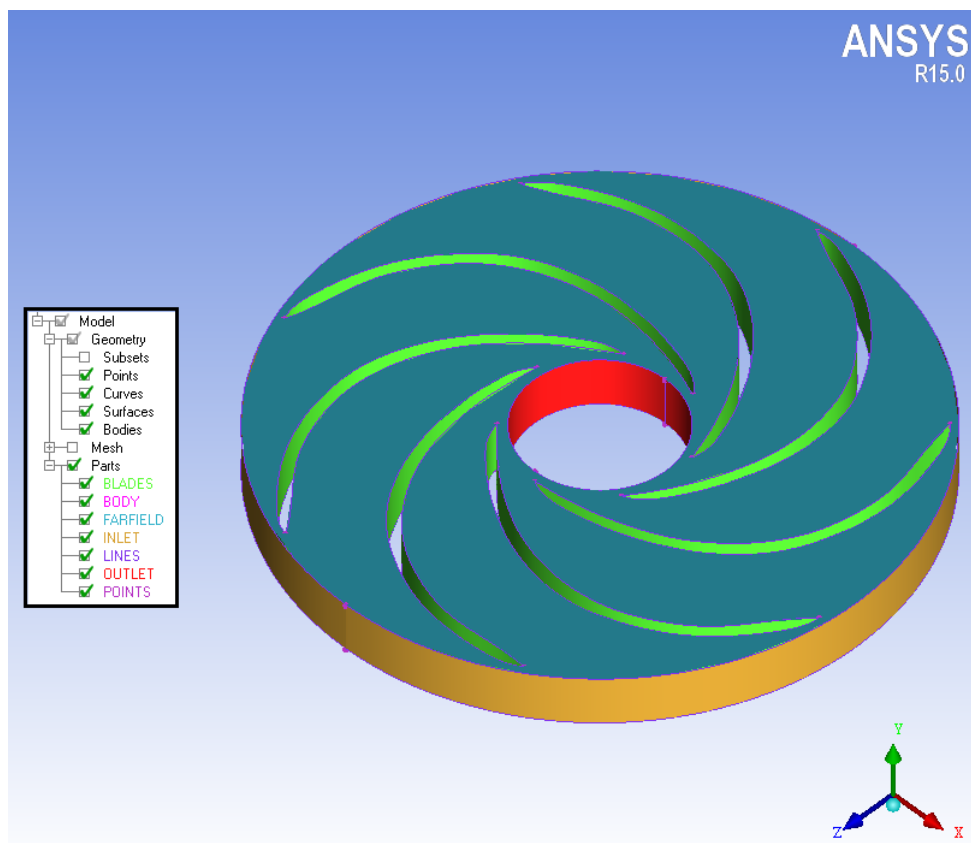


Figure 3.8 Division of the geometry in parts

- Check geometry

Finally, to check that everything is correct, we are going to see if there are errors like duplicate lines, isolated lines, surface holes, reliefs, etc by using the Check Geometry tool. If an error is found, it would be identified to be later fixed and able to move to the meshing section

3.2.2. Meshing

First there has been a division of the entire turbine domain into two parts: rotor and stator. In this way we can work and impose the relevant working conditions on each subdomain independently. Following the real physics of a Francis turbine, we are going to post the stator and impose an angular rotor rotation. With this setup it is pretended to get the rotor slide through the stator outlet by a appropriately configured Interface.

The preprocessing of the stator is not a part of this work as it is a matter of TFG "Simulación de una turbina hidráulica con CFD" by Jordi Lahoz. [40]. Thanks to his permission, I have arranged at any moment to the geometry and meshing archives of the stator as well as, to the necessary data for the realization of this work.

- Stator:

The mesh generation in single block is not efficient and creates problems of adaptability in more complex geometries. That is why in these cases is used the multiblock strategy which consists to subdivide the domain in regions filling in this way the entire domain. Each region or block is formed by a structured mesh. For connecting elements between blocks must be properly associate each block with his attached. In this manner we can achieve greater flexibility and precision.

The area of greatest interest in the stator is residing from the half until the outlet of it. The multiblock strategy allows us to divide the mesh to our interest and independently control each zone. That is why in the stator geometry has been created a structured mesh by blocking. In this manner the mesh in the area of greater computational interest has been refined and that means near the rotor and around the guide vanes by the O-Grid technique (for detailed information see [40]).

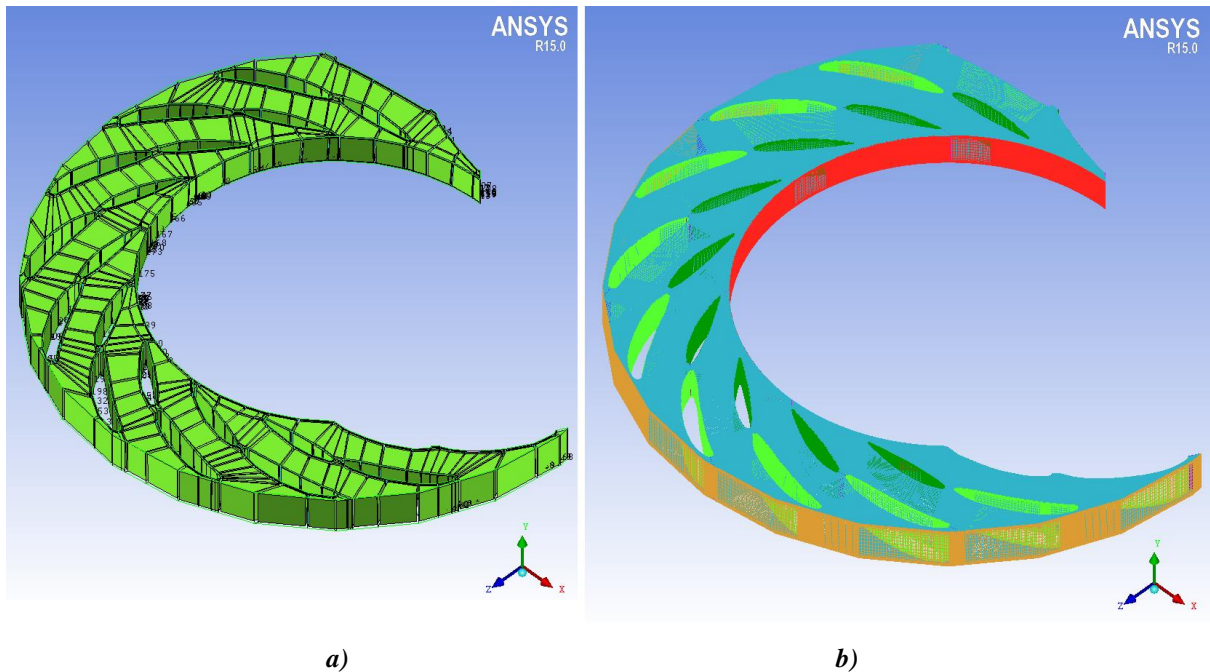


Figure 3.9 a) Strategy employed in distributing the blocks, b) Overview of the stator mesh

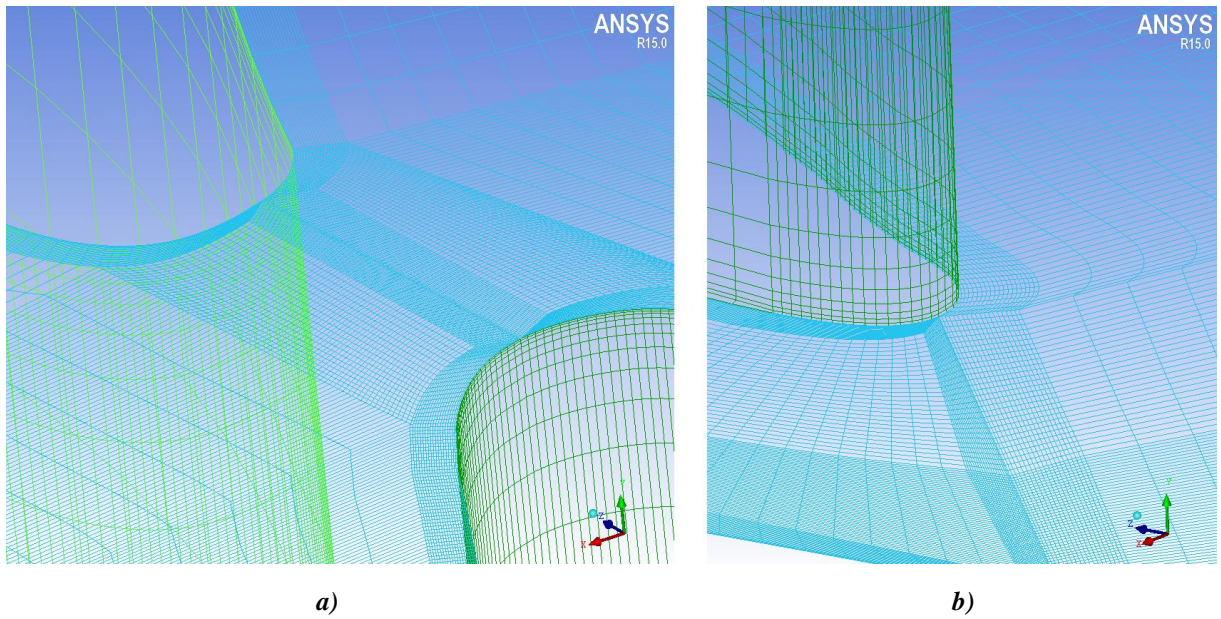


Figure 3.10 a) O-grid mesh refined, b) mesh density at the guide vane trailing edge

As it is shown in Figure 3.11., because of being a partial geometry, periodic areas are defined to make a continuous and stepless simulation.

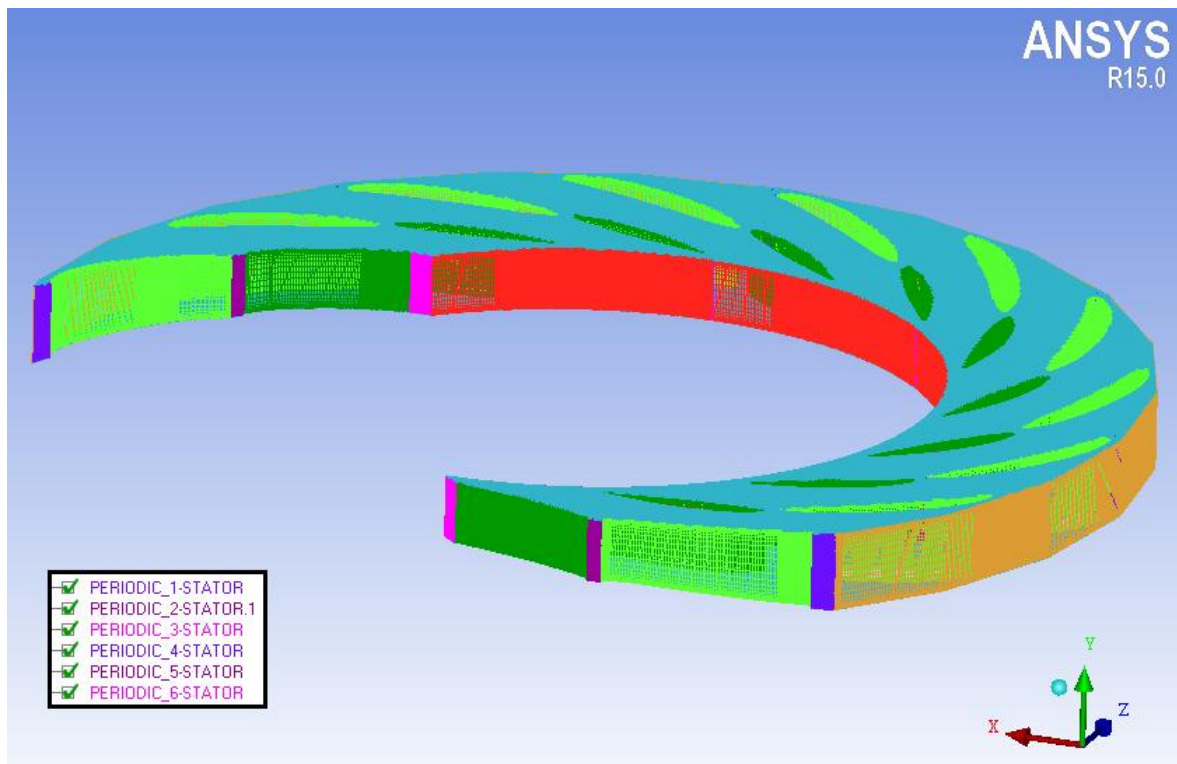


Figure 3.11 Detail view of the stator periodic zones

- Rotor:

For this study, it is not necessary to create a rotor structured mesh. This is possible because the interest computational area is on the periphery so would be an unnecessary waste of resources and time. That is why an automatic unstructured tetrahedral mesh element has been generated (Figure 3.12.). In addition it offers more than enough quality and fulfils the requirements expected.

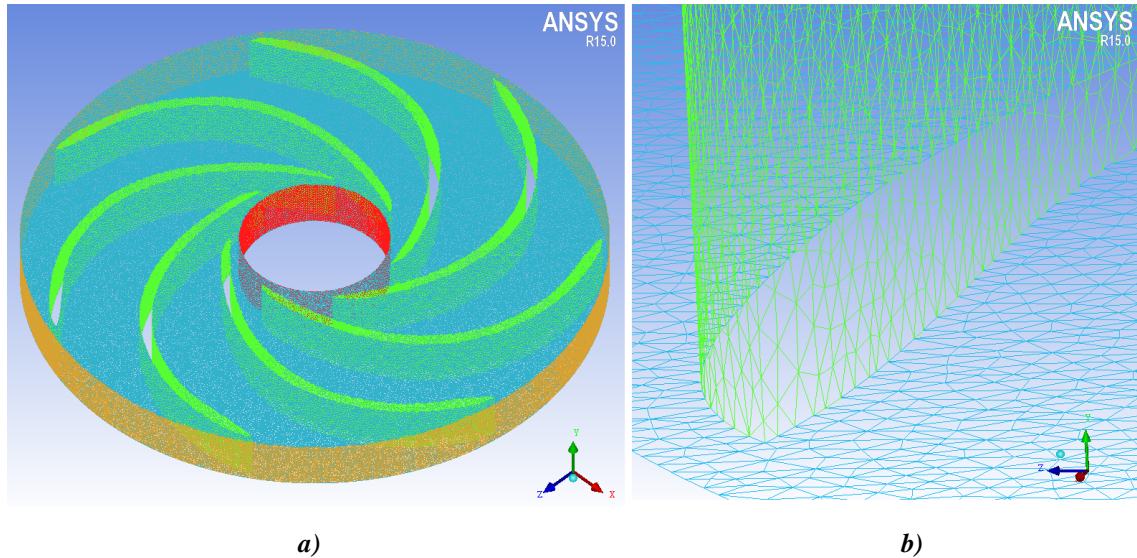


Figure 3.12 a) General view of the rotor mesh, b) Detail view of the tetrahedral elements that conform the rotor mesh

After the geometry meshing, the software that will solve the equations must set. In our case we are going to use ANSYS FLUENT 15.0. Afterwards we are going to predefine the boundary conditions in this way the Fluent can recognise them and we also can do the set later. Finally we are going to export the mesh to a single .msh file that is recognizable by Fluent and thus the setup can start.

As a summary in Table 3.1. can be observed the computational domain general characteristics:

	Geometry	Vane shape	Number of vanes	Meshing type	Element type	Number of elements
Runner	2D extruded	Default	7	Unstructured	Tetra	2.519.721
Stator	3D	Default	16	Structured (Multiblocking)	Hexa	9.293.952

Table 3.1 Features Summary of both meshes

3.2.3. Physics

This section establishes the physical parameters with a more tangible nature of the problem.

- General parameters:

As it has been mentioned in previous chapters, have been firstly defined the unsteady flow character as well as the turbulence model Spallart-Almaras, unique in this problem because they are not involved other relevant physical phenomena in the study.

Regarding to assigned materials in the geometry, it has been set by default the aluminum for the solid and water in each volume for the flow, that means in the rotor and in the four periodic stator volumes.

Analogously the rotor angular velocity has been imposed to 600 rpm. The stator has been established in the resting inertial reference frame.

	General parameter	Observations
Flow type	Transient	-
Turbulence model	Spallart-Almaras	-
Fluid	Water-liquid	-
Cell zone conditions stator	Resting mesh	0 rpm
Cell zone conditions runner	Sliding mesh	600 rpm

Table 3.2 Initial pre-established general parameters

- **Boundary Conditions:**

This section has associated to each surface or surfaces group, a specific type of predefined treatment in ANSYS Icem 15.0. Each assigned boundary contour will be determined depending on the role and characteristics that take each area.

The fluid inlet is given by the peripheral stator surfaces in the guide vane's arrow direction. In these surfaces has been assigned, as a boundary contour, a treatment for velocity-inlet with an absolute speed of 26.4 m / s. Analogously for the flow outlet in the rotor central surface is established a treatment of pressure-outlet.

The computational domain is composed of five meshes, four of them make up the domain of the stator and the resting, the totality of the rotor. The surfaces which delimits them have been defined as interfaces whose only function is to exchange data from one mesh to the other.

Due to the stator domain is not complete, for getting a continuous simulation in cascade, periodic and symmetry conditions in the rotational contact surfaces have been defined as is detailed in Figure 3.11.

Finally, the rest of areas whose function is to close the domain, the wall treatment has been assigned them.

As a summary for better understanding, the used boundary conditions in Table 3.3 were synthesized with the Figure 3.13.

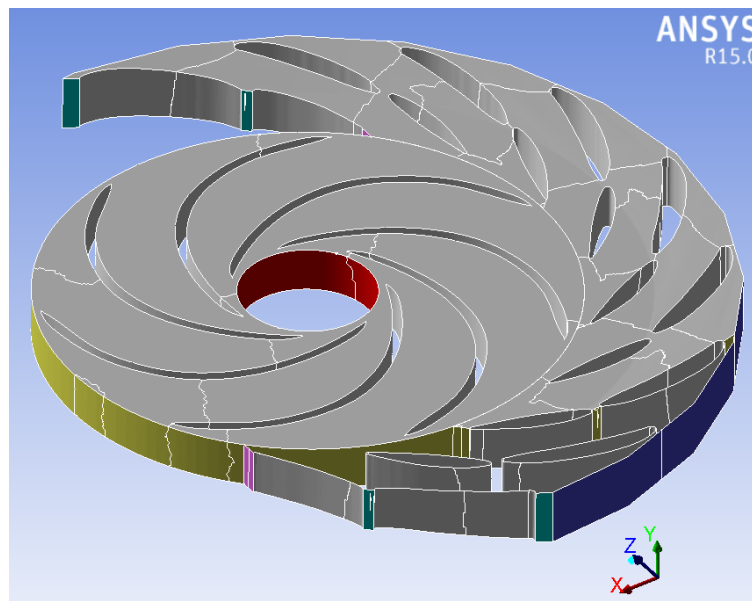


Figure 3.13 Defined boundary conditions in the computational domain

Part	Color	Boundary condition type	Observations
Inlet	Blue	Velocity-inlet	26.4 m/s
Outlet	Red	Pressure-outlet	0 bar
Interfaces	Yellow	Interface / Interior	-
Periodic ext. stator	Aquamarine	Periodic	-
Periodic mid stator	Aquamarine	Periodic	-
Symmetry int. stator	Fuchsia	Symmetry	-
Stator far field	Grey	Wall	-
Runner far field	Grey	Wall	-
Guide vanes	Grey	Wall	-
Wicket gates	Grey	Wall	-
Runner blades	Grey	Wall	-

Table 3.3 Detail of the used boundary conditions

3.2.4. Solver settings.

The parameters for simulation control have been established in this section:

- Solution Controls (Relaxing factors):

During the simulation there are instabilities that can irreversibly alter the process, This is the reason why in the iteration calculation are introduced coefficients that amortize these kind of instabilities with the aim that the solution converges.

A misuse of these factors can break down the simulation as we reduce these coefficients this increases the diffusion phenomena of interest and decreases the reliability of the results.

Factors that have been established in our case are detailed in the following table:

Parameter	Relaxation factor
Pressure	0.3
Density	0.8
Body forces	0.8
Momentum	0.7
Modified turbulent viscosity	0.8
Turbulent viscosity	0.8

Table 3.4 Established relaxing parameters

Another tool that allows us to maintain stable simulation are the limit values of the solution that will be imposed to the solver:

Parameter	Solution limit
Minimum absolute pressure (Pa)	1
Maximum absolute pressure (Pa)	5e+10
Maximum turbulent viscosity ratio	1e+20

Table 3.5 Pre-defined limit values

- Monitors:

For subsequent analysis of results and discussion will not be enough to represent graphical contours of pressure or velocity vectors. In order to understand in depth the phenomena involved in this study is essential to complement them with graphs. Thus apart from having a global graphical view, it could also observe how certain parameters evolve in time.

Fluent supplies us with a tool which allows us to define different monitors or sensors in areas of greater computational interest. Its main function is to export in a table data values which takes certain predefined parameters during the course of the simulation. Subsequently, using this data table the data treating will be done by making graphs of F-t, P-t, Hz-t.

In this case we define three types of monitors: residual, strength monitors and surface monitors.

Residual monitors.

In each iteration, the solver calculates the following variables: continuity, x-velocity, y-velocity, z-velocity and nut. Since they are continuous approximations, an assumable residual error is committed corresponding to the difference between the current value they must take and calculation in each iteration. For each variable has assumed a maximum residual error of $1e-03$.

Strength monitors: Lift and drag coefficients.

As has been mentioned in the introduction, the lift and drag coefficients are dimensionless parameters which give us information about the forces generated by pressure gradients present in the guide vanes and wicket gates of the stator.

For observing the fluctuation of these coefficients in time the vane walls were monitored. In addition in the guide vane as well as in the wicket gate have been defined both directions of lift and drag vectors as it is shown in Figures 3.14 y 3.15 respectively.

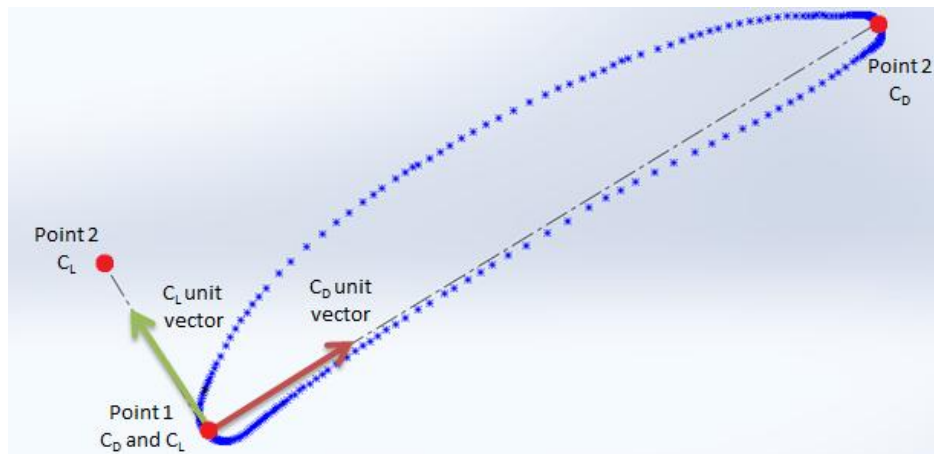


Figure 3.14 Unit vectors of drag and lift of the guide vane

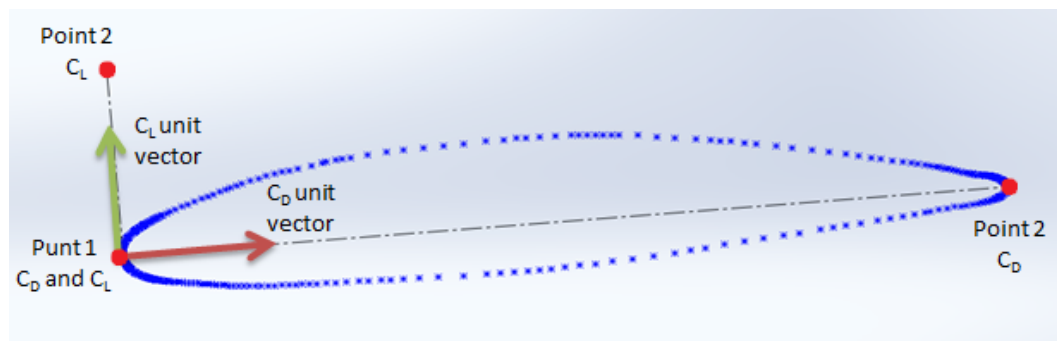


Figure 3.15 Unit vectors of drag and lift of the wicket gate

The following table shows the components of the lift and drag unit vectors defined in both vanes.

	x	y	z
C_D guide vane	-0.8544	0	-0.5197
C_L guide vane	-0.5197	0	-0.8544
C_D wicket gate	-0.9966	0	-0.0827
C_L wicket gate	-0.0827	0	-0.9966

Table 3.6 Unit vectors components of the C_L and C_D

d) Surface monitors.

In order to find the instant when the flow is stabilized, that means when the results become relevant and meaningful, it has monitored on the outlet surface the full volumetric output rate.

On the other hand different radial points have been defined which are monitored in each instantaneous static pressure in order to observe the variation of the runner blades passage.

The following table shows the coordinates of the monitoring points:

	X (m)	Y (m)	Z (m)	Radi (m)
Punt 1	-0,25439	0	-1,442743	1,465
Punt 2	-0,50106	0	-1,376650	1,465
Punt 3	-0,7325	0	-1,268727	1,465
Punt 4	-0,94168	0	-1,122255	1,465
Punt 5	-0,71845	0	-1,540723	1,700
Punt 6	-1,30228	0	-1,092739	1,700
Punt 7	-1,30815	0	-1,308148	1,850

Table 3.7 Geometric coordinates of the punctual monitors

- Time step:

For the calculation of a problem with non-steady flow must be defined a time step. In each time step the problem performs calculations and iterations required to reach convergence and get a result. The results of each time step are shown as a function of total time.

The calculation is more precise as small as this time step would be. If the step is too large it is possible to loss information and if it is too small, the calculation time is excessive. So it is important to calculate the step time for each problem before starting the numerical simulation.

In this issue will be taken this time step that is equivalent to advance 1° of 360° that has a revolution. First, the turbine period will be calculated by knowing the velocity at which it will rotate. Te time step (dt), which is the relation between an appropriate angle (°) and the turbine period (T). It is going to be calculated as follows:

$$T = 1rev \cdot \frac{1min}{600rev} \cdot \frac{60s}{1min} = 0,1s \quad (3.1)$$

$$dt = \frac{0,1s}{360^\circ} = 2,778 \times 10^{-4}s \quad (3.2)$$

By performing calculations is obtained a time step of $2.778e-04$ s ., that means 360 time steps are calculated in each rotor revolution.

Per each time step it has determined a maximum number of 25 iterations thus If in 25 iterations the solution will not converge with a predefined error assumed in the residuals, the time will jump to the next time step.

3.3. Solve

When a commercial CFD code is used, the partial differential equations of momentum conservation and scalars such as conservation of mass and turbulence are solved by integrating them numerically. The commercial codes use a technique based on control volumes, which consist of three basic steps:

- Domain division in discrete volumes control by using the computational mesh.
- Integration of the equations in control volumes to create an algebraic equation for variables such as pressure, velocity and other scalar properties.
- Solving discretized equations by an iterative method.

The equations are solved sequentially. These equations are coupled and therefore is necessary to calculate them by iterating loops to get the results convergence. The loop of calculation is achieved with seven steps that are performed in sequential order and they are shown as follows (see Figure 3.16):

1. The equation of momentum is solved for all directions, using the instant pressure value (initially the boundary conditions are used), in order to update the velocity field.
2. The obtained velocities cannot achieve locally the continuity equation. Using the continuity equation and the linearized momentum equation, is derived an equation for the pressure correction. Are going to be used the corrected pressure, the original pressure and the velocity in order to achieve the continuity.
3. The turbulence equations are solved with the corrected velocity fields.
4. All other equations (energy, etc.) are solved by using the corrected variables.
5. Fluid properties are updated.
6. All additional terms of the sources are updated.
7. It is carried out a convergence control.

These seven steps are performed until the convergence is achieved.

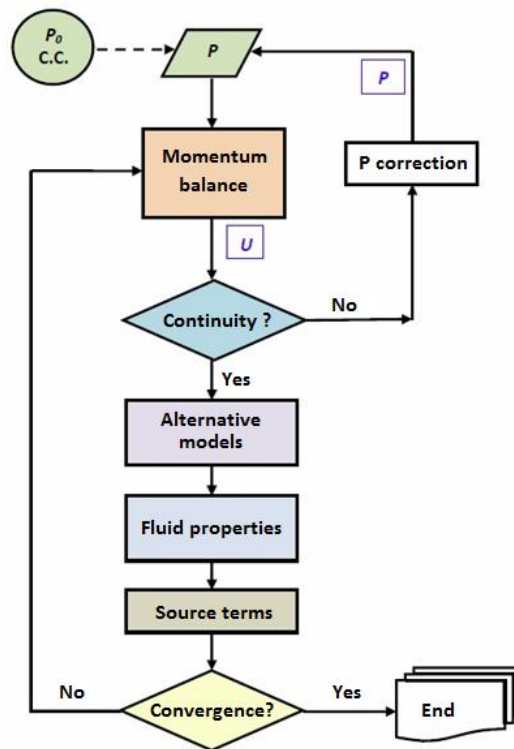


Figure 3.16 Flowchart of the numerical solution in commercial CFD programs (Fontanals, Alfred 2012)

3.4. Post-processing

When the simulation has converged, the last simulation data are stored. This file has information in all the control volumes about the velocity, pressure, density, etc. The display of all these data is called post processing and let us to compare results between different simulations or external data.

There are different ways to display the results such as in two-dimensional charts, where a variable is faced in front of the other. These graphics are useful for visualizing the flow velocity at the wall boundary layer, the lift coefficient fluctuation in a profile or the characteristic frequencies, etc.

For obtaining the characteristic frequencies from the pressure values it has been used the "ProcessaLift_pos" application that is developed in Scilab. This application develops the Fourier transformation and converts pressure values in characteristic frequencies.

The contour images allow us to represent graphically in a plane or in a volume how a variable changes in time. The velocity vector graphic show the velocity vectors in each surface control volume or the selected volume. It provides a better information about the local characteristics of the flux.

For carrying out the frequencies calculation will be analyzed by Fourier transform, which of them are the most repeated during the simulation at all over the points, as well as with the lift coefficient. In this way will be determined which points capture better the frequency information for later draw conclusions.

The calculation of the Fourier transform with each results file was performed using the "ProcessaLift" application in Scilab, which sorts the frequencies as they appear, showing a chart with the frequency spectrum.

As the problem lasts until it is actually considered stationary, the area where the flow is stabilizing must be removed to avoid frequencies which do not exist in reality. As previously indicated, this can be done by looking at the graph of lift coefficient. When the signal become stable is then when the values are coherent and logical.

CHAPTER 4. RESULTS AND DISCUSSION

4.1. Pressure and velocity contours

FLUENT let us to observe in a graphic way the contours about every property we would be interested. In addition, we can capture these images in each time instant and in this way we could make a turbine behaviour simulation. These animations will be annexed in the virtual device of the project.

One complete rotor revolution simulation has been carried out when the problem was completely uniform. The pressure and velocity contours data have been saved. It is interesting to observe the interaction between the rotor blades and the stator wicket gates as is where the peaks and pressure fluctuations occur.

In the Figure 4.1 is shown the number of cycles that occur in one rotor revolution at the point monitor 2 and in the Figure 4.2 we can observe a single cycle in order to determine when the maximum and minimum occurs.

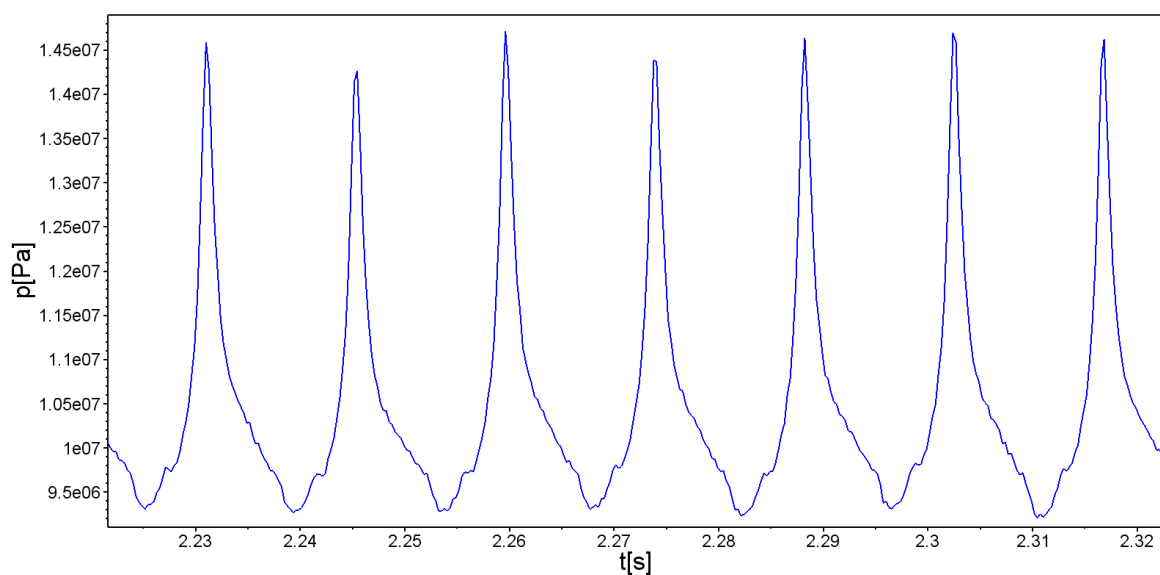


Figure 4.1 Static pressure variation in real time in one complete rotor revolution

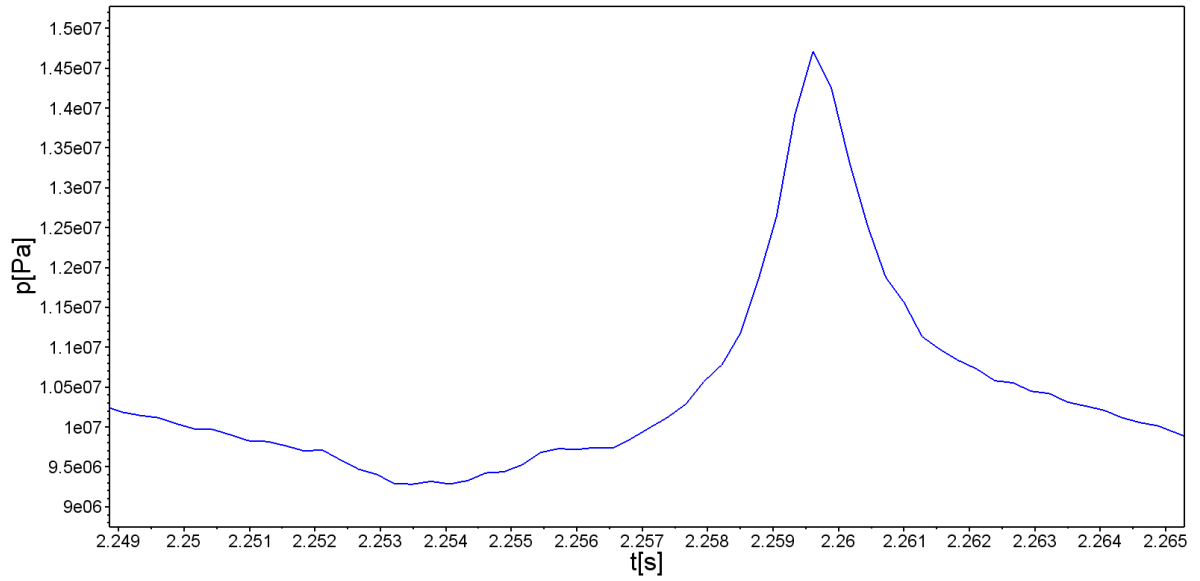


Figure 4.2 Single static pressure cycle at real time

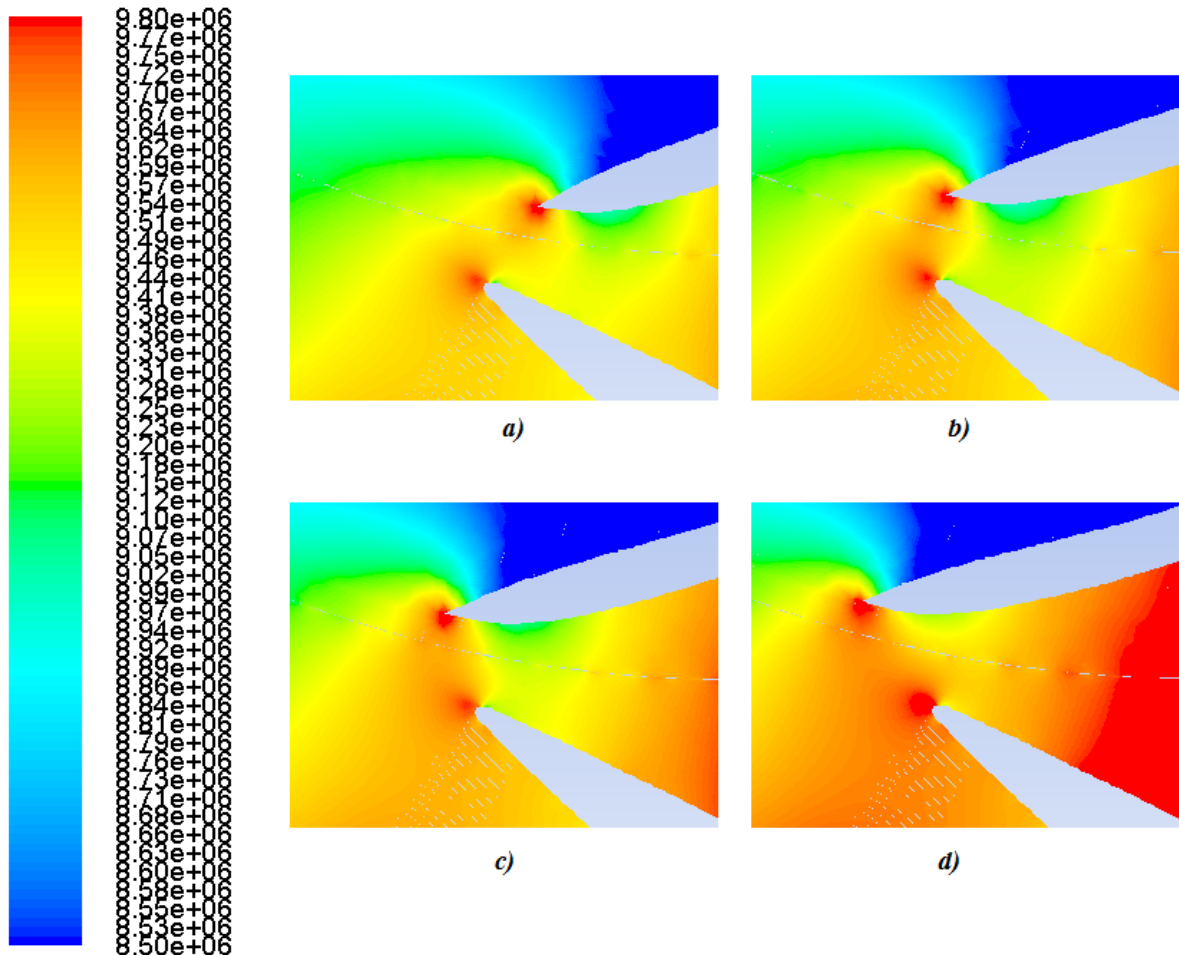


Figure 4.3 Static pressure contours showing the potential phenomena at different time steps; a) Time=2,7396 s b) Time=2,7402 s c) Time=2,7408 s d) Time=2,7414 s

When we observe the static pressure contours between the runner and the stator shown in the Figure 4.3, we can see that as the blades approach, the pressure increases until its maximum value which is reached one instant after the alignment. Immediately, after it the pressure decreases drastically to start

the cycle again. In other words we can tell that before the encounter there is a depression and after of it appear an overpressure zone because of the rotor stator interaction.

In this way the low pressure zone is above the rotor blades and the high pressure below them at the surroundings of the interaction.

Consequently, observing the velocity contours, is clear to see that where the velocity values are higher is behind the rotor blades (see Figure 4.4).

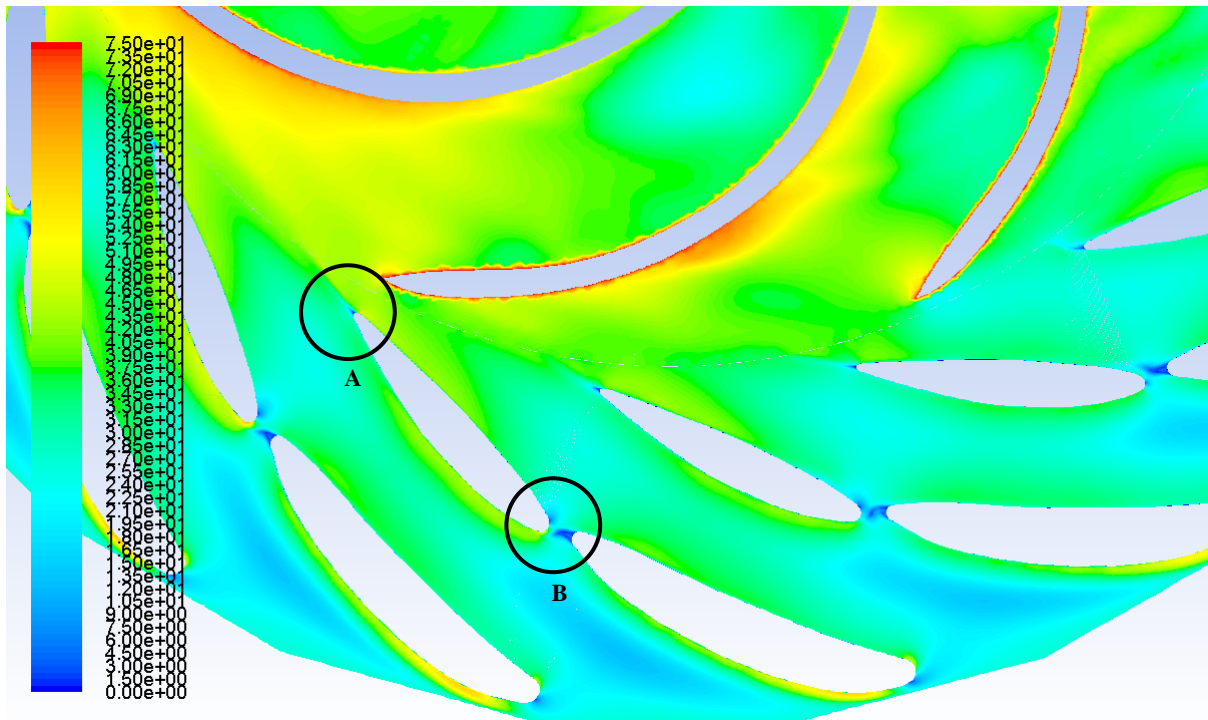


Figure 4.4 Velocity contours of the rotor-stator domain

If we zoom in the detail A, we will see how affect the rotor blade movement around the ending part of the wicket gate (see Figure 4.5).

As we can observe, as well as the continuity law says, to the extent that the flow passage section decreases, the flow will increase the velocity until reaching a maximum value which is corresponded to the blades alignment. This is because the volumetric flow-rate must be the same in each step. So increasing the section, will decrease the velocity and decreasing the section, will increase the velocity.

In the other hand we can see also that there is a permanent velocity gradient at the wicket gate tail which generates vortex shedding and consequently high pressure zones.

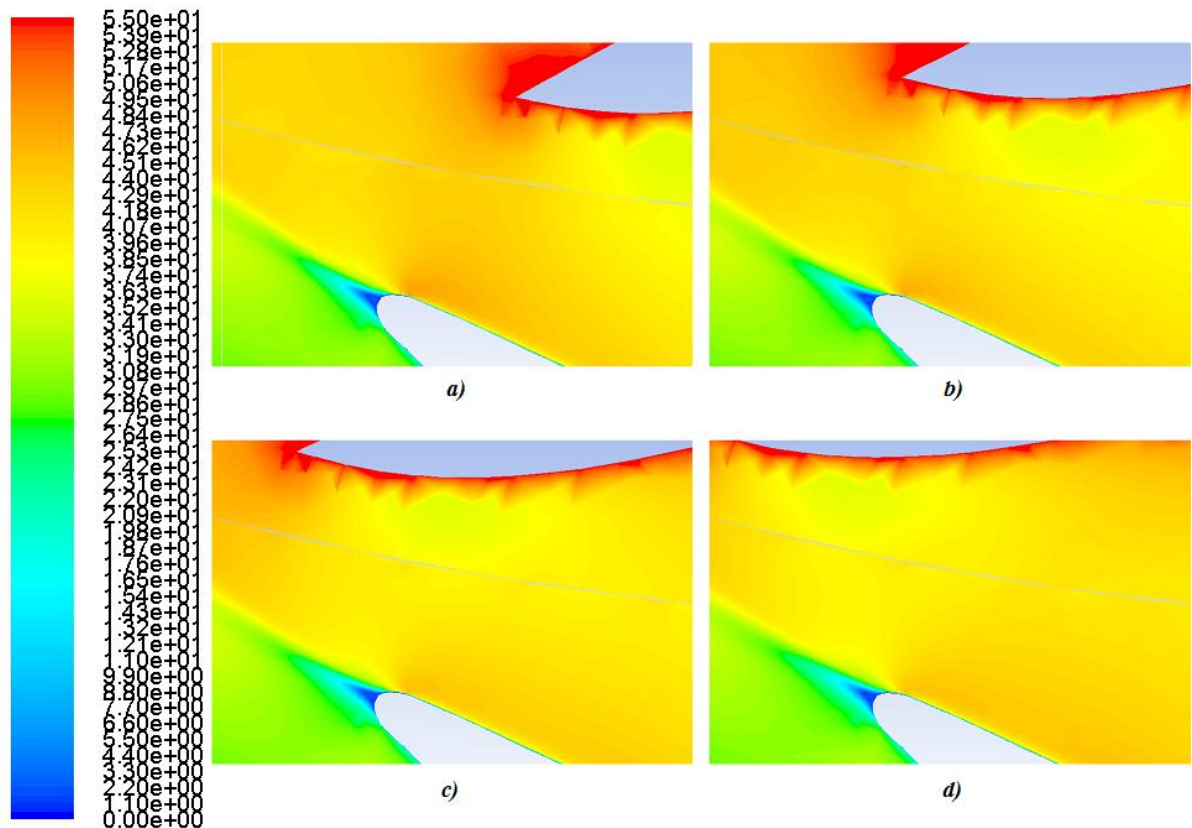


Figure 4.5 Detail A view showing the contours of velocity around the wicket gate trailing edge at different time steps; a) Time=2,7396 s b) Time=2,7402 s c) Time=2,7408 s d) Time=2,7414 s

4.2. Velocity vectors

In the same way as before, FLUENT, also let us to observe in a graphic way the vectors about every non scalar property we would be interested. We will capture these images in each time instant and the animation will be annexed in the virtual device of the project.

If we zoom in the detail B of the figure 4.4, and setting the velocity vectors mode, we could observe clearly which is the behaviour of the flow between the guide vanes and the wicket gates as is shown in the Figure 4.6.

As well as we have commented in the introduction, due to the shearing forces, caused by the velocity gradient, appear the vortex shedding phenomena behind the guide vane. As we can see in the Figures above, because of the vortex shedding the flow fluctuates generating the Von Karman street.

The beginning of the wicket gate, brake this vortex street by accelerating the flow towards the rotor entrance.

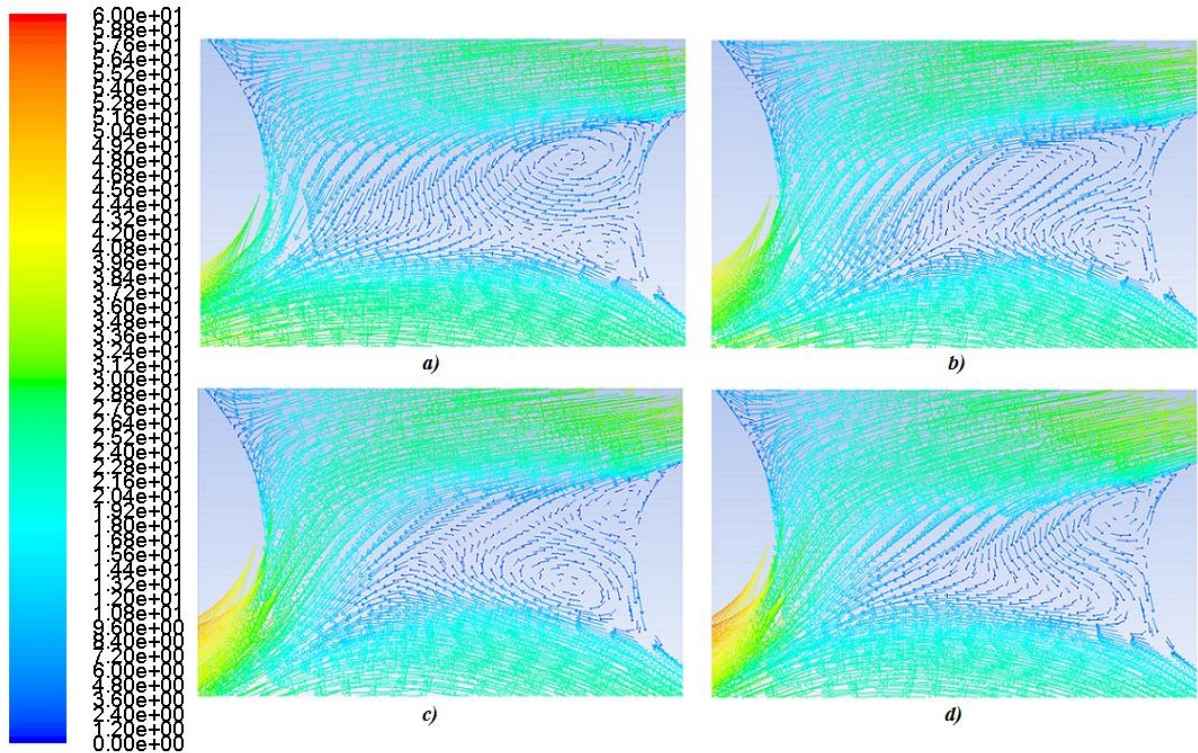


Figure 4.6 Detail B view of the vortex shedding due to the wake effect

4.3. Frequency analysis

The turbine movement type is rotary, which makes the pressure distribution in it be cyclical and harmonious. As well as seen above in Figure 4.1, every certain period of time, the same information is being repeated at the different point monitors. It is interesting to analyze how often this information is repeated in order to verify if the turbine behaves like in reality.

4.3.1. Drag and lift coefficients

For a better understanding of the hydrodynamic forces that the stator is receiving it has been plotted one graph showing the guide vane and wicket gate drag coefficients versus the flow time and the other shows the guide vane and the wicket gate lift coefficients versus the flow time. In this way we could see in a quick look the behaviour of the hydrodynamic coefficients in each vane.

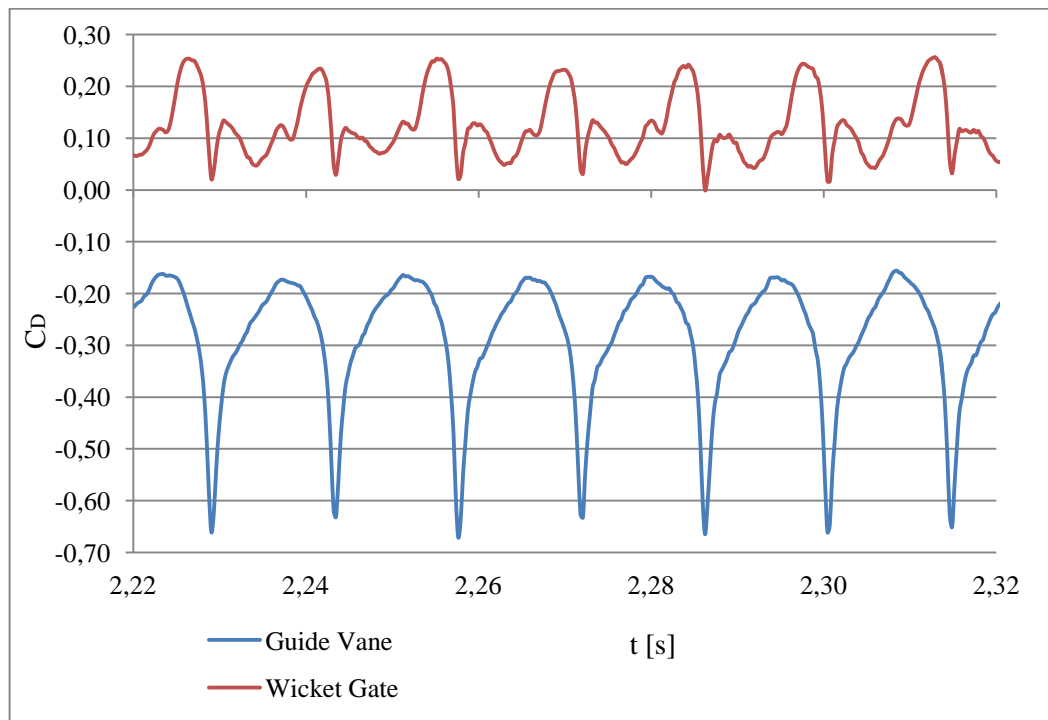


Figure 4.7 Drag coefficient values depending on the vane (wicket gate drag coefficient magnitude $\times 10$)

In this chart, the wicket gate drag coefficient tends to zero unlike the guide vane one that took higher values. That is because the frontal area of the wicket gate is negligible so in this way the resistance tends to zero. Also is frequent to have coefficient drag values between 0.1 to 1. The negative sign means that the hydrodynamic drag forces are always contrary to the flow.

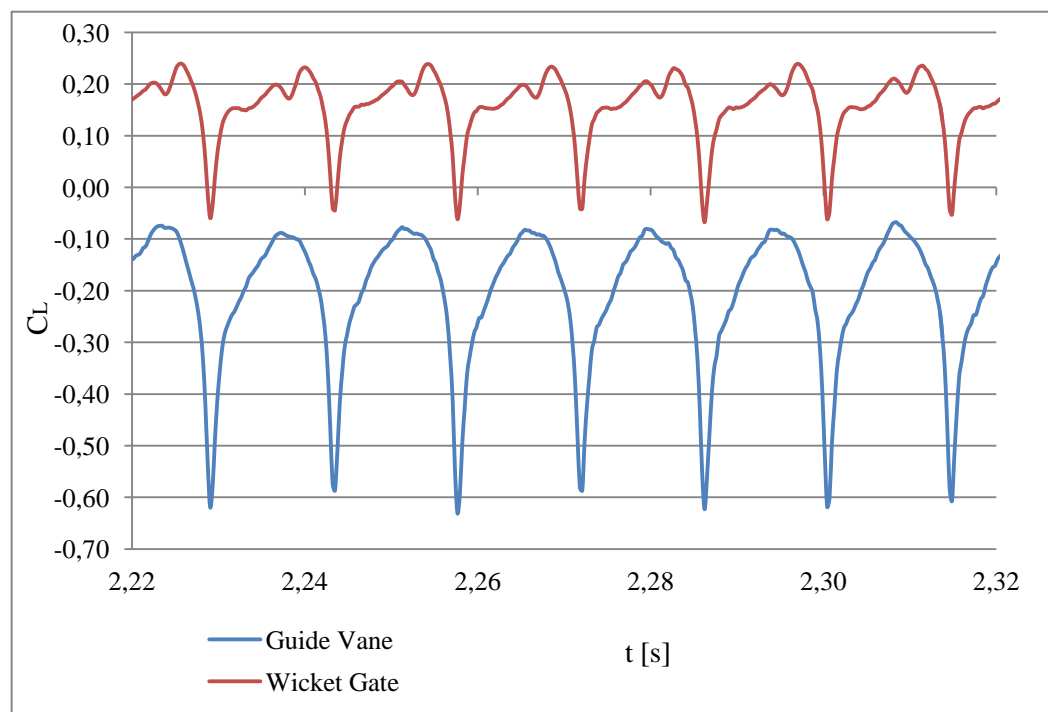


Figure 4.8 Lift coefficient values depending on the vane

Here is interesting to remark that depending on the vane we will have positives or negatives values of lift coefficient. Around the guide vane the hydrodynamic lift forces go approximately from -0,1 to -0,6. Otherwise the wicket gate takes lift values from -0,1 to 0,5 approximately.

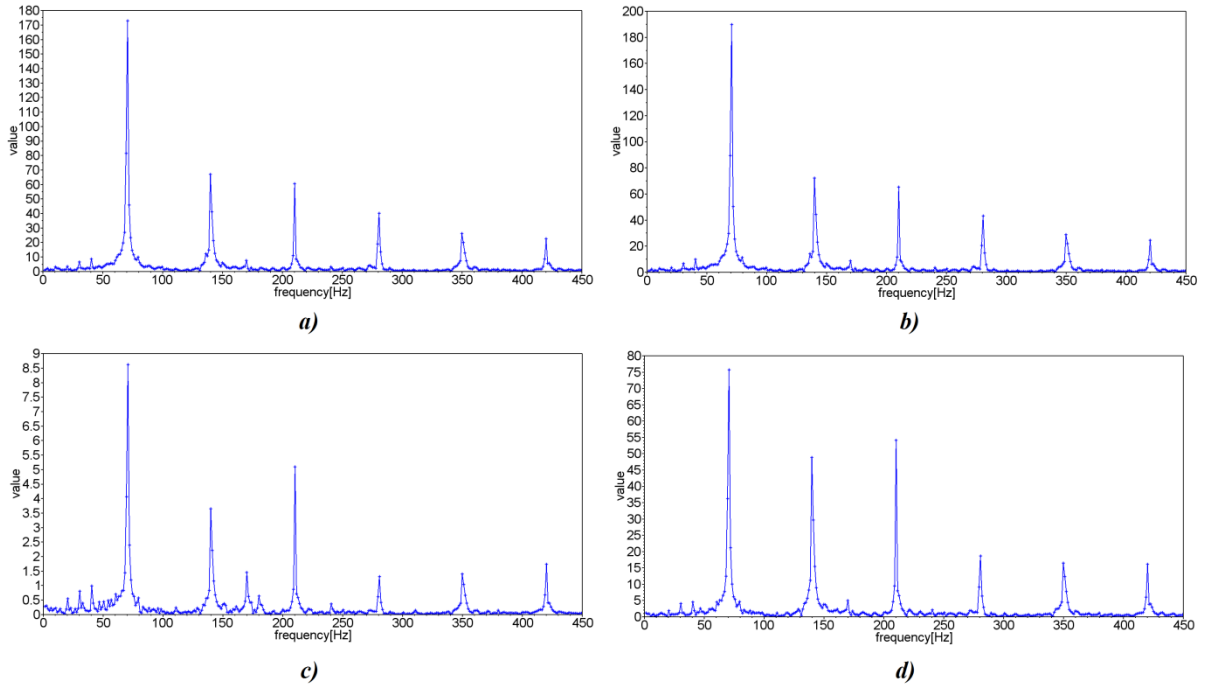


Figure 4.9 Frequencies of the a) C_D around the guide vane, b) C_L around the guide vane, c) C_D around the wicket gate and d) C_L around the wicket gate

	f1[Hz]	f2[Hz]	f3[Hz]	f4[Hz]	f5[Hz]
C_D guide vane	70	140	215	281	350
C_D wicket gate	70	215	140	423	350
C_L guide vane	70	140	215	281	350
C_L wicket gate	70	215	140	281	350

Table 3.8 Characteristic frequencies of the C_D and C_L coefficients

As shown in the Figure 4.9 and in the Table 3.8, the most important frequencies detailed in the spectrum of vibration are the first three. In addition we can see that the fundamental one in all the vanes is 70Hz which corresponds to de first harmonic. However their secondary harmonics don't share the same appearing structure. On the guide vane the following one is the second that vibrates at 140Hz unlike the wicket gate that the following harmonic is the third and vibrates at 215Hz.

4.3.2. Pressure monitors

Another interesting thing to do would be to plot the pressure values captured in the seven monitors in one graph as seen in the Figure 4.11. In this way we could see at a glance how affects the rotor passing blades around the point locations. In section 2.1 of the annexes are detailed all the static pressure monitors tables corresponding to one complete rotor revolution as well as shown in Figure 4.1. The following picture (Figure 4.10) shows the location of the pre-established seven point monitors.

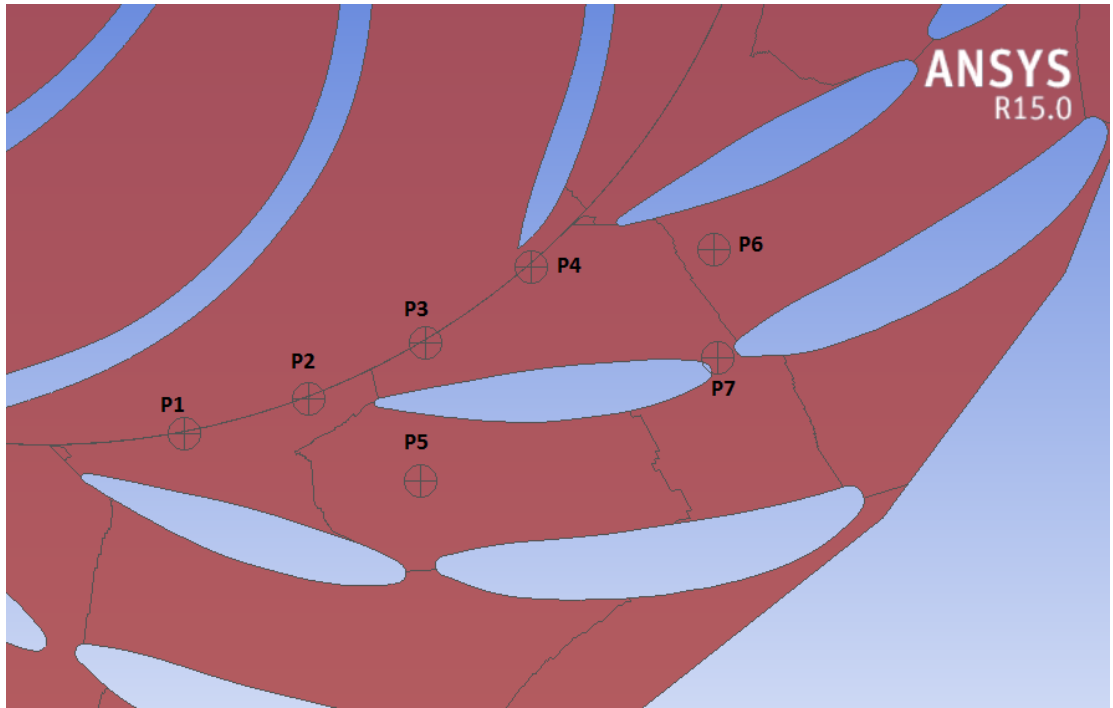


Figure 4.10 Detail of the point monitors location

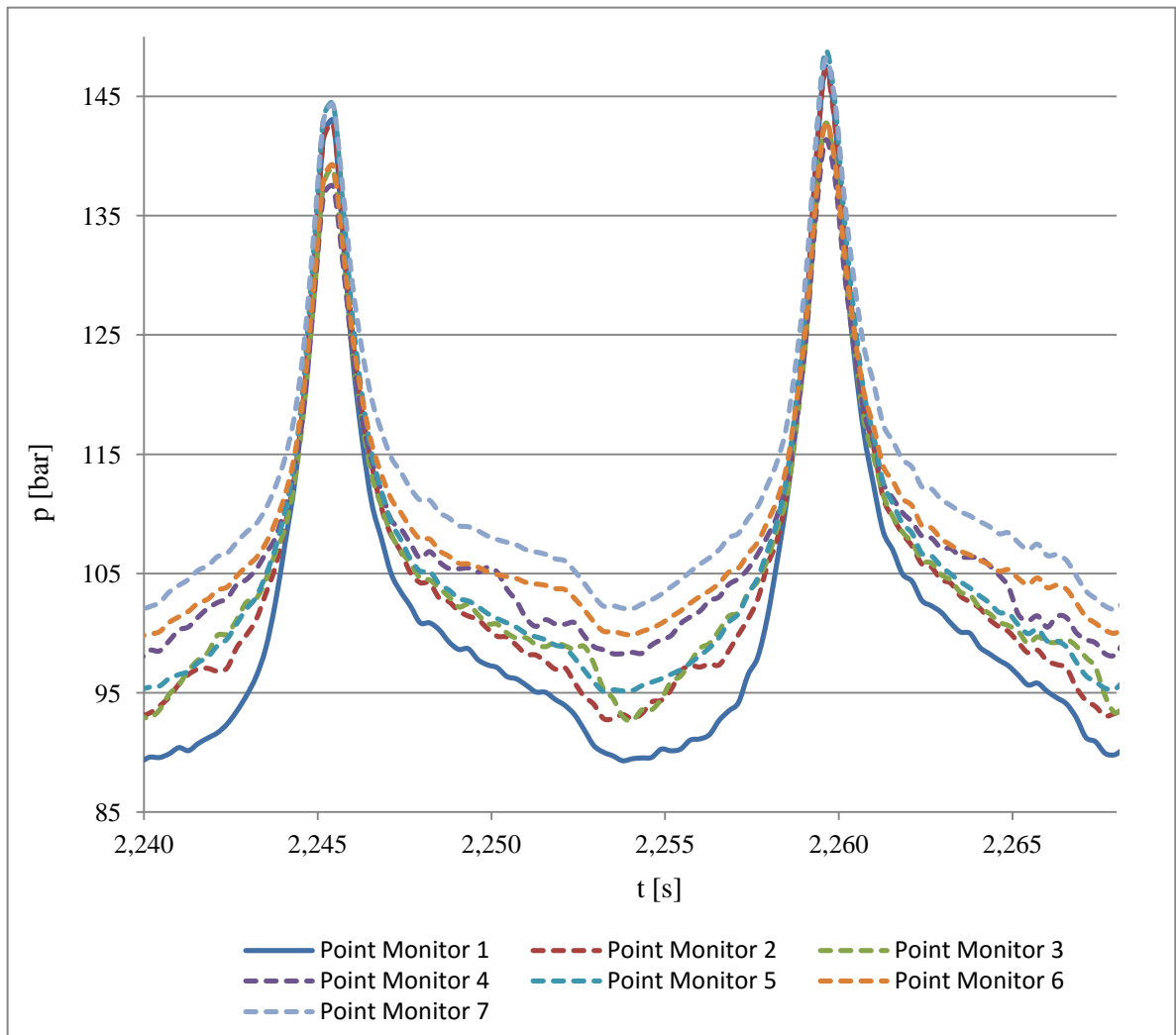


Figure 4.11 Static pressure monitors variation in one complete cycle

As we can see in the Figure 4.11, this chart can be divided into 4 parts. The first one, when the blade is entering to the stator control channel, the point 4, 6 and 7 read moderate values of pressure because of the previous interaction. Otherwise, in this instant the monitor 1 gets low pressure values because is the farthest point. While the rotor blade is approximating to the wicket gate trailing edge, all the point monitors increase their pressure values until their maximum which correspond to one instant after the blade and wicket gate alienation. In this moment the monitors 1, 2, 5 and 7 reach higher pressure values than the rest because they are set in the previous part of the wicket gate where the RSI occurs. Finally, when the blade leave the control channel the pressure values descend until their minimum. Comparing this results with the Figure 4.3 we could see that the values are coherent and approximate.

As a sample, in the Figure 4.12, are detailed only the frequencies corresponding to the pressure monitor 1. That is because as it is shown in the Table 3.9 they are identical in each point monitor. For more detailed information, in the section 2.2 of the Annexes are shown all the frequency graphs corresponding to each of the 7 monitors.

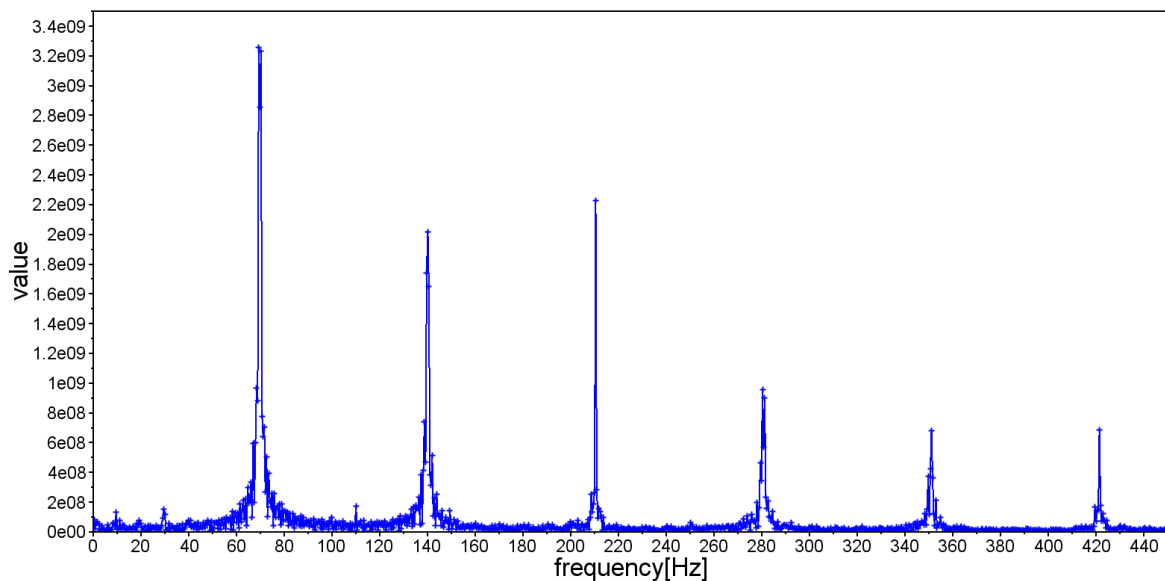


Figure 4.12 Frequencies of the static pressure in the monitor point 1

	f1[Hz]	f2[Hz]	f3[Hz]	f4[Hz]	f5[Hz]
P1	70	215	140	281	423
P2	70	215	140	281	423
P3	70	140	215	281	423
P4	70	215	140	281	423
P5	70	215	140	281	423
P6	70	215	140	281	423
P7	70	215	140	281	423

Table 3.9 Frequencies of the static pressure monitor points

As well as before, we can see in the vibration spectrum that the highest component is the first harmonic which vibrates at 70Hz, then the third that vibrates at 215Hz, followed by the second one that do it at 140Hz and so on.

4.3.3. Surface Monitor

It is obvious that the volumetric flow rate should be constant from the moment that the flux will be uniform. So in order to check it, a graph of volumetric flow versus time flow has been done (see Figure 4.13).

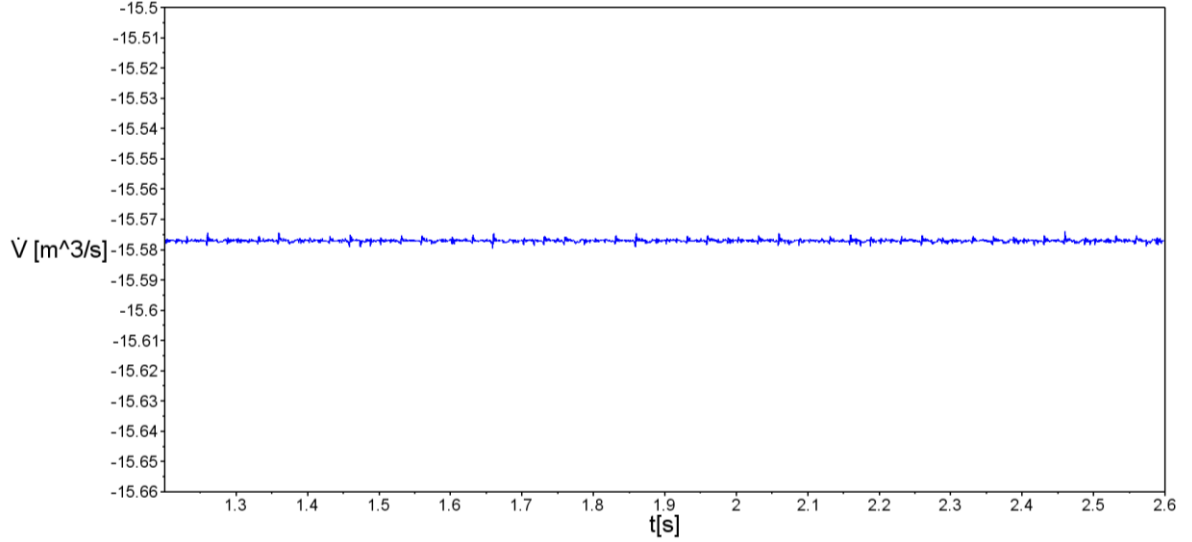


Figure 4.13 Volumetric flow-rate variation

Since the flux is stabilized, the volume flow rate remains practically constant throughout the timescale. As we can see the volumetric flow-rate is more or less about 15,6 m³/s and the one of the real turbine is 32 m³/s. It is relevant to highlight that in our study is exactly the half because we only have simulated 180° of the stator.

4.4. Comparison between theoretical and numerical study

As we have seen, until now the results seem to be logical and coherent. However it would be interesting to verify if the frequencies approximate to its theoretical value.

To determine in a theoretical way which is the fundamental frequency in this study is needed the angular velocity and the number of rotor blades. It is calculated as follows:

$$\Omega = 600 \text{ rpm} \quad (4.1)$$

$$\omega = 600 \frac{\text{rev}}{\text{min}} \cdot \frac{1 \text{ min}}{60 \text{ s}} = 10 \frac{\text{rev}}{\text{s}} \quad (4.2)$$

$$f_{\text{theo}}^1 = 10 \frac{\text{rev}}{\text{s}} \cdot \frac{7 \text{ cycles}}{1 \text{ rev}} = 70 \frac{\text{cycles}}{\text{s}} = 70 \text{ Hz} \quad (4.3)$$

$$f_{\text{num}}^1 = 70 \text{ Hz} \quad (4.4)$$

As we expected, in the theory, the fundamental frequency is 70Hz which exactly coincides with the highest one in the spectrum of vibration that we have calculated in the numerical study. This principal frequency will have its secondary harmonics which will be multiples of it. With this method we can't determine the other harmonics.

CHAPTER 5. CONCLUSIONS

First of all, it has been proved that although the first studies related to fluid mechanics were in the 18th century, it was not until the last decades that thanks to the emergence of computational fluid dynamics has allowed us to deal with almost any type of fluid dynamic problem without big efforts.

The main point of this paper was to make a numerical simulation of a Francis turbine in operating conditions in order to see how the RSI affects in the turbomachine.

The potential effect and the wake interaction have been modelled in order to obtain the pressure variation, the hydrodynamic forces and their fundamental frequencies.

The project turned out to be quite complex to such an extent of having to split it into other students. Thereby the rotor was the geometry with which I had to carry out the CAD design and the meshing.

The first three months were destined to software self-learning as it was highly wide and complex. However, I have been learning new tools and improving my software knowledge during all the project.

Concerning to the CAD design, the original geometries were given to us in .igs format. Despite it had many errors and I could not advance in the project, I have decided to import it in SolidWorks to correct them and redo almost the entire geometry by simplifying it into a 2D extruded problem. Afterwards, I exported them to ANSYS Icem 15.0 in .igs format.

Although the geometry had improved greatly, it had generated duplicate lines and minor errors which I could deal with by repairing them in Icem. So, as a result of export files to .igs, a clear loss of information from the original file geometry occurs.

Regarding to the rotor meshing, a non structured mesh with tetrahedral elements has been done. Previously, the intention was to carry out an structured hexahedral mesh by using blocking strategy in order to get a perfect quality grid.

Nevertheless I realized that the study area where the RSI occurs is in the rotor and stator union so, thereby only the initial part of it has high computational interest. Even so, the obtained quality mesh was pretty acceptable.

On the other hand the stator mesh have been done with a blocking strategy because in this case is interesting to capture all the effects involved in the stator as they play an essential role in the RSI. Therefore a well done boundary layer has been defined around the stator vanes.

With respect to the solution setting, I have established a transient simulation due to the potential effect and the wake interaction which make the flow to be non-stationary. Also is interesting to modify the relaxation parameters which amortize instabilities during the simulation with the aim that the solution converges. It is important to highlight that a wrong use of them could destroy the simulation because

as we reduce these coefficients, increases the diffusion of the interest phenomena and consequently decreases the reliability of the results.

As summary the obtained results of the entire study are satisfying. The numerical model has approximated well to the behaviour of the real turbine. Also the used turbulence model has approximated well the real flow turbulence.

However in future projects it would be interesting to improve both quality meshes to get better results as well as propose other stator vane geometries in order to reduce the RSI effects, such as simulating a rotor-stator domain with Donaldson vanes and to compare both study results.

CHAPTER 6. BIBLIOGRAPHY

6.1. Reference bibliography

1. Zobeiri, A., Kueny, J., Farhat, M., and Avellan, F., 2006. "*Pump-turbine Rotor-Stator Interactions in Generating Mode: Pressure Fluctuation in Distributor Channel*". 23rd IAHR Symposium on Hydraulic Machinery and Systems, Paper Code num. 235.
2. Dring, R.P., Joslyn, H.D., Hardin, L.W., and Wagner, J.H., 1982. "*Turbine Rotor-Stator Interaction*". Journal of Engineering for Power, Oct. 1982, Vol. 104, pp 729-742.
3. Arndt, N., Acosta, A. J., Brennen, C. E., and Caughey, T. K., 1989. "*Rotor-Stator Interaction in a Diffuser Pump*". J. of Turbomachinery (1989) 111:213-221.
4. Giesing, J.P., 1968. "*Nonlinear Two-Dimensional Unsteady Potential Flow with Lift*". J. Aircraft, Mar. – Apr. 1968, Vol. 5, No. 2, pp. 135-143.
5. Giesing, J.P., 1968. "*Nonlinear Interaction of two Lifting Bodies in Arbitrary Unsteady Motion*". ASME Journal of Basic Eng., Sept. 1968, pp. 387-394.
6. Lienhard, J.H., 1966. "Synopsis of lift, drag, and vortex frequency data for rigid circular cylinders", Technical Extension Service (1966).
7. Ausoni, P., Farhat, M., Escaler, X., Egusquiza, E., and Avellan, F., 2007. "*Cavitation Influence on von Kármán Vortex Shedding and Induced Hydrofoil Vibrations*". Journal of fluids engineering-transactions of the ASME ISSN: 0098-2202, Vol.: 129, N°: 8, pp.966-973 (2007).
8. Kármán, T. V., 1921. "*Über laminare und turbulente Reibung*". ZAMM - Journal of Applied Mathematics and Mechanics / Zeitschrift für Angewandte Mathematik und Mechanik, Volume 1, Issue 4, pages 233–252, 1921.
9. Kármán., T.V., and Sears, W.R., 1938. "*Airfoil Theory for Non-Uniform Motion*", Journal of the Aeronautical Sciences, Vol.5, No. 10 (1938), pp. 379-390.
10. Sears, W.R., 1941. "*Some Aspects of Nonstationary Airfoil Theory and Its Practical Applications*". J. Aero. Sci. Vol.B, No.2, pp.4-10B, February 1941.
11. Kemp, N.H., 1952. "*On The Lift And Circulation Of Airfoils In Some Unsteady Motion*". J. of Aero. Sci., 19, pag. 713 (1952).

12. Silkowski, P.D., Rhie, C.M., Copeland, G.S., Eley, J.A., and Bleeg, J.M., 2001. "CFD Investigation of Aeromechanics". ASME Turbo Expo 2001: Power for Land, Sea, and Air, New Orleans, Louisiana, USA, June 4–7, 2001.
13. Horlock, J. H., 1968. "Fluctuating Lift Forces on Aerofoils Moving Through Transverse and Chordwise Gusts". J. Basic Eng. 90(4), 494-500 (Dec 01,1968).
14. Graham, J.M.R., 1970. "Similarity Rules for Thin Airfoils in Non-Stationary Subsonic Flows". J. Fluid Mechanics, 43, pag.753 (1970).
15. Filotas, L. T., 1969. "Response of an Infinite Wing to an Oblique Sinusoidal Gust: a Generalization of Sears' Problem". Basic Aerodynamic Noise Research. NASA SP-207, edited by Ira R. Schwartz, published by NASA, Washington, D.C., 1969, p.231
16. Mugridge, B.D., 1971. "Turbulent Boundary Layers and Surface Pressure Fluctuations on Two-Dimensional Aerofoils". Journal of Sound and Vibration, Volume 18, Issue4, 22 October 1971, Pages 475-486.
17. Adamczyk, J.J., 1974. "The Passage of an Infinite Swept Airfoil Through an Oblique Gust". National Aeronautics and Space Administration • Washington; D. C., May 1974.
18. Osborne, C., 1971. "Compressibility Effects In The Unsteady Interactions Between Blade Rows". Ph.D. Thesis, Cornell University, Ithaca, NY (1971).
19. Parker, R., and Watson, J.F., 1972. "Interaction Effects between Blade Rows in Turbomachines". Proc. I. Mech. E., 186, 21/72 (1971).
20. Kerrebrock, J.L., and Mikolajczak, A.A., 1970. "Intra-Stator Transport of Rotor Wakes and Its Effect on Compressor Performance". J.Eng. Powe 92(4), 359-638, (Oct 1, 1970).
21. Haldeman, C.W., and Dunn, M.G., 2000. "Time-Averaged Heat Flux for a Recessed Tip, Lip, and Platform of a Transonic Turbine Blade". ASME Turbo Expo 2000: Power for Land, Sea, and Air Volume 3 Munich, Germany, May 8–11, (2000).
22. Hwang, R.R., and Yao, C.C., 1997. "A Numerical Study of Vortex Shedding From a Square Cylinder With Ground Effect". J. Fluids Eng. 119(3), 512-518 (Sep 1, 1997).
23. Jordan, S.A., and Ragab, S.A., 1998. "A Large-Eddy Simulation of the Near Wake of a Circular Cylinder". J. Fluids Eng. 120(2), 243-252 (Jun 1, 1998).
24. Doolan, C.J. 2010. "Large Eddy Simulation of the Near Wake of a Circular Cylinder at Sub-critical Reynolds Number". Engineering Applications of Computational Fluid Mechanics Volume 4, Issue 4, pages 496-510 (2010)
25. Brun, C., Aubrun, S., Goossens, T., and Ravier, P., 2008. "Coherent Structures and their Frequency Signature in the Separated Shear Layer on the Sides of a Square Cylinder". Flow, Turbulence and Combustion July 2008, Volume 81, Issue 1, pp 97-114.
26. Ovchinnikov, V., Piomelli, U., and Choudhari, M.M., 2006. "Numerical simulations of boundary-layer transition induced by a cylinder wake". Journal of Fluid Mechanics, 547, pp 413-441.
27. Vu, T.C., Nennemann, B., Ausoni, P., Farhat, M., and Avellan, F., 2007. "Unsteady CFD prediction of von Kármán vortex shedding in hydraulic turbine stay vanes". Hydro 2007, Granada, Spain, 15-17 October 2007.

28. Münch, C., Ausoni, P., Braun, O., Farhat, M., and Avellan, F., 2010. "Fluid–structure coupling for an oscillating hydrofoil". *Journal of Fluids and Structures*, Volume 26, Issue 6, August 2010, Pages 1018–1033
29. Shi, F., and Tsukamoto, H., 2001. "Numerical Study of Pressure Fluctuations Caused by Impeller-Diffuser Interaction in a Diffuser Pump Stage". *J. Fluids Eng.* 123(3), 466-474 (Apr 12, 2001).
30. Wang, H., and Tsukamoto, H., 2001. "Fundamental Analysis on Rotor-Stator Interaction in a Diffuser Pump by Vortex Method". *J. Fluids Eng.* 123(4), 737-747 (Jun 29, 2001).
31. Zhang, M., and Tsukamoto, H., 2005. "Unsteady Hydrodynamic Forces due to Rotor-Stator Interaction on a Diffuser Pump With Identical Number of Vanes on the Impeller and Diffuser". *J. Fluids Eng.* 127(4), 743-751 (Apr 1, 2005).
32. Byskov, R.K. Jacobsen, C.B. and Pedersen, N., 2003. "Flow in a Centrifugal Pump Impeller at Design and Off-Design Conditions—Part II: Large Eddy Simulations". *J. Fluids Eng.* 125(1), 73-83 (Jan 22, 2003).
33. Guleren, K.M., and Pinarbasi A., 2004. "Numerical Simulation of the Stalled Flow Within a Vaned Centrifugal Pump". *Journal of Mechanical Engineering Science*, April 1, 2004 vol. 218 no. 4.
34. González, J., Parrondo, J., Santolaria, C., and Blanco, E., 2006. "Steady and Unsteady Radial Forces for a Centrifugal Pump With Impeller to Tongue Gap Variation". *J. Fluids Eng* 128(3), 454-462 (Sep 29, 2005).
35. Wang, J., Feng, T., Liu, K., and Zhou, Q., 2007 "Experimental Research on the Relationship between the Flow-induced Noise and the Hydraulic Parameters in Centrifugal Pump". Beijing Technology and Business University (2007).
36. K., Vasudeva, K., and Sharma, N.Y., 2009. "Numerical analysis on the effect of varying number of diffuser vanes on impeller - Diffuser flow interaction in a centrifugal fan". *World Journal of Medellín and Simulation*, Vol. 5 (2009) No. 1, pp. 63-71.
37. Feng, J., Benra, F., and Dohmen, H.J., 2010. "Investigation of Periodically Unsteady Flow in a Radial Pump by CFD Simulations and LDV Measurements". *J. Turbomach* 133(1), 011004 (Sep 07, 2010)
38. Cavazzini, G., Pavesi, G., and Ardizzon, G., 2011. "Pressure Instabilities in a Vaned Centrifugal Pump". *Journal of Power and Energy* November 2011 vol. 225 no. 7.
39. Denton, J.D., 2010. "Some Limitations of Turbomachinery CFD". *ASME Turbo Expo 2010: Power for Land, Sea, and Air* Volume 7: Turbomachinery, Parts A, B, and C pp. 735-745; Glasgow, UK, June 14–18, 2010.
40. Lahoz, J., 2015. "Simulación de una turbina hidráulica con CFD" Proyecto Final de Grado. Universitat Politècnica de Catalunya (UPC), Escola d'Enginyeria Tècnica Industrial de Barcelona (EUETIB)

6.2. Consultation bibliography

1. Fernandez, J. Manuel, *"Interacción No Estacionaria Entre el Rotor y el Estator en Una Turbomáquina Axial"*, Ph.D. Thesis. Universidad de Oviedo Biblioteca Universitaria, 2007.
2. Ausoni, P., Farhat, M., Avellan F., *"Cavitation in Kármán Vortex Shedding from 2D Hydrofoil. Wall Roughness Effects"*, article (2007). ASME/JSME Fluids Engineering Conference July 30-August 2, 2007.
3. Tedy, Muhammad, *"CFD Simulation of Vortex Induced Vibration of a Cylindrical Structure"*, Master Thesis. Faculty of Engineering Science and Technology Department of Civil and Transport Engineering.
4. S., Mittal, and A., Raghuvanshi, *"Control of Vortex Shedding Behind Circular Cylinder for Flows at Low Reynolds Numbers"*, article (2001). John Wiley & Sons. Ltd. 2001.
5. Oro, J.M. Fernández, and Pérez, J. González, *"Perspectiva histórica de la simulación numérica del flujo en máquinas hidráulicas"*, article (2014). 2014, IWA Publishing, Editorial UPV, FFIA.
6. Guardo, A., Fontanals, A., and Coussirat, M.G., *"Estudio Numerico de la Interaccion Rotor Estator en el Difusor de una Bomba"*, article (2013). 2013 Asociación Argentina de Mecánica Computacional.
7. George W. and Jones, Jr., *"Unsteady Lift Forces Generated by Vortex Shedding about a Large, Stationary, and Oscillating Cylinder at High Reynolds Numbers"*, Paper (1968), ASME Symposium on Unsteady Flow.
8. Laín S., García M. Julio, Quintero B., and Orrego S., *"Simulación Numérica del Flujo en Turbomáquinas Hidráulicas. Estado del Arte y Fuentes de Error. Aplicación a Turbinas Francis"*, article (2008). Revista Universidad EAFIT, Vol. 44. No. 152. 2008. pp. 90-114
9. Fontanals. A., *"Caracterització del flux a causa de la interacció rotor-estator en turbomàquines mitjançant CFD"*, Ph.D. Thesis (2012).
10. Yan, J., Koutnik, J., Seidel, U., Hübner, B., and Scherer, T., *"Compressible Simulation of Rotor-Stator Interaction in a Pump-Turbine"*, article (2009).
11. Guardo, A., Fontanals, A., and Coussirat, M.G., and Panella, L., *"Estudio del Fenómeno de Interacción Rotor Estator (Rsi) en una Bomba Radial, Trabajando Fuera de las Condiciones de Diseño Óptimo"*, article (2014). 2014 Asociación Argentina de Mecánica Computacional.
12. Rodriguez, C.G., Egusquiza, E., Santos, I.F., *"Frequencies in the Vibration Induced by the Rotor Stator Interaction in a Centrifugal Pump Turbine"*, article (2007). 2007 by ASME.
13. Rodriguez, C., Mateos-Prieto, B., and Egusquiza, E., *"Monitoring of Rotor-Stator Interaction in Pump-Turbine Using Vibrations Measured with On-Board Sensors Rotating with Shaft"*, article (2013). Hindawi Publishing Corporation Shock and Vibration Volume 2014.
14. Bartrons, J., *"Estudio Hidrodinámico por CFD del Casco de una Lancha Motora"*, Degree Paper (2014), Facultat De Nàutica De Barcelona, UPC
15. Laín S., García M. Julio, Avellan, F., Quintero B., and Orrego S., *"Simulación numérica de turbinas Francis"*, Book (2011). Fondo Editorial Universidad EAFIT 2011.

16. Arias, I., Parés, N., Gesto, J.M., Pozo, F., Gibergans, J., Pujol, G., Ikhouane, F., Vidal, Y., "*Cálculo Avanzado para Ingeniería*" Book 2008. Edicions UPC, 2010
17. Anthony, W., "*Cálculo Diferencial e Integral*", Book (2009). 2009, Editorial Limusa, S.A.
18. Burgos, J., "*Cálculo Infinitesimal de Varias Variables*", Book (1995). 1995, The McGraw-Hill Companies, Inc.
19. Anderson, J.D., "*Governing Equations of Fluid Dynamics*". J.F. Wendt (ed.), Computational Fluid Dynamics, 3rd ed., Springer-Verlag Berlin Heidelberg 2009
20. Versteeg, H.K., and Malalasekera, W., "*An Introduction to Computational Fluid Dynamics*" Book (1995). Pearson Education Limited 1995, 2007.
21. Petrova, R., "*Finite Volume Method-Powerful Means of Engineering Design*", Book (2012). INTECH Open Science /Open Minds 2012.
22. Anonymous, "*Método de los Volúmenes Finitos*", Book (2002).
23. Kubota, Y., Suzuki, T., Tomita, H., Nagafugi, T., and Okamura, C., "*Vibration of Rotating Bladed Disc Excited by Stationary Distributed Forces*", article (1983). JSME, Vol. 26, No. 221, Nov 1983.
24. White F.M., "*Mecánica de Fluidos*", Book (2008). 2008, The McGraw-Hill Companies, Inc.
25. Ansys, Inc, "*ANSYS ICEM CFD User Manual*", Book (2012). 2012 SAS IP, Inc.
26. Ansys, Inc, "*ANSYS ICEM CFD Tutorial Manual* ", Book (2013). 2013 SAS IP, Inc.
27. Ansys, Inc, "*ANSYS Fluent User's Guide*", Book (2013). 2013 SAS IP, Inc.
28. Ansys, Inc, "*ANSYS Fluent Tutorial Guide*", Book (2013). 2013 SAS IP, Inc.
29. Ansys, Inc, "*ANSYS Fluent Theory Guide*", Book (2013). 2013 SAS IP, Inc.
30. CFD Online: <http://www.cfd-online.com>
31. http://www.unet.edu.ve/~fenomeno/F_DE_T-164.htm
32. LEAP Australia, CFD Blog: <http://www.computationalfluidynamics.com.au/>



Escola Universitària d'Enginyeria
Tècnica Industrial de Barcelona
Consorci Escola Industrial de Barcelona

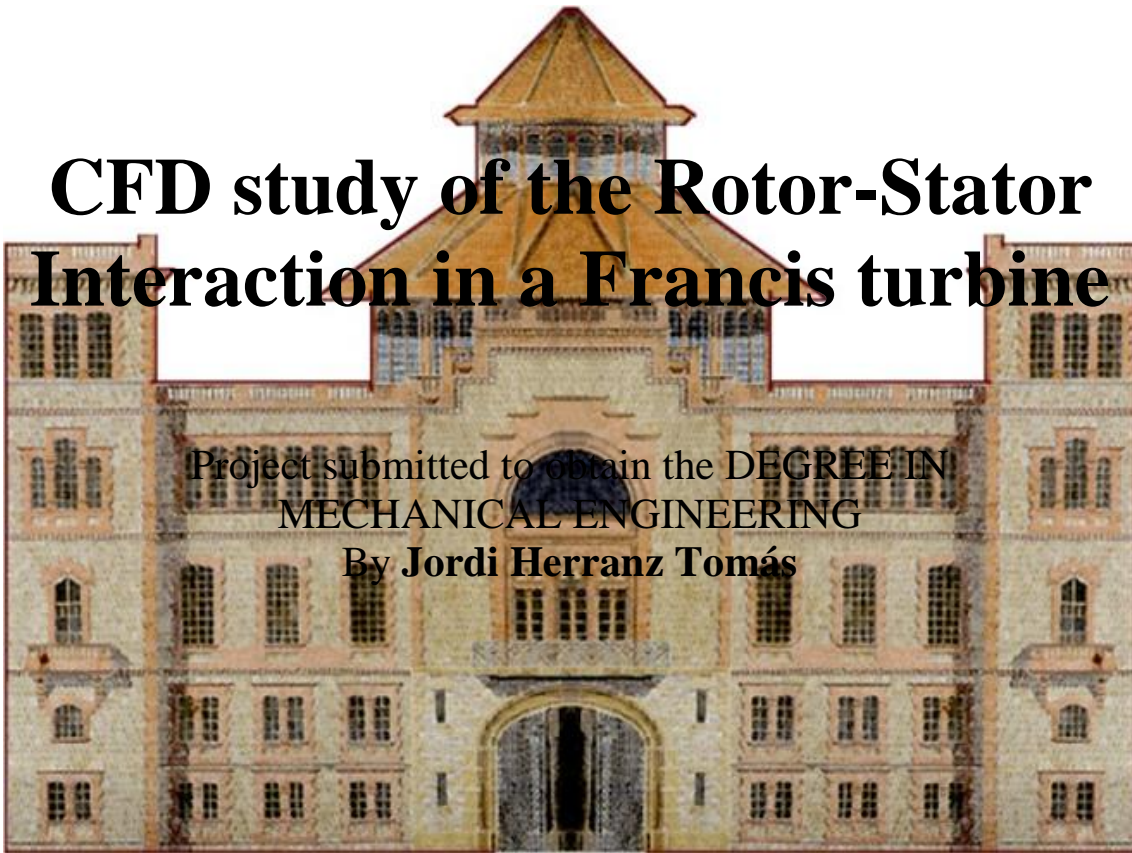
UNIVERSITAT POLITÈCNICA DE CATALUNYA

Budget

CFD study of the Rotor-Stator Interaction in a Francis turbine

Project submitted to obtain the **DEGREE IN
MECHANICAL ENGINEERING**

By Jordi Herranz Tomás



Barcelona, 26th April 2016

Director: Alfredo Guardo Zabaleta
Fluids Mechanics Department (MF)
Universitat Politècnica de Catalunya (UPC)

BUDGET TABLE OF CONTENTS

Budget table of contents	i
CHAPTER 1. Previous considerations.....	1
CHAPTER 2. Budget	2

CHAPTER 1. PREVIOUS CONSIDERATIONS

For carrying out the following budget has taken into account various concepts:

- Working hours do not take into account the self-learning hours regarding to the software, but only has been considered the working hours relating to the study.
- The engineering working hours will be spread across the four main parts of the study:
 - a. Geometry: Dedicated hours by specialized personnel to carry out the required CAD design.

Meshing: Dedicated hours by specialized personnel to carry out the domain meshes. This section is the most tedious, but also the most important. Every little detail not taken into account could wreck the simulation. Therefore a large amount of hours are required to avoid errors and mistakes.
 - b. Solution setting: Dedicated hours by specialized personnel to plan, define and set all the CFD study.
 - c. Results analysis and discussion: Dedicated hours by specialized personnel to obtain the results from the simulations, process the data and to draw conclusions about the complete CFD study. This section is the most specialized and thereby is the one that needs more qualified staff. Therefore the results analysis and discussion hours are the most expensive
- It is estimated that the software license cost used (Ansys 15.0) is about 1,5€/hour.
- The calculation hours in CSUC as well as in personal computers have a cost. This price is 0,05€ per hour and per processor used in the CSUC (<http://www.csuc.cat>) and it is estimated that the computational cost is the same for personal computers.

CHAPTER 2. BUDGET

Code	Concept	Unit	Quantity	Unit price	Sum
PB01	Engineering costs				
	Geometry	h	35	12	420,00 €
	Meshing	h	50	12	600,00 €
	Solution setting	h	20	12	240,00 €
	Results analysis and discussion	h	15	18	270,00 €
Partial Budget 1					1.530,00 €
PB02	Computing resource costs				
	4 core 3,40GHz Pcs.	h*pcs	500	0,05	25,00 €
	16 core 2,7GHz (CSUC Pcs.)	h*pcs	1344	0,05	67,20 €
Partial Budget 2					92,20 €
PB03	Licensing costs				
	ANSYS License	h	1844	1,5	2.766,00 €
Partial Budget 3					2.766,00 €
Material Execution Budget (MEB)					4.388,20 €
				13,00%	570,47 €
				6,00%	263,29 €
Contract Budget (CB)					5.221,96 €
				21,00%	1.096,61 €
Total Budget					6.318,57 €

This total budget ascend to the sum of six thousand, three hundred and eighteen Euro and fifty-seven cents (6.318,57€).



Escola Universitària d'Enginyeria
Tècnica Industrial de Barcelona
Consorci Escola Industrial de Barcelona

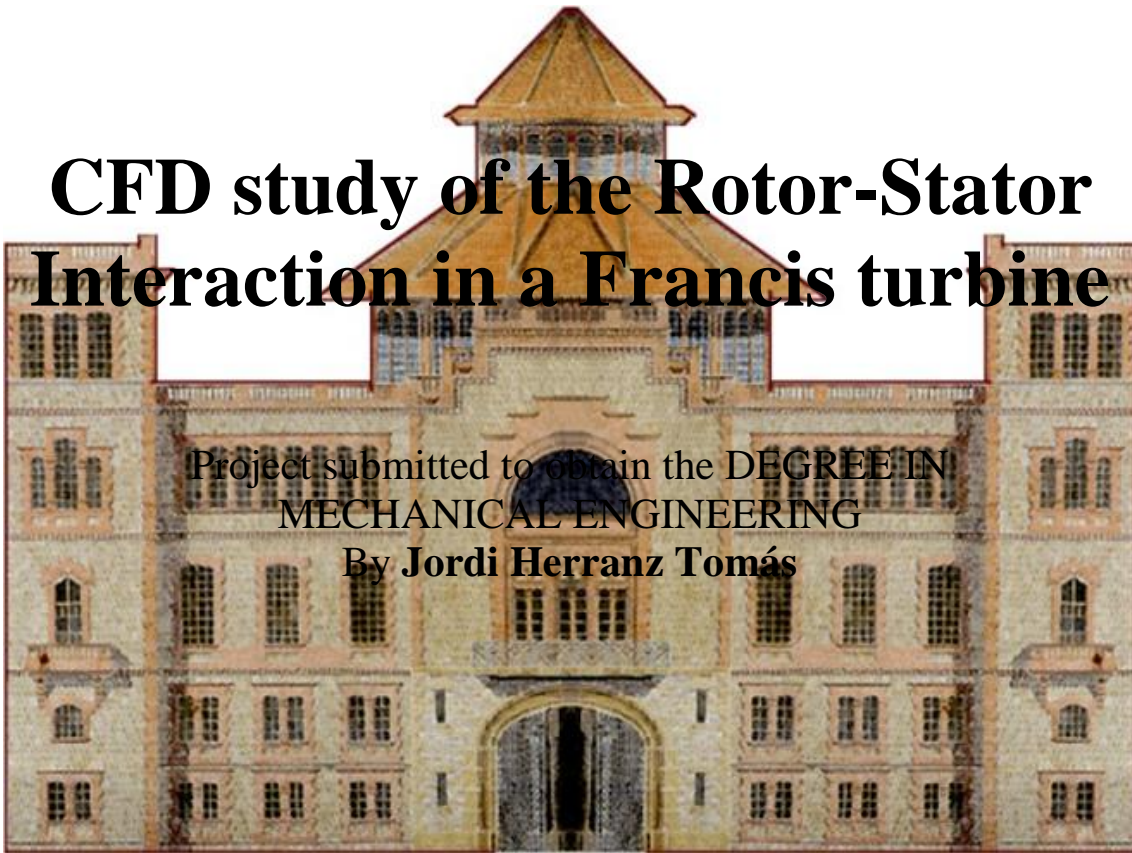
UNIVERSITAT POLITÈCNICA DE CATALUNYA

Annexes

CFD study of the Rotor-Stator Interaction in a Francis turbine

Project submitted to obtain the **DEGREE IN
MECHANICAL ENGINEERING**

By Jordi Herranz Tomás



Barcelona, 26th April 2016

Director: Alfredo Guardo Zabaleta
Fluids Mechanics Department (MF)
Universitat Politècnica de Catalunya (UPC)

ANNEXES TABLE OF CONTENTS

Annexes table of contents	i
CHAPTER 1. Meshing.....	1
1.1. Annex A: Rotor meshing quality	1
1.2. Annex B: Stator meshing quality	3
CHAPTER 2. Results.....	5
2.1. Annex C: Static pressure point monitors	5
2.2. Annex D: Frequencies of the pressure monitors	32

CHAPTER 1. MESHING

1.1. Annex A: Rotor meshing quality

Min = 0.433876, max = 1, mean = 0.930828097131	Min = 2.00047, max = 10.2767, mean = 3.39705200692
2849871 elements with the "Orthogonal Quality" diagnostic	2849871 elements with the "Aspect Ratio (Fluent)" diagnostic
Histogram of Orthogonal Quality values	Histogram of Aspect Ratio (Fluent) values
0.95 -> 1.0 : 89322 (3.134%)	9.762865 -> 10.2767 : 21 (0.001%)
0.9 -> 0.95 : 2438277 (85.557%)	9.24903 -> 9.762865 : 118 (0.004%)
0.85 -> 0.9 : 109279 (3.835%)	8.735195 -> 9.24903 : 377 (0.013%)
0.8 -> 0.85 : 74239 (2.605%)	8.22136 -> 8.735195 : 1025 (0.036%)
0.75 -> 0.8 : 51134 (1.794%)	7.707525 -> 8.22136 : 2489 (0.087%)
0.7 -> 0.75 : 36704 (1.288%)	7.19369 -> 7.707525 : 5583 (0.196%)
0.65 -> 0.7 : 24878 (0.873%)	6.679855 -> 7.19369 : 11113 (0.390%)
0.6 -> 0.65 : 15483 (0.543%)	6.16602 -> 6.679855 : 20709 (0.727%)
0.55 -> 0.6 : 7359 (0.258%)	5.652185 -> 6.16602 : 33511 (1.176%)
0.5 -> 0.55 : 2577 (0.090%)	5.13835 -> 5.652185 : 52040 (1.826%)
0.45 -> 0.5 : 586 (0.021%)	4.624515 -> 5.13835 : 80094 (2.810%)
0.4 -> 0.45 : 33 (0.001%)	4.11068 -> 4.624515 : 114158 (4.006%)
0.35 -> 0.4 : 0 (0.000%)	3.596845 -> 4.11068 : 110047 (3.861%)
0.3 -> 0.35 : 0 (0.000%)	3.08301 -> 3.596845 : 2343778 (82.242%)
0.25 -> 0.3 : 0 (0.000%)	2.569175 -> 3.08301 : 17039 (0.598%)
0.2 -> 0.25 : 0 (0.000%)	2.05534 -> 2.569175 : 56282 (1.975%)
0.15 -> 0.2 : 0 (0.000%)	1.541505 -> 2.05534 : 1487 (0.052%)
0.1 -> 0.15 : 0 (0.000%)	1.02767 -> 1.541505 : 0 (0.000%)
0.05 -> 0.1 : 0 (0.000%)	0.513835 -> 1.02767 : 0 (0.000%)
0.0 -> 0.05 : 0 (0.000%)	0.0 -> 0.513835 : 0 (0.000%)

Figure 1.1 Rotor diagnostic about the orthogonal quality, on the left and the aspect ratio, on the right

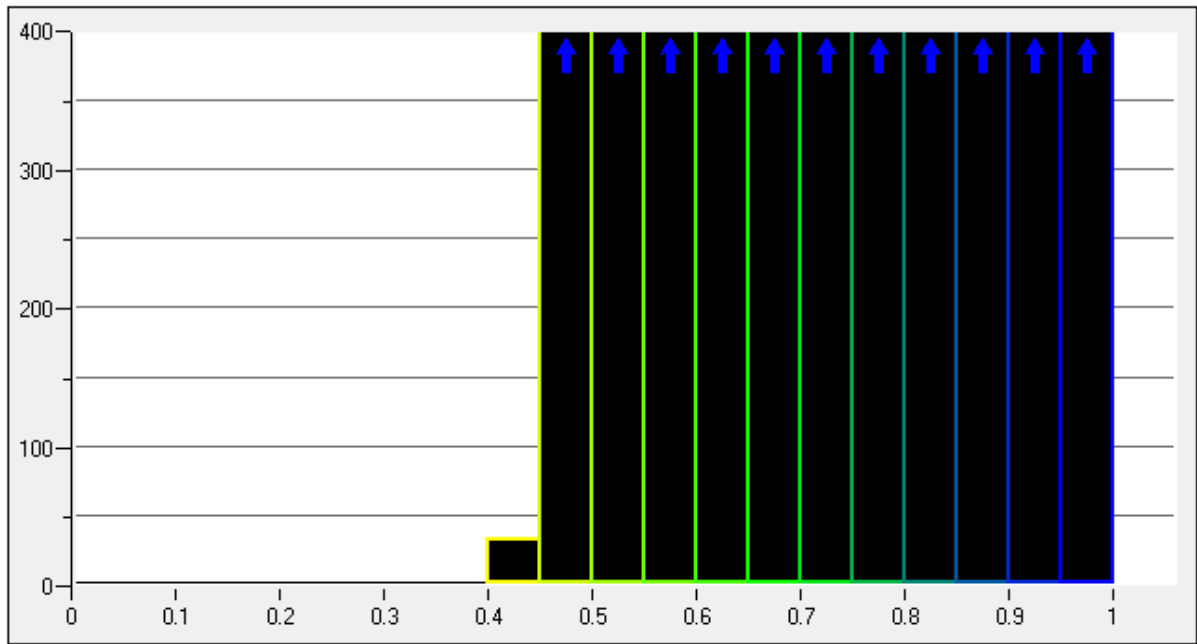


Figure 1.2 Orthogonal quality histogram for the rotor mesh

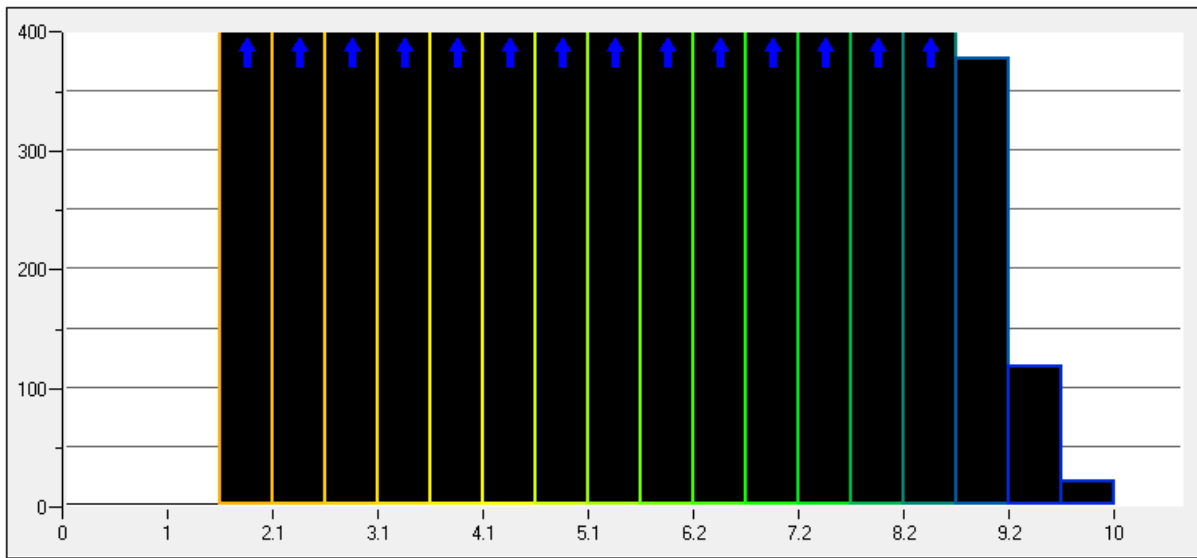


Figure 1.3 Aspect ratio histogram for the rotor mesh

1.2. Annex B: Stator meshing quality

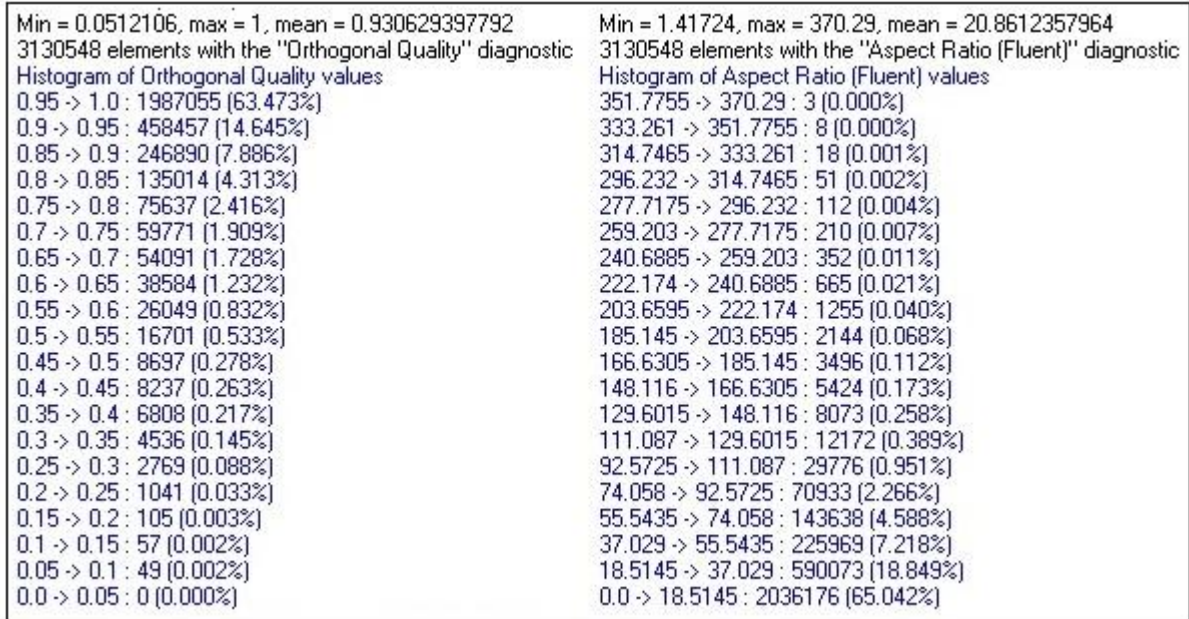


Figure 1.4 Stator diagnostic about the orthogonal quality, on the left and the aspect ratio, on the right

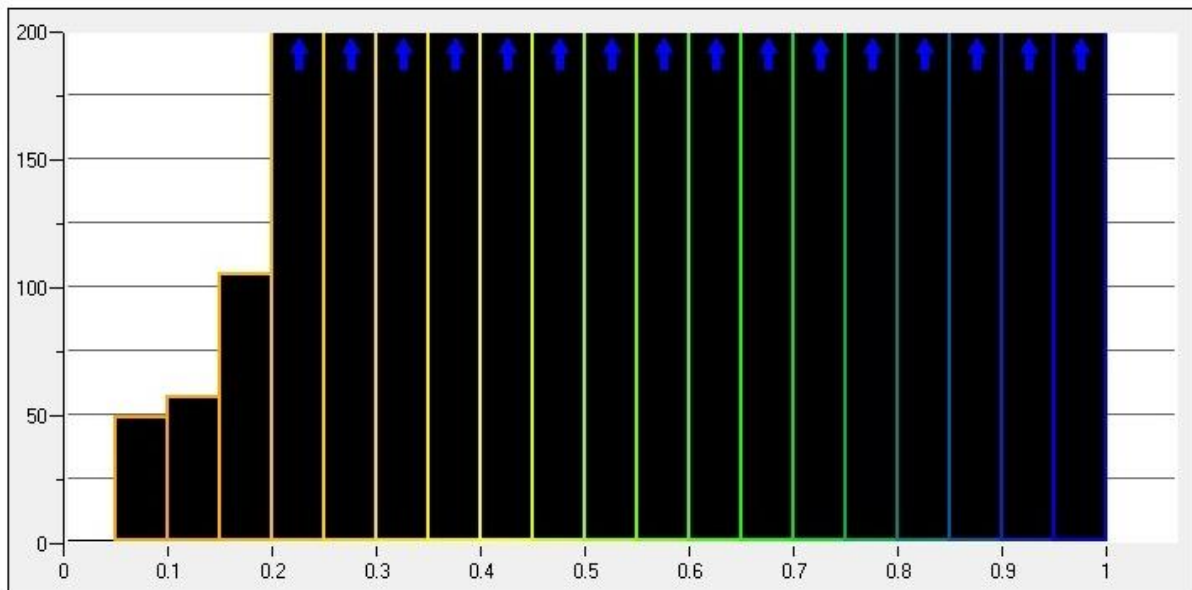


Figure 1.5 Orthogonal quality histogram for the stator mesh

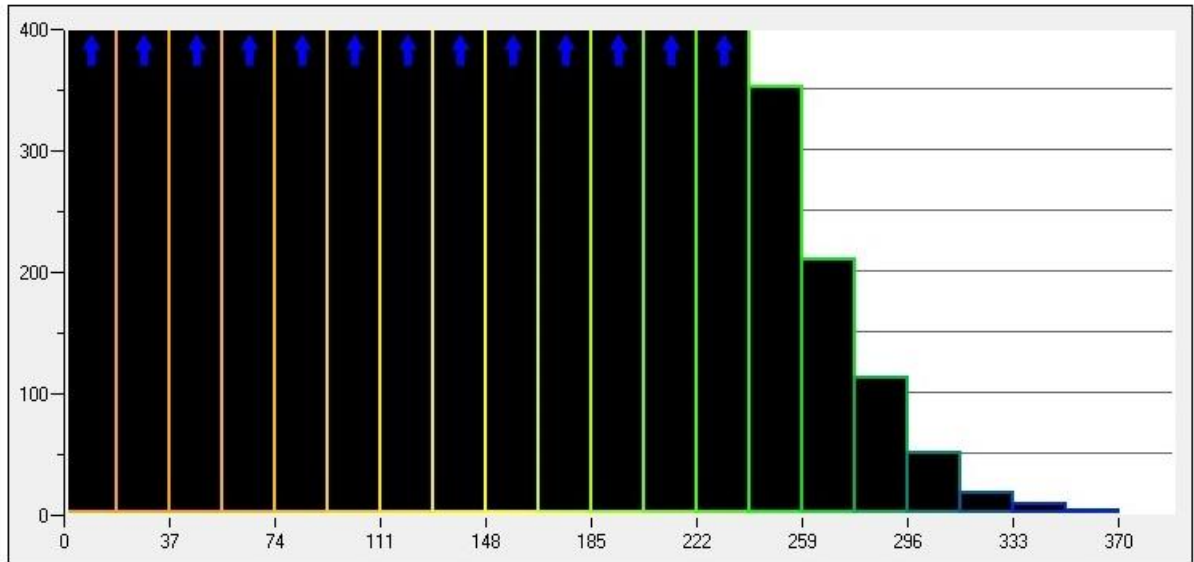


Figure 1.6 Aspect ratio histogram for the stator mesh

CHAPTER 2. RESULTS

2.1. Annex C: Static pressure point monitors

t(s)	p[Pa]	t(s)	p[Pa]
2,222107887	9675935	2,272111893	10075611
2,222385645	9648982	2,27238965	10423909
2,222663403	9642454	2,272667408	10937435
2,22294116	9567883	2,272945166	11544229
2,223219156	9540700	2,273222923	12220614
2,223496914	9526789	2,273500919	13310371
2,223774672	9411754	2,273778677	14388974
2,224052429	9293260	2,274056435	14377641
2,224330187	9182454	2,274334192	13305670
2,224607944	9046894	2,27461195	12483273
2,224885941	9013882	2,274889946	11796978
2,225163698	9008310	2,275167704	11164937
2,225441456	8963095	2,275445461	10931255
2,225719213	8995786	2,275723219	10639474
2,225996971	9011572	2,276000977	10493264
2,226274729	9003948	2,276278734	10369192
2,226552725	9052122	2,27655673	10316114
2,226830482	9073128	2,276834488	10190051
2,22710824	9076336	2,277112246	10114982
2,227385998	9139571	2,277390003	10113746
2,227663755	9180853	2,277667761	9997376
2,227941751	9224293	2,277945518	9930486
2,228219509	9352338	2,278223515	9899192
2,228497267	9449359	2,278501272	9822951
2,228775024	9574132	2,27877903	9737276
2,229052782	9824551	2,279056787	9669251
2,22933054	10080767	2,279334545	9674147
2,229608536	10518672	2,279612541	9561280
2,229886293	11091200	2,279890299	9494261
2,230164051	11663382	2,280168056	9470342
2,230441809	12547334	2,280445814	9477654

2,230719566	13789505	2,280723572	9364790
2,230997562	14633214	2,281001329	9311573
2,23127532	14191773	2,281279325	9129424
2,231553078	13211701	2,281557083	9009726
2,231830835	12283591	2,281834841	9001095
2,232108593	11687627	2,282112598	8910806
2,232386351	11230260	2,282390356	8953658
2,232664347	10880384	2,282668352	8892563
2,232942104	10652859	2,28294611	8935178
2,233219862	10572208	2,283223867	8969796
2,23349762	10384129	2,283501625	8950888
2,233775377	10280098	2,283779383	9000154
2,234053135	10274215	2,28405714	9014296
2,234331131	10140645	2,284335136	9042038
2,234608889	10070655	2,284612894	9110320
2,234886646	10031204	2,284890652	9151612
2,235164404	9960741	2,285168409	9208309
2,235442162	9848811	2,285446167	9353353
2,235720158	9798369	2,285724163	9406100
2,235997915	9721683	2,286001921	9651514
2,236275673	9674043	2,286279678	9820880
2,236553431	9629924	2,286557436	10185460
2,236831188	9520855	2,286835194	10621477
2,237108946	9497403	2,287112951	11236114
2,237386942	9474055	2,287390947	11829353
2,2376647	9403763	2,287668705	12830294
2,237942457	9384871	2,287946463	14084317
2,238220215	9245965	2,28822422	14653815
2,238497972	9086415	2,288501978	13954476
2,23877573	9086587	2,288779736	12951139
2,239053726	8964289	2,289057732	12054866
2,239331484	8940892	2,289335489	11480247
2,239609241	8964539	2,289613247	11081819
2,239886999	8927839	2,289891005	10788448
2,240164757	8961099	2,290168762	10558183
2,240442753	8958144	2,290446758	10442262
2,24072051	8989034	2,290724516	10337825
2,240998268	9040832	2,291002274	10240680
2,241276026	9015556	2,291280031	10147018
2,241553783	9075169	2,291557789	10111985
2,241831541	9121096	2,291835546	10073627
2,242109537	9165221	2,292113543	9961682
2,242387295	9238415	2,2923913	9940098
2,242665052	9346392	2,292669058	9891374
2,24294281	9475716	2,292946815	9800326
2,243220568	9635210	2,293224573	9796961
2,243498325	9871624	2,293502331	9682996
2,243776321	10253755	2,293780327	9637416

2,244054079	10748254	2,294058084	9658786
2,244331837	11259074	2,294335842	9533920
2,244609594	12006266	2,2946136	9487880
2,244887352	13028634	2,294891357	9520276
2,245165348	14165137	2,295169353	9376494
2,245443106	14291712	2,295447111	9313845
2,245720863	13323968	2,295724869	9118704
2,245998621	12319974	2,296002626	9043625
2,246276379	11622327	2,296280384	9020301
2,246554136	11087485	2,296558142	8990668
2,246832132	10792228	2,296836138	8976305
2,24710989	10498850	2,297113895	9030830
2,247387648	10346613	2,297391653	8971995
2,247665405	10227693	2,297669411	9012945
2,247943163	10087734	2,297947168	9114250
2,248220921	10086451	2,298224926	9064528
2,248498917	10027005	2,298502922	9110720
2,248776674	9926095	2,29878068	9210379
2,249054432	9864063	2,299058437	9200806
2,24933219	9869465	2,299336195	9293751
2,249609947	9777092	2,299613953	9392599
2,249887943	9733962	2,299891949	9453387
2,250165701	9710705	2,300169706	9676390
2,250443459	9636507	2,300447464	9833916
2,250721216	9616387	2,300725222	10052105
2,250998974	9564307	2,301002979	10575659
2,251276731	9507279	2,301280737	11028406
2,251554728	9504174	2,301558733	11627017
2,251832485	9445180	2,301836491	12491901
2,252110243	9395304	2,302114248	13657958
2,252388	9317707	2,302392006	14783886
2,252665758	9191602	2,302669764	14569048
2,252943754	9058476	2,302947521	13364621
2,253221512	9002531	2,303225517	12568068
2,253499269	8971314	2,303503275	11757711
2,253777027	8930571	2,303781033	11314348
2,254054785	8947637	2,30405879	10952082
2,254332542	8954563	2,304336548	10686562
2,254610538	8959260	2,304614544	10559815
2,254888296	9028006	2,304892302	10399567
2,255166054	9014040	2,305170059	10252454
2,255443811	9028527	2,305447817	10224996
2,255721569	9103868	2,305725574	10151380
2,255999327	9113960	2,306003332	10020275
2,256277323	9150458	2,306281328	10006346
2,25655508	9269862	2,306559086	9964796
2,256832838	9348985	2,306836843	9893470
2,257110596	9418242	2,307114601	9744685

2,257388353	9653128	2,307392359	9756858
2,257666349	9800009	2,307670116	9664047
2,257944107	10134541	2,307948112	9657944
2,258221865	10601274	2,30822587	9533488
2,258499622	11113837	2,308503628	9522888
2,25877738	11765490	2,308781385	9420518
2,259055138	12635195	2,309059143	9413776
2,259333134	13893185	2,309337139	9372053
2,259610891	14742601	2,309614897	9222035
2,259888649	14290872	2,309892654	9060464
2,260166407	13172641	2,310170412	8992167
2,260444164	12324749	2,31044817	8888129
2,26072216	11676545	2,310726166	8886089
2,260999918	11241714	2,311003923	8912502
2,261277676	10851528	2,311281681	8880107
2,261555433	10695164	2,311559439	8894017
2,261833191	10495480	2,311837196	8953301
2,262110949	10433613	2,312114954	8959656
2,262388945	10274662	2,31239295	8991252
2,262666702	10228987	2,312670708	9064560
2,26294446	10175735	2,312948465	9079021
2,263222218	10084348	2,313226223	9111860
2,263499975	10010100	2,313503981	9233868
2,263777733	9998364	2,313781738	9283492
2,264055729	9882608	2,314059734	9385915
2,264333487	9827655	2,314337492	9491766
2,264611244	9773323	2,31461525	9688167
2,264889002	9725243	2,314893007	9976003
2,265166759	9647875	2,315170765	10240750
2,265444756	9566192	2,315448761	10796366
2,265722513	9581347	2,315726519	11402968
2,266000271	9512044	2,316004276	12034749
2,266278028	9457995	2,316282034	13102484
2,266555786	9406842	2,316559792	14387870
2,266833544	9292741	2,316837549	14643124
2,26711154	9126532	2,317115545	13588165
2,267389297	9090572	2,317393303	12680404
2,267667055	8993249	2,317671061	11792251
2,267944813	8981030	2,317948818	11362720
2,26822257	9024517	2,318226576	11004432
2,268500328	8970912	2,318504333	10712288
2,268778324	9030634	2,31878233	10523764
2,269056082	8996500	2,319060087	10383193
2,269333839	9074228	2,319337845	10277171
2,269611597	9042531	2,319615602	10231802
2,269889355	9120748	2,31989336	10096809
2,270167351	9155149	2,320171356	10060372
2,270445108	9186057	2,320449114	10027907

2,270722866	9309044	2,320726871	9896850
2,271000624	9324880	2,321004629	9910113
2,271278381	9452620	2,321282387	9828802
2,271556139	9613563	2,321560144	9739463
2,271834135	9768064	2,32183814	9726694

Table 1 Static pressure variation versus flow time on the point monitor 1

t(s)	p[Pa]	t(s)	p[Pa]
2,222107887	9962454	2,272111893	10511613
2,222385645	9957083	2,27238965	10715177
2,222663403	9867527	2,272667408	11091078
2,22294116	9854459	2,272945166	11569075
2,223219156	9828529	2,273222923	12280131
2,223496914	9744570	2,273500919	13370003
2,223774672	9712214	2,273778677	14381343
2,224052429	9588400	2,274056435	14375435
2,224330187	9439568	2,274334192	13424500
2,224607944	9382550	2,27461195	12685081
2,224885941	9339102	2,274889946	12030447
2,225163698	9305784	2,275167704	11443302
2,225441456	9356934	2,275445461	11219003
2,225719213	9366048	2,275723219	10943476
2,225996971	9390520	2,276000977	10801311
2,226274729	9492171	2,276278734	10661887
2,226552725	9545290	2,27655673	10643969
2,226830482	9649270	2,276834488	10500140
2,22710824	9778552	2,277112246	10408047
2,227385998	9761650	2,277390003	10366275
2,227663755	9731873	2,277667761	10334171
2,227941751	9797184	2,277945518	10241250
2,228219509	9836073	2,278223515	10202203
2,228497267	9960710	2,278501272	10098719
2,228775024	10144269	2,27877903	10036067
2,229052782	10287885	2,279056787	9988758
2,22933054	10483246	2,279334545	9886313
2,229608536	10814775	2,279612541	9872882
2,229886293	11129335	2,279890299	9780893
2,230164051	11693844	2,280168056	9736031
2,230441809	12658259	2,280445814	9741973
2,230719566	13756586	2,280723572	9630896
2,230997562	14587555	2,281001329	9566613
2,23127532	14260066	2,281279325	9429704
2,231553078	13293641	2,281557083	9298874
2,231830835	12472221	2,281834841	9305593
2,232108593	11983100	2,282112598	9234647
2,232386351	11461249	2,282390356	9246062
2,232664347	11174604	2,282668352	9277316

2,232942104	10997511	2,28294611	9303058
2,233219862	10816701	2,283223867	9343269
2,23349762	10705867	2,283501625	9441811
2,233775377	10622075	2,283779383	9520648
2,234053135	10531323	2,28405714	9634905
2,234331131	10463251	2,284335136	9717366
2,234608889	10392897	2,284612894	9686167
2,234886646	10282576	2,284890652	9733526
2,235164404	10290827	2,285168409	9736147
2,235442162	10148804	2,285446167	9836521
2,235720158	10046835	2,285724163	9987834
2,235997915	10055760	2,286001921	10163584
2,236275673	9943471	2,286279678	10270937
2,236553431	9877148	2,286557436	10599365
2,236831188	9831074	2,286835194	10785265
2,237108946	9747695	2,287112951	11276057
2,237386942	9741463	2,287390947	11912855
2,2376647	9691320	2,287668705	12843414
2,237942457	9627527	2,287946463	14076294
2,238220215	9558126	2,28822422	14634757
2,238497972	9385414	2,288501978	13944702
2,23877573	9344389	2,288779736	13107749
2,239053726	9305742	2,289057732	12282639
2,239331484	9269776	2,289335489	11684248
2,239609241	9291644	2,289613247	11398517
2,239886999	9302153	2,289891005	11083573
2,240164757	9332224	2,290168762	10819210
2,240442753	9389976	2,290446758	10781723
2,24072051	9464826	2,290724516	10625797
2,240998268	9572394	2,291002274	10523757
2,241276026	9654490	2,291280031	10492916
2,241553783	9700242	2,291557789	10376395
2,241831541	9705456	2,291835546	10358958
2,242109537	9682403	2,292113543	10303592
2,242387295	9709278	2,2923913	10190184
2,242665052	9880347	2,292669058	10184875
2,24294281	9985570	2,292946815	10119325
2,243220568	10112614	2,293224573	10041744
2,243498325	10330045	2,293502331	9970167
2,243776321	10557742	2,293780327	9929555
2,244054079	10905752	2,294058084	9880460
2,244331837	11314691	2,294335842	9831789
2,244609594	12021918	2,2946136	9758044
2,244887352	13111033	2,294891357	9745790
2,245165348	14144651	2,295169353	9705537
2,245443106	14261626	2,295447111	9587936
2,245720863	13467649	2,295724869	9381154
2,245998621	12499408	2,296002626	9394004

2,246276379	11858062	2,296280384	9323377
2,246554136	11404761	2,296558142	9313115
2,246832132	11051665	2,296836138	9354639
2,24710989	10822434	2,297113895	9376410
2,247387648	10686191	2,297391653	9393557
2,247665405	10506889	2,297669411	9465171
2,247943163	10424223	2,297947168	9566195
2,248220921	10419044	2,298224926	9696927
2,248498917	10293576	2,298502922	9773559
2,248776674	10263590	2,29878068	9825567
2,249054432	10185751	2,299058437	9811566
2,24933219	10143935	2,299336195	9814485
2,249609947	10115307	2,299613953	9921136
2,249887943	10038194	2,299891949	9992995
2,250165701	9974610	2,300169706	10176638
2,250443459	9967613	2,300447464	10365107
2,250721216	9898252	2,300725222	10489812
2,250998974	9824402	2,301002979	10840086
2,251276731	9817179	2,301280737	11142145
2,251554728	9763422	2,301558733	11661759
2,251832485	9699558	2,301836491	12572873
2,252110243	9711919	2,302114248	13675399
2,252388	9587881	2,302392006	14692609
2,252665758	9470808	2,302669764	14588159
2,252943754	9405128	2,302947521	13501245
2,253221512	9285430	2,303225517	12707221
2,253499269	9283697	2,303503275	11995222
2,253777027	9318230	2,303781033	11613848
2,254054785	9284599	2,30405879	11229586
2,254332542	9326701	2,304336548	10976513
2,254610538	9423944	2,304614544	10833355
2,254888296	9437821	2,304892302	10741185
2,255166054	9526042	2,305170059	10568861
2,255443811	9678876	2,305447817	10513842
2,255721569	9728424	2,305725574	10481168
2,255999327	9716786	2,306003332	10337518
2,256277323	9742965	2,306281328	10314159
2,25655508	9734862	2,306559086	10259828
2,256832838	9853513	2,306836843	10198391
2,257110596	9988825	2,307114601	10049305
2,257388353	10121125	2,307392359	10063461
2,257666349	10286471	2,307670116	9929898
2,257944107	10570169	2,307948112	9939269
2,258221865	10784030	2,30822587	9848833
2,258499622	11173094	2,308503628	9749141
2,25877738	11851563	2,308781385	9692632
2,259055138	12648392	2,309059143	9719382
2,259333134	13912806	2,309337139	9603470

2,259610891	14710598	2,309614897	9504303
2,259888649	14259317	2,309892654	9398944
2,260166407	13323193	2,310170412	9262435
2,260444164	12522296	2,31044817	9203895
2,26072216	11876211	2,310726166	9252911
2,260999918	11563484	2,311003923	9214147
2,261277676	11132749	2,311281681	9251155
2,261555433	10970430	2,311559439	9297065
2,261833191	10834198	2,311837196	9339637
2,262110949	10727915	2,312114954	9468538
2,262388945	10580269	2,31239295	9544632
2,262666702	10553417	2,312670708	9685760
2,26294446	10448878	2,312948465	9768970
2,263222218	10419067	2,313226223	9734884
2,263499975	10311608	2,313503981	9783024
2,263777733	10261931	2,313781738	9826138
2,264055729	10209876	2,314059734	9952411
2,264333487	10116166	2,314337492	10029052
2,264611244	10054406	2,31461525	10250520
2,264889002	10012888	2,314893007	10423351
2,265166759	9922801	2,315170765	10598777
2,265444756	9836930	2,315448761	10980290
2,265722513	9858179	2,315726519	11432645
2,266000271	9767640	2,316004276	12097538
2,266278028	9737397	2,316282034	13125575
2,266555786	9706684	2,316559792	14351684
2,266833544	9546241	2,316837549	14619178
2,26711154	9437252	2,317115545	13669009
2,267389297	9385936	2,317393303	12821021
2,267667055	9307032	2,317671061	12064477
2,267944813	9328131	2,317948818	11618248
2,26822257	9352882	2,318226576	11276835
2,268500328	9329668	2,318504333	11030988
2,268778324	9423817	2,31878233	10810868
2,269056082	9425835	2,319060087	10715126
2,269333839	9541082	2,319337845	10591126
2,269611597	9620395	2,319615602	10504027
2,269889355	9750676	2,31989336	10450533
2,270167351	9810069	2,320171356	10363976
2,270445108	9767615	2,320449114	10302438
2,270722866	9796230	2,320726871	10246714
2,271000624	9880353	2,321004629	10190676
2,271278381	9979913	2,321282387	10118959
2,271556139	10104870	2,321560144	10074996
2,271834135	10314810	2,32183814	9976052

Table 2 Static pressure variation versus flow time on the point monitor 2

t(s)	p[Pa]	t(s)	p[Pa]
2,222107887	10033372	2,272111893	10619062
2,222385645	10000424	2,27238965	10777606
2,222663403	10007575	2,272667408	11093308
2,22294116	9973626	2,272945166	11506260
2,223219156	9961668	2,273222923	12119481
2,223496914	9987793	2,273500919	13063483
2,223774672	9977740	2,273778677	14012072
2,224052429	9923915	2,274056435	13983577
2,224330187	9860030	2,274334192	13143844
2,224607944	9653368	2,27461195	12456876
2,224885941	9466163	2,274889946	11969220
2,225163698	9406577	2,275167704	11413726
2,225441456	9336312	2,275445461	11216461
2,225719213	9347529	2,275723219	10935405
2,225996971	9438559	2,276000977	10834586
2,226274729	9486176	2,276278734	10733121
2,226552725	9567589	2,27655673	10613548
2,226830482	9720738	2,276834488	10579303
2,22710824	9768468	2,277112246	10465958
2,227385998	9860768	2,277390003	10399773
2,227663755	10001437	2,277667761	10378054
2,227941751	10023234	2,277945518	10265629
2,228219509	10093835	2,278223515	10216200
2,228497267	10244214	2,278501272	10156010
2,228775024	10294965	2,27877903	10072292
2,229052782	10427000	2,279056787	10041596
2,22933054	10628686	2,279334545	9954908
2,229608536	10805622	2,279612541	9922539
2,229886293	11105004	2,279890299	9927281
2,230164051	11635959	2,280168056	9863244
2,230441809	12389110	2,280445814	9884396
2,230719566	13415009	2,280723572	9892201
2,230997562	14193132	2,281001329	9855225
2,23127532	13837308	2,281279325	9812235
2,231553078	13046705	2,281557083	9678816
2,231830835	12333369	2,281834841	9500697
2,232108593	11845023	2,282112598	9371037
2,232386351	11455679	2,282390356	9270810
2,232664347	11171385	2,282668352	9226523
2,232942104	10967300	2,28294611	9330924
2,233219862	10892012	2,283223867	9320408
2,23349762	10724055	2,283501625	9418192
2,233775377	10632789	2,283779383	9576564
2,234053135	10609420	2,28405714	9620740
2,234331131	10482066	2,284335136	9738240
2,234608889	10430260	2,284612894	9860528

2,234886646	10337348	2,284890652	9917570
2,235164404	10290815	2,285168409	10010004
2,235442162	10213688	2,285446167	10122464
2,235720158	10091086	2,285724163	10170425
2,235997915	10062324	2,286001921	10368414
2,236275673	10028456	2,286279678	10423190
2,236553431	9931808	2,286557436	10640020
2,236831188	9910990	2,286835194	10849381
2,237108946	9867019	2,287112951	11237052
2,237386942	9866944	2,287390947	11749957
2,2376647	9890564	2,287668705	12634436
2,237942457	9863870	2,287946463	13678536
2,238220215	9860171	2,28822422	14169465
2,238497972	9773813	2,288501978	13634858
2,23877573	9650142	2,288779736	12830931
2,239053726	9497732	2,289057732	12123949
2,239331484	9315320	2,289335489	11648369
2,239609241	9250115	2,289613247	11311516
2,239886999	9298817	2,289891005	11081649
2,240164757	9288745	2,290168762	10873510
2,240442753	9358363	2,290446758	10762866
2,24072051	9488101	2,290724516	10670885
2,240998268	9566676	2,291002274	10581894
2,241276026	9688821	2,291280031	10493791
2,241553783	9776094	2,291557789	10442010
2,241831541	9837859	2,291835546	10404155
2,242109537	9982107	2,292113543	10302130
2,242387295	9993307	2,2923913	10283196
2,242665052	10113059	2,292669058	10215224
2,24294281	10258721	2,292946815	10135798
2,243220568	10287781	2,293224573	10139377
2,243498325	10447066	2,293502331	10015116
2,243776321	10671410	2,293780327	9996699
2,244054079	10882597	2,294058084	10009695
2,244331837	11268167	2,294335842	9922039
2,244609594	11908147	2,2946136	9942575
2,244887352	12797620	2,294891357	9959289
2,245165348	13762422	2,295169353	9923780
2,245443106	13885234	2,295447111	9978157
2,245720863	13129366	2,295724869	9759033
2,245998621	12338827	2,296002626	9654537
2,246276379	11768677	2,296280384	9505059
2,246554136	11321578	2,296558142	9345953
2,246832132	11062766	2,296836138	9351764
2,24710989	10831820	2,297113895	9361685
2,247387648	10688050	2,297391653	9354226
2,247665405	10588073	2,297669411	9506246
2,247943163	10463429	2,297947168	9588585

2,248220921	10445524	2,298224926	9702287
2,248498917	10376645	2,298502922	9799949
2,248776674	10304774	2,29878068	9912075
2,249054432	10220278	2,299058437	10030459
2,24933219	10241283	2,299336195	10070035
2,249609947	10157345	2,299613953	10153095
2,249887943	10079351	2,299891949	10260716
2,250165701	10075836	2,300169706	10416983
2,250443459	10001850	2,300447464	10484813
2,250721216	9958551	2,300725222	10601769
2,250998974	9960735	2,301002979	10924358
2,251276731	9904494	2,301280737	11133607
2,251554728	9887532	2,301558733	11573986
2,251832485	9921656	2,301836491	12355125
2,252110243	9895043	2,302114248	13388941
2,252388	9865734	2,302392006	14262259
2,252665758	9890351	2,302669764	14171110
2,252943754	9746966	2,302947521	13262050
2,253221512	9534264	2,303225517	12540001
2,253499269	9453297	2,303503275	11904336
2,253777027	9301019	2,303781033	11566815
2,254054785	9267457	2,30405879	11225137
2,254332542	9358336	2,304336548	10994072
2,254610538	9358707	2,304614544	10881021
2,254888296	9449145	2,304892302	10760436
2,255166054	9591570	2,305170059	10607258
2,255443811	9641106	2,305447817	10590490
2,255721569	9756270	2,305725574	10472619
2,255999327	9872863	2,306003332	10368142
2,256277323	9914754	2,306281328	10384780
2,25655508	10023610	2,306559086	10248405
2,256832838	10142937	2,306836843	10228469
2,257110596	10174705	2,307114601	10133506
2,257388353	10341814	2,307392359	10065874
2,257666349	10438012	2,307670116	9976791
2,257944107	10620744	2,307948112	10043972
2,258221865	10872439	2,30822587	9890946
2,258499622	11145901	2,308503628	9860718
2,25877738	11721403	2,308781385	9847554
2,259055138	12478321	2,309059143	9867009
2,259333134	13540230	2,309337139	9876617
2,259610891	14269808	2,309614897	9821779
2,259888649	13908385	2,309892654	9771746
2,260166407	13040337	2,310170412	9635283
2,260444164	12384540	2,31044817	9430943
2,26072216	11792727	2,310726166	9354907
2,260999918	11479305	2,311003923	9253791
2,261277676	11157589	2,311281681	9283253

2,261555433	10975149	2,311559439	9286476
2,261833191	10847876	2,311837196	9386740
2,262110949	10759167	2,312114954	9461338
2,262388945	10609940	2,31239295	9578163
2,262666702	10587703	2,312670708	9716618
2,26294446	10491086	2,312948465	9797903
2,263222218	10443493	2,313226223	9891530
2,263499975	10343861	2,313503981	10005521
2,263777733	10319415	2,313781738	10086000
2,264055729	10213491	2,314059734	10211623
2,264333487	10165094	2,314337492	10245694
2,264611244	10093706	2,31461525	10397570
2,264889002	10063050	2,314893007	10587398
2,265166759	10014983	2,315170765	10665340
2,265444756	9913042	2,315448761	10983938
2,265722513	9969493	2,315726519	11398684
2,266000271	9926327	2,316004276	11935764
2,266278028	9923134	2,316282034	12885790
2,266555786	9947762	2,316559792	13951057
2,266833544	9892711	2,316837549	14159110
2,267111154	9798001	2,317115545	13409962
2,267389297	9711468	2,317393303	12610701
2,267667055	9474114	2,317671061	11925105
2,267944813	9333871	2,317948818	11600763
2,26822257	9381324	2,318226576	11228841
2,268500328	9305681	2,318504333	11021812
2,268778324	9365492	2,31878233	10867503
2,269056082	9459435	2,319060087	10701532
2,269333839	9549371	2,319337845	10631672
2,269611597	9618492	2,319615602	10574025
2,269889355	9793433	2,31989336	10438904
2,270167351	9866277	2,320171356	10421114
2,270445108	9940744	2,320449114	10355601
2,270722866	10066127	2,320726871	10235028
2,271000624	10155707	2,321004629	10252112
2,271278381	10222555	2,321282387	10165646
2,271556139	10317698	2,321560144	10074622
2,271834135	10498868	2,32183814	10044373

Table 3 Static pressure variation versus flow time on the point monitor 3

t(s)	p[Pa]	t(s)	p[Pa]
2,222107887	10273994	2,272111893	10855646
2,222385645	10236607	2,27238965	10955830
2,222663403	10163968	2,272667408	11231686
2,22294116	10119994	2,272945166	11596745
2,223219156	10189680	2,273222923	12164577
2,223496914	10169897	2,273500919	13061381

2,223774672	10132842	2,273778677	13839339
2,224052429	10106382	2,274056435	13898324
2,224330187	9989908	2,274334192	13134250
2,224607944	9903498	2,27461195	12460161
2,224885941	9930239	2,274889946	12012667
2,225163698	9886998	2,275167704	11504375
2,225441456	9860958	2,275445461	11308795
2,225719213	9923572	2,275723219	11103288
2,225996971	9923369	2,276000977	10971089
2,226274729	9948508	2,276278734	10892588
2,226552725	10053079	2,27655673	10819127
2,226830482	10094355	2,276834488	10732184
2,22710824	10139465	2,277112246	10718120
2,227385998	10243620	2,277390003	10649914
2,227663755	10268818	2,277667761	10613972
2,227941751	10323864	2,277945518	10630431
2,228219509	10404948	2,278223515	10574872
2,228497267	10448738	2,278501272	10585115
2,228775024	10533274	2,27877903	10546423
2,229052782	10657893	2,279056787	10367885
2,22933054	10754437	2,279334545	10234191
2,229608536	10984238	2,279612541	10129705
2,229886293	11241645	2,279890299	10044592
2,230164051	11661447	2,280168056	10079944
2,230441809	12429909	2,280445814	10076083
2,230719566	13340448	2,280723572	10040925
2,230997562	14027257	2,281001329	10060901
2,23127532	13766897	2,281279325	9916259
2,231553078	12990223	2,281557083	9823838
2,231830835	12339709	2,281834841	9844135
2,232108593	11932776	2,282112598	9769913
2,232386351	11513910	2,282390356	9781127
2,232664347	11302972	2,282668352	9792476
2,232942104	11117972	2,28294611	9799398
2,233219862	10997009	2,283223867	9834710
2,23349762	10925132	2,283501625	9905739
2,233775377	10810822	2,283779383	9952332
2,234053135	10791159	2,28405714	10033880
2,234331131	10728171	2,284335136	10107045
2,234608889	10659563	2,284612894	10144876
2,234886646	10636942	2,284890652	10254199
2,235164404	10625949	2,285168409	10295802
2,235442162	10573600	2,285446167	10346924
2,235720158	10542390	2,285724163	10444409
2,235997915	10457427	2,286001921	10563932
2,236275673	10334431	2,286279678	10600735
2,236553431	10149248	2,286557436	10850365
2,236831188	10028091	2,286835194	10959143

2,237108946	10043399	2,287112951	11331702
2,237386942	10018113	2,287390947	11843907
2,2376647	10035641	2,287668705	12585829
2,237942457	10063004	2,287946463	13594119
2,238220215	9965199	2,28822422	14069697
2,238497972	9898795	2,288501978	13493803
2,23877573	9867159	2,288779736	12828546
2,239053726	9786189	2,289057732	12179845
2,239331484	9819462	2,289335489	11669101
2,239609241	9787943	2,289613247	11450569
2,239886999	9787513	2,289891005	11208577
2,240164757	9856666	2,290168762	10977130
2,240442753	9851727	2,290446758	10959531
2,24072051	9935999	2,290724516	10838544
2,240998268	10026783	2,291002274	10756380
2,241276026	10052955	2,291280031	10745951
2,241553783	10135180	2,291557789	10650307
2,241831541	10208798	2,291835546	10682003
2,242109537	10256480	2,292113543	10636712
2,242387295	10293547	2,2923913	10575708
2,242665052	10405439	2,292669058	10654043
2,24294281	10449600	2,292946815	10585767
2,243220568	10534976	2,293224573	10504882
2,243498325	10667094	2,293502331	10351016
2,243776321	10798103	2,293780327	10183166
2,244054079	11050858	2,294058084	10176199
2,244331837	11389368	2,294335842	10115956
2,244609594	11918344	2,2946136	10080050
2,244887352	12795592	2,294891357	10172296
2,245165348	13669295	2,295169353	10099500
2,245443106	13744110	2,295447111	10092892
2,245720863	13108809	2,295724869	9918393
2,245998621	12362811	2,296002626	9872763
2,246276379	11796233	2,296280384	9907321
2,246554136	11446137	2,296558142	9848453
2,246832132	11189590	2,296836138	9837188
2,24710989	10949671	2,297113895	9906676
2,247387648	10875486	2,297391653	9917463
2,247665405	10751566	2,297669411	9952558
2,247943163	10628277	2,297947168	10024478
2,248220921	10684070	2,298224926	10137643
2,248498917	10596430	2,298502922	10187118
2,248776674	10541508	2,29878068	10251917
2,249054432	10539788	2,299058437	10322620
2,24933219	10546734	2,299336195	10424554
2,249609947	10512141	2,299613953	10445686
2,249887943	10550742	2,299891949	10490274
2,250165701	10511647	2,300169706	10662896

2,250443459	10369781	2,300447464	10718766
2,250721216	10268019	2,300725222	10791838
2,250998974	10124993	2,301002979	11070043
2,251276731	10057193	2,301280737	11287359
2,251554728	10113232	2,301558733	11663901
2,251832485	10078728	2,301836491	12393874
2,252110243	10075458	2,302114248	13331197
2,252388	10087898	2,302392006	14125005
2,252665758	9978563	2,302669764	14080087
2,252943754	9888266	2,302947521	13185383
2,253221512	9860685	2,303225517	12539625
2,253499269	9828081	2,303503275	11996643
2,253777027	9828317	2,303781033	11627866
2,254054785	9838982	2,30405879	11329126
2,254332542	9831747	2,304336548	11167938
2,254610538	9901492	2,304614544	11012438
2,254888296	9946357	2,304892302	10917033
2,255166054	9979405	2,305170059	10830223
2,255443811	10080221	2,305447817	10756234
2,255721569	10136967	2,305725574	10710261
2,255999327	10184775	2,306003332	10654599
2,256277323	10272232	2,306281328	10633609
2,25655508	10304577	2,306559086	10602903
2,256832838	10409054	2,306836843	10624621
2,257110596	10456633	2,307114601	10547359
2,257388353	10540336	2,307392359	10536290
2,257666349	10664097	2,307670116	10331248
2,257944107	10813020	2,307948112	10285704
2,258221865	10983859	2,30822587	10088209
2,258499622	11298266	2,308503628	10055704
2,25877738	11785334	2,308781385	10028345
2,259055138	12474453	2,309059143	10090012
2,259333134	13478906	2,309337139	10055501
2,259610891	14130956	2,309614897	9981599
2,259888649	13812264	2,309892654	9918026
2,260166407	13008945	2,310170412	9814317
2,260444164	12392377	2,31044817	9774046
2,26072216	11860732	2,310726166	9809002
2,260999918	11597236	2,311003923	9768470
2,261277676	11257419	2,311281681	9810683
2,261555433	11131070	2,311559439	9820500
2,261833191	11010587	2,311837196	9857950
2,262110949	10931028	2,312114954	9958941
2,262388945	10814496	2,31239295	10003171
2,262666702	10796875	2,312670708	10096820
2,26294446	10713984	2,312948465	10197530
2,263222218	10709358	2,313226223	10203183
2,263499975	10643011	2,313503981	10337045

2,263777733	10635980	2,313781738	10395667
2,264055729	10632174	2,314059734	10431196
2,264333487	10568029	2,314337492	10519712
2,264611244	10487429	2,31461525	10627726
2,264889002	10384133	2,314893007	10742971
2,265166759	10157501	2,315170765	10876520
2,265444756	10104557	2,315448761	11110841
2,265722513	10145136	2,315726519	11481944
2,266000271	10050759	2,316004276	12022021
2,266278028	10141628	2,316282034	12822252
2,266555786	10130003	2,316559792	13840116
2,266833544	10004595	2,316837549	14067753
2,26711154	9947408	2,317115545	13297087
2,267389297	9918722	2,317393303	12618769
2,267667055	9827745	2,317671061	12003025
2,267944813	9815353	2,317948818	11625278
2,26822257	9912397	2,318226576	11363493
2,268500328	9826553	2,318504333	11172885
2,268778324	9866093	2,31878233	10970523
2,269056082	9948276	2,319060087	10896659
2,269333839	9998959	2,319337845	10834405
2,269611597	10024168	2,319615602	10729878
2,269889355	10162043	2,31989336	10691923
2,270167351	10235239	2,320171356	10672729
2,270445108	10271541	2,320449114	10599174
2,270722866	10343953	2,320726871	10575156
2,271000624	10442220	2,321004629	10608136
2,271278381	10499627	2,321282387	10553444
2,271556139	10550359	2,321560144	10544952
2,271834135	10652737	2,32183814	10434766

Table 4 Static pressure variation versus flow time on the point monitor 4

t(s)	p[Pa]	t(s)	p[Pa]
2,222107887	10114982	2,272111893	10670714
2,222385645	10097419	2,27238965	10872683
2,222663403	10049461	2,272667408	11207644
2,22294116	10026799	2,272945166	11694280
2,223219156	10004767	2,273222923	12430497
2,223496914	9957612	2,273500919	13518006
2,223774672	9909086	2,273778677	14519413
2,224052429	9794576	2,274056435	14554644
2,224330187	9670503	2,274334192	13580311
2,224607944	9598463	2,27461195	12771661
2,224885941	9571900	2,274889946	12162164
2,225163698	9560924	2,275167704	11577991
2,225441456	9570421	2,275445461	11318631
2,225719213	9601908	2,275723219	11041188

2,225996971	9616339	2,276000977	10921816
2,226274729	9654436	2,276278734	10778629
2,226552725	9683776	2,27655673	10691079
2,226830482	9728285	2,276834488	10614259
2,22710824	9768391	2,277112246	10535739
2,227385998	9832719	2,277390003	10478603
2,227663755	9900158	2,277667761	10419072
2,227941751	9979788	2,277945518	10364179
2,228219509	10066598	2,278223515	10300667
2,228497267	10187359	2,278501272	10234934
2,228775024	10306779	2,27877903	10176122
2,229052782	10463629	2,279056787	10110739
2,22933054	10651524	2,279334545	10049381
2,229608536	10923691	2,279612541	10009635
2,229886293	11270624	2,279890299	9956321
2,230164051	11840133	2,280168056	9920575
2,230441809	12754536	2,280445814	9896338
2,230719566	13925163	2,280723572	9836661
2,230997562	14773560	2,281001329	9767064
2,23127532	14386134	2,281279325	9628411
2,231553078	13445029	2,281557083	9526008
2,231830835	12614574	2,281834841	9505171
2,232108593	12070893	2,282112598	9469867
2,232386351	11590585	2,282390356	9486683
2,232664347	11293940	2,282668352	9481620
2,232942104	11076160	2,28294611	9538662
2,233219862	10932752	2,283223867	9544775
2,23349762	10806218	2,283501625	9586739
2,233775377	10701047	2,283779383	9639237
2,234053135	10642734	2,28405714	9663255
2,234331131	10555285	2,284335136	9733235
2,234608889	10490001	2,284612894	9791796
2,234886646	10402861	2,284890652	9882968
2,235164404	10386991	2,285168409	9957206
2,235442162	10270802	2,285446167	10066776
2,235720158	10187965	2,285724163	10163167
2,235997915	10158905	2,286001921	10361898
2,236275673	10100477	2,286279678	10444465
2,236553431	10030276	2,286557436	10721018
2,236831188	9964904	2,286835194	10933808
2,237108946	9927082	2,287112951	11411986
2,237386942	9909199	2,287390947	12020759
2,2376647	9867260	2,287668705	13001187
2,237942457	9826889	2,287946463	14235323
2,238220215	9729956	2,28822422	14798454
2,238497972	9597808	2,288501978	14116397
2,23877573	9558207	2,288779736	13238220
2,239053726	9507255	2,289057732	12405594

2,239331484	9499103	2,289335489	11824839
2,239609241	9500175	2,289613247	11493467
2,239886999	9526635	2,289891005	11199958
2,240164757	9548832	2,290168762	10945663
2,240442753	9557844	2,290446758	10863821
2,24072051	9621098	2,290724516	10736991
2,240998268	9653370	2,291002274	10628107
2,241276026	9681432	2,291280031	10566723
2,241553783	9755074	2,291557789	10491327
2,241831541	9800569	2,291835546	10468659
2,242109537	9895952	2,292113543	10386643
2,242387295	9952475	2,2923913	10320107
2,242665052	10079900	2,292669058	10312217
2,24294281	10204064	2,292946815	10233314
2,243220568	10302268	2,293224573	10199158
2,243498325	10486515	2,293502331	10117120
2,243776321	10713705	2,293780327	10081217
2,244054079	11020320	2,294058084	10063153
2,244331837	11450660	2,294335842	9989745
2,244609594	12168845	2,2946136	9946634
2,244887352	13234648	2,294891357	9954892
2,245165348	14321149	2,295169353	9873011
2,245443106	14439600	2,295447111	9810680
2,245720863	13590535	2,295724869	9603041
2,245998621	12646805	2,296002626	9585757
2,246276379	11991316	2,296280384	9563738
2,246554136	11503701	2,296558142	9545507
2,246832132	11190050	2,296836138	9569671
2,24710989	10932410	2,297113895	9611651
2,247387648	10785336	2,297391653	9582903
2,247665405	10624821	2,297669411	9651218
2,247943163	10520422	2,297947168	9708253
2,248220921	10518697	2,298224926	9732932
2,248498917	10411138	2,298502922	9792096
2,248776674	10361937	2,29878068	9876558
2,249054432	10290718	2,299058437	9933592
2,24933219	10270780	2,299336195	10029104
2,249609947	10223751	2,299613953	10123454
2,249887943	10165182	2,299891949	10215771
2,250165701	10122998	2,300169706	10381861
2,250443459	10087052	2,300447464	10515006
2,250721216	10049137	2,300725222	10654794
2,250998974	9998161	2,301002979	10973374
2,251276731	9970314	2,301280737	11273676
2,251554728	9945683	2,301558733	11801266
2,251832485	9900951	2,301836491	12673495
2,252110243	9880027	2,302114248	13845807
2,252388	9793521	2,302392006	14887146

2,252665758	9691860	2,302669764	14746754
2,252943754	9592030	2,302947521	13628391
2,253221512	9512980	2,303225517	12862620
2,253499269	9525348	2,303503275	12135317
2,253777027	9517186	2,303781033	11692730
2,254054785	9520208	2,30405879	11357453
2,254332542	9561200	2,304336548	11107801
2,254610538	9589733	2,304614544	10937396
2,254888296	9618592	2,304892302	10830188
2,255166054	9655940	2,305170059	10685105
2,255443811	9693969	2,305447817	10624160
2,255721569	9750183	2,305725574	10538573
2,255999327	9812998	2,306003332	10452244
2,256277323	9877442	2,306281328	10439072
2,25655508	9965398	2,306559086	10338316
2,256832838	10092886	2,306836843	10331486
2,257110596	10164837	2,307114601	10194585
2,257388353	10328190	2,307392359	10177802
2,257666349	10466684	2,307670116	10080776
2,257944107	10692677	2,307948112	10109271
2,258221865	10937781	2,30822587	9985459
2,258499622	11311123	2,308503628	9921711
2,25877738	11965152	2,308781385	9886426
2,259055138	12799681	2,309059143	9886366
2,259333134	14069561	2,309337139	9807539
2,259610891	14876976	2,309614897	9719961
2,259888649	14443341	2,309892654	9580860
2,260166407	13454265	2,310170412	9490492
2,260444164	12663768	2,31044817	9434688
2,26072216	12013596	2,310726166	9460085
2,260999918	11654730	2,311003923	9461907
2,261277676	11261433	2,311281681	9480370
2,261555433	11086194	2,311559439	9517769
2,261833191	10919901	2,311837196	9553647
2,262110949	10837679	2,312114954	9603580
2,262388945	10670141	2,31239295	9657302
2,262666702	10648098	2,312670708	9708946
2,26294446	10561512	2,312948465	9786860
2,263222218	10497024	2,313226223	9838737
2,263499975	10431515	2,313503981	9947110
2,263777733	10378791	2,313781738	10048663
2,264055729	10312990	2,314059734	10142752
2,264333487	10255060	2,314337492	10239158
2,264611244	10175119	2,31461525	10411003
2,264889002	10165312	2,314893007	10593222
2,265166759	10070486	2,315170765	10754879
2,265444756	9996830	2,315448761	11091538
2,265722513	10034211	2,315726519	11576413

2,266000271	9935180	2,316004276	12217703
2,266278028	9933943	2,316282034	13273217
2,266555786	9884522	2,316559792	14529532
2,266833544	9759989	2,316837549	14758202
2,267111154	9644390	2,317115545	13831321
2,267389297	9593034	2,317393303	12961221
2,267667055	9539345	2,317671061	12165815
2,267944813	9531425	2,317948818	11755514
2,26822257	9592672	2,318226576	11390058
2,268500328	9559478	2,318504333	11138292
2,268778324	9616820	2,31878233	10934389
2,269056082	9618646	2,319060087	10796710
2,269333839	9674285	2,319337845	10699868
2,269611597	9695189	2,319615602	10616329
2,269889355	9780001	2,31989336	10518571
2,270167351	9827599	2,320171356	10475169
2,270445108	9905095	2,320449114	10415168
2,270722866	10009882	2,320726871	10326606
2,271000624	10073721	2,321004629	10320864
2,271278381	10205326	2,321282387	10246006
2,271556139	10318575	2,321560144	10177224
2,271834135	10466700	2,32183814	10128694

Table 5 Static pressure variation versus flow time on the point monitor 5

t(s)	p[Pa]	t(s)	p[Pa]
2,222107887	10510072	2,272111893	10925837
2,222385645	10511625	2,27238965	11075373
2,222663403	10474825	2,272667408	11332680
2,22294116	10469902	2,272945166	11715730
2,223219156	10466004	2,273222923	12309709
2,223496914	10427500	2,273500919	13180871
2,223774672	10398576	2,273778677	14000871
2,224052429	10299250	2,274056435	14039482
2,224330187	10178712	2,274334192	13274284
2,224607944	10110977	2,27461195	12619871
2,224885941	10080586	2,274889946	12138665
2,225163698	10059841	2,275167704	11663594
2,225441456	10055822	2,275445461	11454072
2,225719213	10071363	2,275723219	11228165
2,225996971	10085460	2,276000977	11130429
2,226274729	10130503	2,276278734	11010847
2,226552725	10172379	2,27655673	10931910
2,226830482	10229612	2,276834488	10859638
2,22710824	10276534	2,277112246	10784353
2,227385998	10330537	2,277390003	10729690
2,227663755	10376806	2,277667761	10685369
2,227941751	10427230	2,277945518	10647582

2,228219509	10470549	2,278223515	10608453
2,228497267	10550835	2,278501272	10565780
2,228775024	10625248	2,27877903	10531064
2,229052782	10736079	2,279056787	10487741
2,22933054	10873093	2,279334545	10445567
2,229608536	11079509	2,279612541	10427931
2,229886293	11342392	2,279890299	10394345
2,230164051	11799531	2,280168056	10372120
2,230441809	12538789	2,280445814	10365143
2,230719566	13482193	2,280723572	10322857
2,230997562	14186625	2,281001329	10263870
2,23127532	13892117	2,281279325	10129909
2,231553078	13150226	2,281557083	10029446
2,231830835	12488494	2,281834841	9994427
2,232108593	12066303	2,282112598	9949768
2,232386351	11676844	2,282390356	9944974
2,232664347	11442065	2,282668352	9928022
2,232942104	11265741	2,28294611	9969995
2,233219862	11149842	2,283223867	9978027
2,23349762	11040925	2,283501625	10027336
2,233775377	10943332	2,283779383	10095063
2,234053135	10883262	2,28405714	10137942
2,234331131	10799307	2,284335136	10207371
2,234608889	10734209	2,284612894	10262082
2,234886646	10661497	2,284890652	10329983
2,235164404	10657392	2,285168409	10378412
2,235442162	10563332	2,285446167	10462891
2,235720158	10502065	2,285724163	10524306
2,235997915	10490881	2,286001921	10671615
2,236275673	10454575	2,286279678	10726954
2,236553431	10398731	2,286557436	10946617
2,236831188	10357695	2,286835194	11095013
2,237108946	10337211	2,287112951	11476749
2,237386942	10336441	2,287390947	11960380
2,2376647	10314411	2,287668705	12745296
2,237942457	10288883	2,287946463	13742113
2,238220215	10208539	2,28822422	14206422
2,238497972	10081556	2,288501978	13669694
2,23877573	10041628	2,288779736	12973421
2,239053726	9985564	2,289057732	12316279
2,239331484	9968243	2,289335489	11837455
2,239609241	9957034	2,289613247	11579417
2,239886999	9974992	2,289891005	11354222
2,240164757	9992437	2,290168762	11137795
2,240442753	10012964	2,290446758	11077200
2,24072051	10090528	2,290724516	10968847
2,240998268	10137269	2,291002274	10871230
2,241276026	10183340	2,291280031	10811800

2,241553783	10253093	2,291557789	10736676
2,241831541	10285456	2,291835546	10729649
2,242109537	10360798	2,292113543	10669122
2,242387295	10386853	2,2923913	10619022
2,242665052	10478596	2,292669058	10639701
2,24294281	10560845	2,292946815	10582900
2,243220568	10630428	2,293224573	10571609
2,243498325	10752481	2,293502331	10509922
2,243776321	10930172	2,293780327	10496776
2,244054079	11158100	2,294058084	10494402
2,244331837	11493936	2,294335842	10437062
2,244609594	12067888	2,2946136	10408966
2,244887352	12924106	2,294891357	10435615
2,245165348	13800096	2,295169353	10359266
2,245443106	13918996	2,295447111	10308717
2,245720863	13243843	2,295724869	10107129
2,245998621	12496431	2,296002626	10085906
2,246276379	11969478	2,296280384	10056220
2,246554136	11583547	2,296558142	10027114
2,246832132	11330452	2,296836138	10036194
2,24710989	11126267	2,297113895	10070472
2,247387648	11011655	2,297391653	10036841
2,247665405	10884485	2,297669411	10114174
2,247943163	10788600	2,297947168	10182699
2,248220921	10787873	2,298224926	10224130
2,248498917	10691885	2,298502922	10287960
2,248776674	10644863	2,29878068	10368920
2,249054432	10585945	2,299058437	10410079
2,24933219	10581162	2,299336195	10477316
2,249609947	10554439	2,299613953	10540267
2,249887943	10515435	2,299891949	10600465
2,250165701	10491899	2,300169706	10718434
2,250443459	10474249	2,300447464	10812741
2,250721216	10457963	2,300725222	10917069
2,250998974	10424936	2,301002979	11159963
2,251276731	10412701	2,301280737	11395047
2,251554728	10401572	2,301558733	11811289
2,251832485	10374103	2,301836491	12507609
2,252110243	10365498	2,302114248	13458152
2,252388	10291809	2,302392006	14298488
2,252665758	10199341	2,302669764	14219879
2,252943754	10095685	2,302947521	13320804
2,253221512	10016264	2,303225517	12710842
2,253499269	10016709	2,303503275	12126632
2,253777027	9994868	2,303781033	11766492
2,254054785	9984570	2,30405879	11497480
2,254332542	10015295	2,304336548	11295327
2,254610538	10042946	2,304614544	11151194

2,254888296	10082164	2,304892302	11066850
2,255166054	10136484	2,305170059	10926321
2,255443811	10187068	2,305447817	10868531
2,255721569	10251561	2,305725574	10787420
2,255999327	10307648	2,306003332	10702703
2,256277323	10356110	2,306281328	10708428
2,25655508	10418345	2,306559086	10621032
2,256832838	10512018	2,306836843	10642595
2,257110596	10545672	2,307114601	10531767
2,257388353	10665757	2,307392359	10533185
2,257666349	10763582	2,307670116	10461064
2,257944107	10934180	2,307948112	10510094
2,258221865	11117494	2,30822587	10410331
2,258499622	11404131	2,308503628	10367928
2,25877738	11927290	2,308781385	10350455
2,259055138	12596275	2,309059143	10366603
2,259333134	13617477	2,309337139	10309825
2,259610891	14278707	2,309614897	10236310
2,259888649	13948176	2,309892654	10106378
2,260166407	13164831	2,310170412	10016780
2,260444164	12524024	2,31044817	9951176
2,26072216	12017454	2,310726166	9966543
2,260999918	11732170	2,311003923	9954284
2,261277676	11400104	2,311281681	9954613
2,261555433	11274754	2,311559439	9976685
2,261833191	11127708	2,311837196	10015926
2,262110949	11067521	2,312114954	10071850
2,262388945	10901855	2,31239295	10136927
2,262666702	10881823	2,312670708	10194757
2,26294446	10791675	2,312948465	10273993
2,263222218	10739299	2,313226223	10312526
2,263499975	10688530	2,313503981	10404178
2,263777733	10654884	2,313781738	10468579
2,264055729	10611311	2,314059734	10536249
2,264333487	10573966	2,314337492	10590297
2,264611244	10519404	2,31461525	10721516
2,264889002	10532242	2,314893007	10863289
2,265166759	10459093	2,315170765	10963820
2,265444756	10407217	2,315448761	11239451
2,265722513	10463291	2,315726519	11619130
2,266000271	10381591	2,316004276	12133371
2,266278028	10402547	2,316282034	12980061
2,266555786	10367964	2,316559792	13998731
2,266833544	10254764	2,316837549	14196685
2,26711154	10138831	2,317115545	13466557
2,267389297	10084286	2,317393303	12768473
2,267667055	10025038	2,317671061	12132201
2,267944813	9999594	2,317948818	11793832

2,26822257	10048108	2,318226576	11503513
2,268500328	10005881	2,318504333	11300216
2,268778324	10058310	2,31878233	11131498
2,269056082	10071123	2,319060087	11013378
2,269333839	10140021	2,319337845	10930873
2,269611597	10179342	2,319615602	10850551
2,269889355	10270700	2,31989336	10753924
2,270167351	10315244	2,320171356	10725559
2,270445108	10381597	2,320449114	10657603
2,270722866	10459680	2,320726871	10597832
2,271000624	10493496	2,321004629	10618551
2,271278381	10584185	2,321282387	10568390
2,271556139	10661917	2,321560144	10520147
2,271834135	10763664	2,32183814	10489862

Table 6 Static pressure variation versus flow time on the point monitor 6

t(s)	p[Pa]	t(s)	p[Pa]
2,222107887	10798903	2,272111893	11231167
2,222385645	10795790	2,27238965	11386470
2,222663403	10755992	2,272667408	11656842
2,22294116	10744134	2,272945166	12062874
2,223219156	10729748	2,273222923	12691786
2,223496914	10683171	2,273500919	13621678
2,223774672	10640979	2,273778677	14495581
2,224052429	10527958	2,274056435	14538703
2,224330187	10396843	2,274334192	13723502
2,224607944	10320848	2,27461195	13035060
2,224885941	10284395	2,274889946	12525375
2,225163698	10262717	2,275167704	12026033
2,225441456	10260850	2,275445461	11808320
2,225719213	10283554	2,275723219	11570720
2,225996971	10304544	2,276000977	11469888
2,226274729	10358754	2,276278734	11346310
2,226552725	10410527	2,27655673	11266725
2,226830482	10477698	2,276834488	11195466
2,22710824	10534389	2,277112246	11120949
2,227385998	10599425	2,277390003	11067732
2,227663755	10655693	2,277667761	11019333
2,227941751	10714976	2,277945518	10976949
2,228219509	10767609	2,278223515	10930550
2,228497267	10853952	2,278501272	10881420
2,228775024	10933285	2,27877903	10836347
2,229052782	11047493	2,279056787	10785446
2,22933054	11190244	2,279334545	10734057
2,229608536	11406043	2,279612541	10704287
2,229886293	11683920	2,279890299	10659808

2,230164051	12165734	2,280168056	10626111
2,230441809	12949500	2,280445814	10605385
2,230719566	13954190	2,280723572	10549697
2,230997562	14700564	2,281001329	10480470
2,23127532	14384959	2,281279325	10335987
2,231553078	13594506	2,281557083	10230790
2,231830835	12892323	2,281834841	10195965
2,232108593	12443029	2,282112598	10154086
2,232386351	12032602	2,282390356	10158591
2,232664347	11786513	2,282668352	10152633
2,232942104	11604063	2,28294611	10206771
2,233219862	11484326	2,283223867	10227114
2,23349762	11374272	2,283501625	10285782
2,233775377	11279513	2,283779383	10360332
2,234053135	11223034	2,28405714	10406298
2,234331131	11142057	2,284335136	10481400
2,234608889	11079885	2,284612894	10538446
2,234886646	11005913	2,284890652	10611543
2,235164404	10999238	2,285168409	10660858
2,235442162	10897935	2,285446167	10746258
2,235720158	10830774	2,285724163	10809361
2,235997915	10811827	2,286001921	10962883
2,236275673	10765780	2,286279678	11017159
2,236553431	10700236	2,286557436	11246516
2,236831188	10645791	2,286835194	11408388
2,237108946	10613256	2,287112951	11814403
2,237386942	10598760	2,287390947	12333071
2,2376647	10559817	2,287668705	13175579
2,237942457	10518264	2,287946463	14243115
2,238220215	10423314	2,28822422	14742375
2,238497972	10284479	2,288501978	14173242
2,23877573	10237290	2,288779736	13432534
2,239053726	10178423	2,289057732	12732697
2,239331484	10164081	2,289335489	12226275
2,239609241	10161474	2,289613247	11951289
2,239886999	10191701	2,289891005	11703791
2,240164757	10222821	2,290168762	11477322
2,240442753	10256326	2,290446758	11409095
2,24072051	10344396	2,290724516	11294261
2,240998268	10400240	2,291002274	11191701
2,241276026	10450922	2,291280031	11133565
2,241553783	10527021	2,291557789	11058960
2,241831541	10563855	2,291835546	11049397
2,242109537	10641378	2,292113543	10985747
2,242387295	10670199	2,2923913	10933707
2,242665052	10762666	2,292669058	10950283
2,24294281	10847017	2,292946815	10889786
2,243220568	10914904	2,293224573	10874558

2,243498325	11042437	2,293502331	10807418
2,243776321	11226036	2,293780327	10789450
2,244054079	11468637	2,294058084	10781812
2,244331837	11826750	2,294335842	10715763
2,244609594	12440260	2,2946136	10678240
2,244887352	13357937	2,294891357	10693051
2,245165348	14298529	2,295169353	10605916
2,245443106	14427254	2,295447111	10540497
2,245720863	13715689	2,295724869	10325557
2,245998621	12922845	2,296002626	10295990
2,246276379	12367938	2,296280384	10261320
2,246554136	11958570	2,296558142	10228920
2,246832132	11692342	2,296836138	10240058
2,24710989	11474146	2,297113895	10279457
2,247387648	11350547	2,297391653	10252745
2,247665405	11213677	2,297669411	10339181
2,247943163	11114868	2,297947168	10418486
2,248220921	11112732	2,298224926	10470047
2,248498917	11012487	2,298502922	10545755
2,248776674	10964753	2,29878068	10638091
2,249054432	10900977	2,299058437	10689486
2,24933219	10891877	2,299336195	10766042
2,249609947	10858742	2,299613953	10836668
2,249887943	10813854	2,299891949	10901043
2,250165701	10784635	2,300169706	11025121
2,250443459	10761668	2,300447464	11120589
2,250721216	10739088	2,300725222	11225518
2,250998974	10699024	2,301002979	11480540
2,251276731	10680210	2,301280737	11724156
2,251554728	10661428	2,301558733	12164423
2,251832485	10623813	2,301836491	12904226
2,252110243	10605924	2,302114248	13914691
2,252388	10521801	2,302392006	14810095
2,252665758	10420503	2,302669764	14721242
2,252943754	10311442	2,302947521	13767112
2,253221512	10226938	2,303225517	13121518
2,253499269	10228681	2,303503275	12503726
2,253777027	10209052	2,303781033	12127043
2,254054785	10204395	2,30405879	11845552
2,254332542	10243500	2,304336548	11634418
2,254610538	10279892	2,304614544	11487998
2,254888296	10326185	2,304892302	11400760
2,255166054	10387541	2,305170059	11261932
2,255443811	10445047	2,305447817	11207408
2,255721569	10515015	2,305725574	11127635
2,255999327	10577744	2,306003332	11044307
2,256277323	10632191	2,306281328	11047448
2,256555508	10699802	2,306559086	10955663

2,256832838	10799717	2,306836843	10969870
2,257110596	10836711	2,307114601	10850254
2,257388353	10961739	2,307392359	10844080
2,257666349	11063206	2,307670116	10761402
2,257944107	11242447	2,307948112	10801208
2,258221865	11436702	2,30822587	10688458
2,258499622	11742502	2,308503628	10632819
2,25877738	12298466	2,308781385	10602350
2,259055138	13012061	2,309059143	10603833
2,259333134	14104221	2,309337139	10531089
2,259610891	14809897	2,309614897	10444208
2,259888649	14458613	2,309892654	10303289
2,260166407	13623069	2,310170412	10207545
2,260444164	12945598	2,31044817	10141089
2,26072216	12401182	2,310726166	10160950
2,260999918	12097654	2,311003923	10156774
2,261277676	11747862	2,311281681	10171351
2,261555433	11608687	2,311559439	10207801
2,261833191	11456380	2,311837196	10260163
2,262110949	11390498	2,312114954	10327702
2,262388945	11227143	2,31239295	10400930
2,262666702	11209006	2,312670708	10465187
2,26294446	11121671	2,312948465	10548408
2,263222218	11070139	2,313226223	10590777
2,263499975	11018337	2,313503981	10684472
2,263777733	10982896	2,313781738	10752319
2,264055729	10935751	2,314059734	10819056
2,264333487	10894589	2,314337492	10875215
2,264611244	10833558	2,31461525	11008307
2,264889002	10840609	2,314893007	11153092
2,265166759	10759762	2,315170765	11263445
2,265444756	10698960	2,315448761	11551637
2,265722513	10745673	2,315726519	11959149
2,266000271	10651050	2,316004276	12509367
2,266278028	10657766	2,316282034	13419238
2,266555786	10608792	2,316559792	14510017
2,266833544	10480440	2,316837549	14726052
2,267111154	10354103	2,317115545	13950440
2,267389297	10290061	2,317393303	13212843
2,267667055	10226698	2,317671061	12537408
2,267944813	10200497	2,317948818	12181876
2,26822257	10253585	2,318226576	11870720
2,268500328	10218230	2,318504333	11653197
2,268778324	10281141	2,31878233	11472951
2,269056082	10304080	2,319060087	11347120
2,269333839	10384268	2,319337845	11256332
2,269611597	10432800	2,319615602	11176020
2,269889355	10534403	2,31989336	11076560

2,270167351	10588118	2,320171356	11045693
2,270445108	10662260	2,320449114	10980051
2,270722866	10747710	2,320726871	10914184
2,271000624	10786711	2,321004629	10930164
2,271278381	10883099	2,321282387	10874755
2,271556139	10962150	2,321560144	10822997
2,271834135	11066854	2,32183814	10789774

Table 7 Static pressure variation versus flow time on the point monitor 7

2.2. Annex D: Frequencies of the pressure monitors

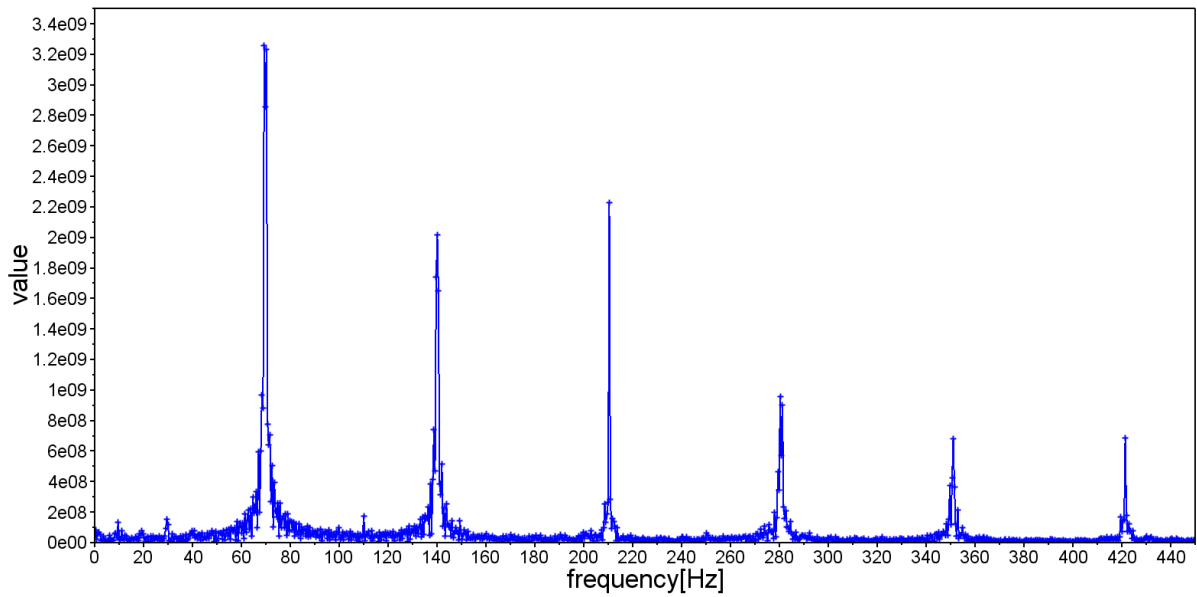


Figure 2.1 Static pressure frequencies on the point monitor 1

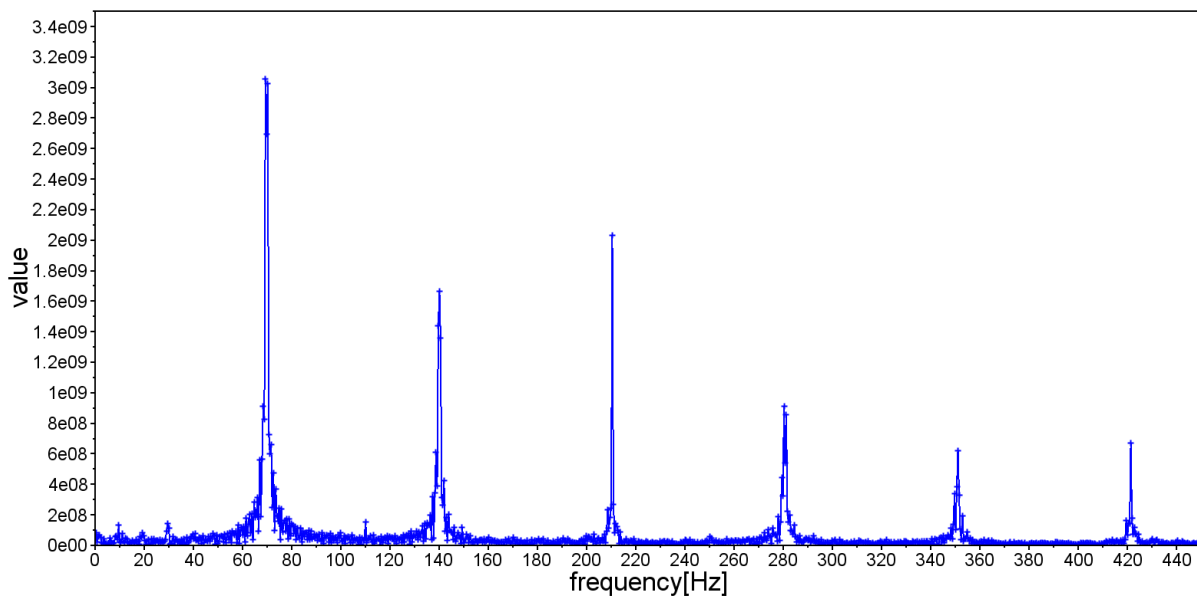


Figure 2.2 Static pressure frequencies on the point monitor 2

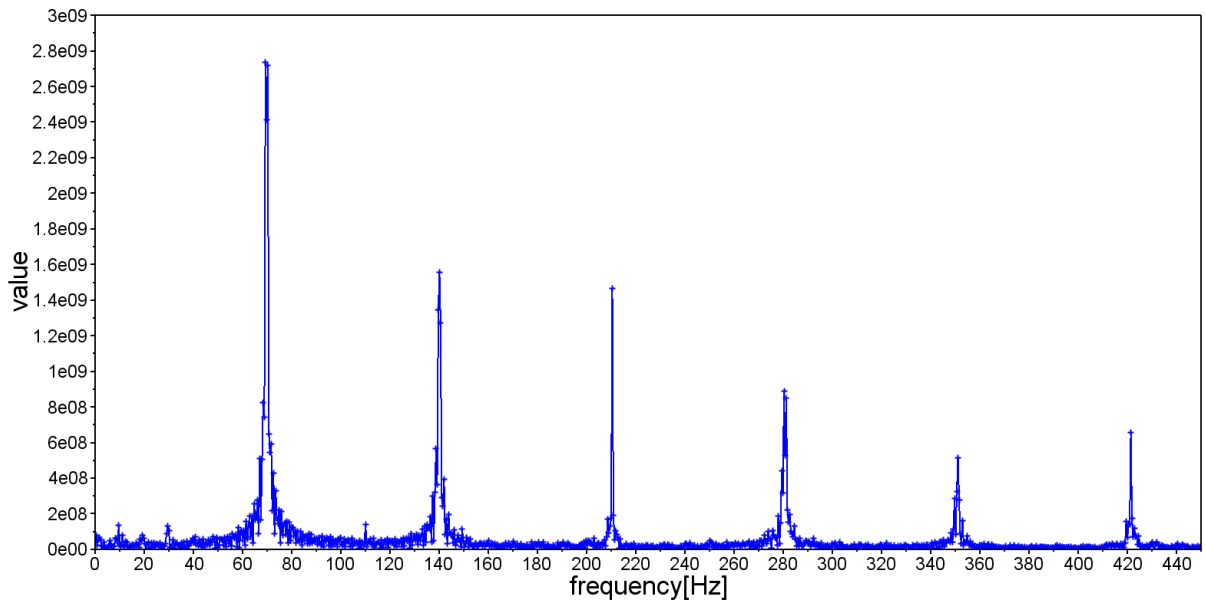


Figure 2.3 Static pressure frequencies on the point monitor 3

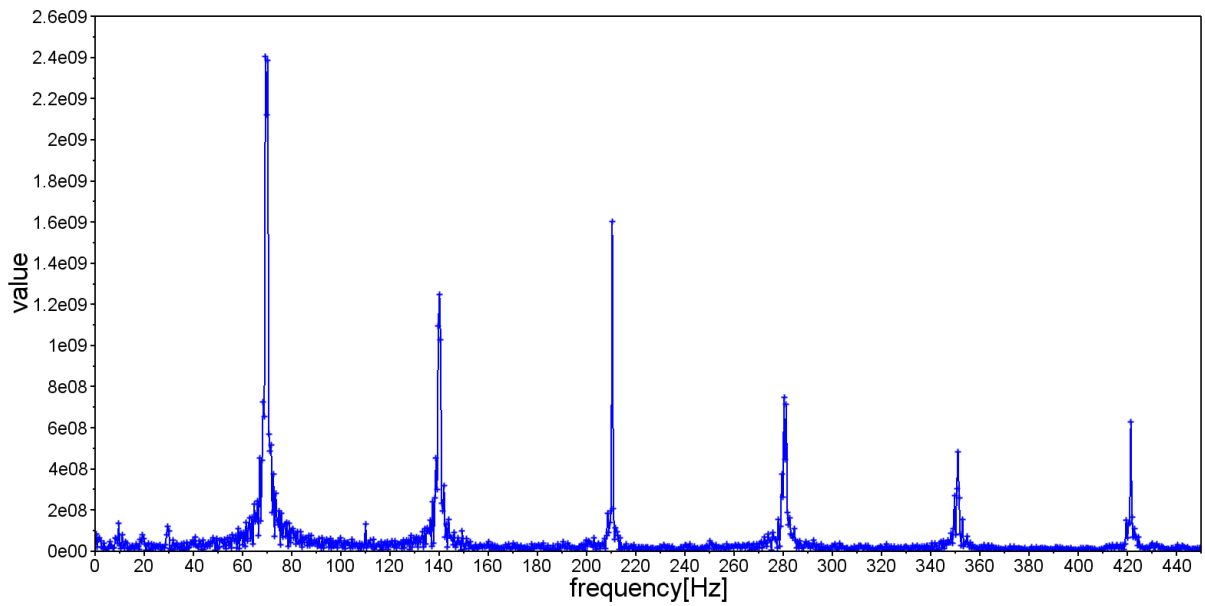


Figure 2.4 Static pressure frequencies on the point monitor 4

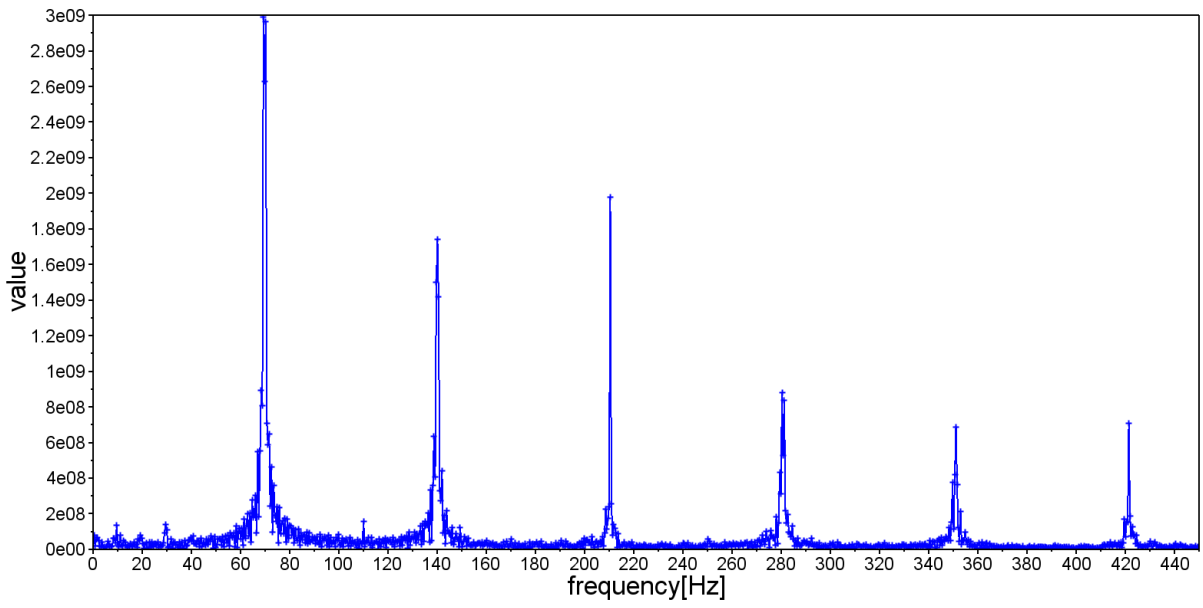


Figure 2.5 Static pressure frequencies on the point monitor 5

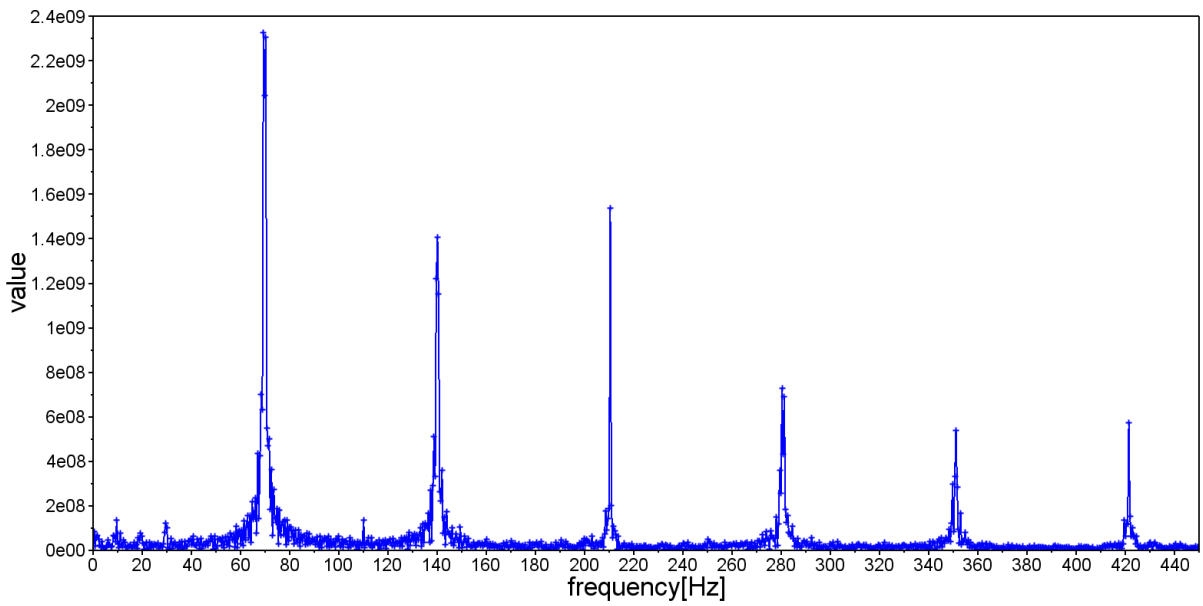


Figure 2.6 Static pressure frequencies on the point monitor 6

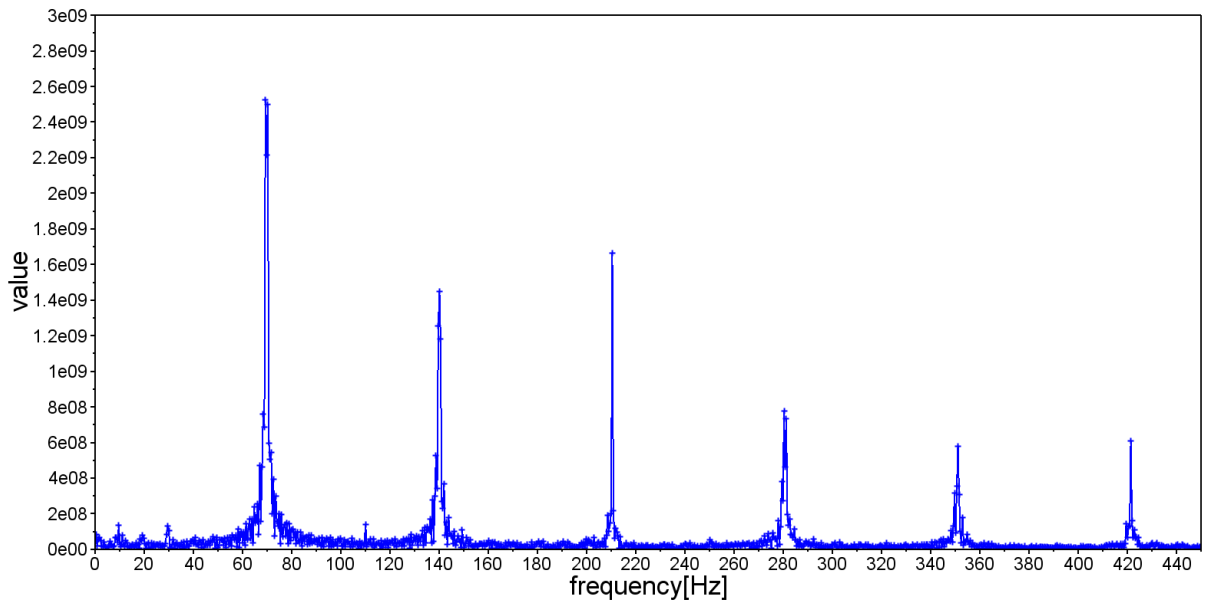


Figure 2.7 Static pressure frequencies on the point monitor 7